

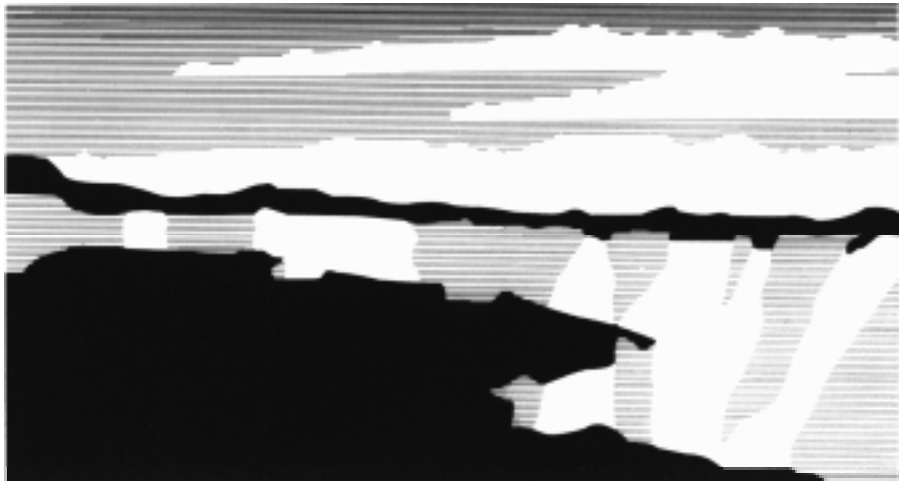
LA-UR-97-3826

Title: **Long-Term Global Nuclear
and Fuel Cell Strategies**

Author(s): R. A. Krakowski

Submitted to:

<http://lib-www.lanl.gov/la-pubs/00412590.pdf>



Los Alamos
NATIONAL LABORATORY

Los Alamos National Laboratory, an affirmative action/equal opportunity employer, is operated by the University of California for the U.S. Department of Energy under contract W-7405-ENG-36. By acceptance of this article, the publisher recognizes that the U.S. Government retains a nonexclusive, royalty-free license to publish or reproduce the published form of this contribution, or to allow others to do so, for U.S. Government purposes. The Los Alamos National Laboratory requests that the publisher identify this article as work performed under the auspices of the U.S. Department of Energy. Los Alamos National Laboratory strongly supports academic freedom and a researcher's right to publish; therefore, the Laboratory as an institution does not endorse the viewpoint of a publication or guarantee its technical correctness.

LONG-TERM GLOBAL NUCLEAR ENERGY AND FUEL CYCLE STRATEGIES

R. A. Krakowski

Systems Engineering and Integration Group
Technology and Safety Assessment Division
Los Alamos National Laboratory
Los Alamos, New Mexico 87545
September 24, 1997

SUMMARY ABSTRACT

The Global Nuclear Vision Project at the Los Alamos National Laboratory is examining, using scenario building techniques, a range of long-term nuclear energy futures. The exploration and assessment of optimal nuclear fuel-cycle and material strategies is an essential element of the Los Alamos study. To this end, an established global E³ (energy/economics/ environmental) model has been adopted and modified with a simplified, but comprehensive and multi-regional (13), nuclear energy module. Consistent nuclear energy scenarios are constructed using this multi-regional E³ model, wherein future demands for nuclear power are projected in price competition with other energy sources under a wide range of long-term (~2100) demographic (population, workforce size and productivity), economic (price-, population-, and income-determined demand for energy services, price- and population-modified GNP, resource depletion, world-market fossil energy prices), policy (taxes, tariffs, sanctions), and top-level technological (energy intensity and end-use efficiency improvements) drivers.

Long-term futures are constructed and studied at two levels in a hierarchy of scenario attributes. The higher levels attributes define external (to nuclear energy) drivers (*e.g.*, demographics, global economic growth, trade policies, sanctions, major technology advances) and largely determine the long-term policy-constrained market demand for nuclear energy. Within the context established by these upper hierarchal scenario attributes, lower-level attributes specify the nuclear fuel cycle *per se* and, thereby, the internal drivers of long-term demand for nuclear power at both market and non-market levels. Using the framework provided by the global E³ model, the impacts of both external and internal drivers are investigated. The ability to connect external and internal drivers through this modeling framework allows the study of impacts and tradeoffs between fossil- *versus* nuclear-fuel burning, that includes interactions between cost, environmental, proliferation, resource, and policy issues.

With a focus on a range of nuclear energy demand scenarios, the results reported herein center on departures from a "basis scenario" and are presented in the following order of increasing specificity: a) definition and parametric variations of the basis scenario; b) comparison of the basis scenario with other recent studies of this kind; c) parametric studies based on variations of the upper-level hierarchal scenario attributes (*e.g.*, external drivers); and d) variations of the lower-level scenario attributes (*e.g.*, internal drivers). This focus leads to the examination of a range of nuclear fuel-cycle scenarios (*e.g.*, once-through, plutonium recycle in thermal-spectrum reactors, fast-spectrum plutonium burners, breeder reactors), the impacts of which are reflected back to the higher-level scenario attributes that define

the particular nuclear energy growth scenario under investigation. Key sensitivities between and optimal strategies associated with external and internal drivers are reported. Special attention is given to understanding the role of nuclear materials inventories (in magnitude, location, and form) in contributing to proliferation risk, to the long-term sustainability of nuclear energy, and to the economic competitiveness of both conventional and advanced nuclear reactors in the broader global and long-term competitiveness. Lastly, by combining economic (GNP) and proliferation-risk metrics with computed carbon-dioxide emission rates and a global warming model, top-level tradeoffs between economic impacts, proliferation risk, and global temperature rise are evaluated under a range of carbon-tax driven scenarios, wherein supply-side forces enhance nuclear-energy market share.

Using the basis scenario and parametric departures therefrom, a series of comparative/benchmarking scenarios are generated and evaluated. The status of the present approach is critically evaluated and areas of future work and development are identified. This report of the limited cases considered provides a technical basis document of work presented at a recent symposium on the nuclear fuel cycle.⁺ The material contained herein also serves as a basis document for follow-on work that attempts to define better the specific role of nuclear energy in stemming long-term greenhouse warming.*

⁺ R. A. Krakowski, J. W. Davidson, C. G. Bathke, E. D. Arthur, and R. L. Wagner, Jr., "Nuclear Energy and Materials in the 21st Century, Intern. Symp. on Nuclear Fuel Cycle and Reactor Strategies: Adjusting to New Realities," IAEA, Vienna (June 3-6, 1997).

* R. A. Krakowski, "The Role of Nuclear Power in Mitigating Greenhouse Warming," Los Alamos National Laboratory document (in preparation, 1997).

CONTENTS

	page
I. INTRODUCTION	1
II. APPROACH.....	5
A. Scenario Hierarchy.....	5
1. Background.....	5
2. Scenario Attribute Hierarchy	6
B. Global Economics/Energy/Environmental E ³ Model.....	8
1. Overview of ERB Model.....	8
2. Additions to ERB Model	11
a. Nuclear Energy Model.....	12
b. Costing.....	13
c. Material Flows.....	14
d. Proliferation Risk	15
C. Basis Scenario	16
1. Description of Basis Scenario	17
2. Comparisons with Other Studies.....	18
III. RESULTS	21
A. Top-Level Hierarchal Variations: Impacts of External Drivers.....	21
1. Population	22
2. Workforce Productivity (GNP)	22
3. Energy Intensity (End-Use Efficiency).....	23
4. Carbon Tax	24
5. Nuclear Economics	25
a. Capital Cost.....	25
b. Uranium Resource	25
6. Composite Impacts of External Drivers	27
B. Lower-Level Hierarchal Variations: Impacts of Internal Drivers.....	28
1. Once-Through LWRs	28
a. Nuclear Materials.....	28
b. Demand Variants.....	28
c. Basis Scenario Realignment	29
2. Plutonium Recycle in Light-Water Reactors (LWRs)	29
3. Liquid-Metal Breeder Reactors (LMRs).....	34
4. Fast-Spectrum Plutonium Burners (FSBs)	36
a. Approach.....	36
b. Results	39
C. Integrated Risk Comparison: Nuclear Proliferation <i>versus</i> Global Warming.....	41
1. Scope and Approach.....	41
2. Comparative Results.....	42
IV. SUMMARY	49
REFERENCES	69

NOMENCLATURE.....	73
APPENDIX A. Simple Models to Estimate Plutonium Accumulations, LWR-Recycle, and Fast-Spectrum Burner Impacts.....	57
I. INTRODUCTION.....	57
II. BACKGROUND.....	57
III. MODELS AND RESULTS.....	57
A. Steady-State Analysis.....	59
B. Time-Dependent Analysis.....	61
C. Fast-Spectrum Burners.....	62
1. General Considerations.....	62
2. Economic Considerations.....	63
a. Support Ratio.....	64
b. Cost Impacts.....	64
IV. SUMMARY.....	67
TABLES.....	79
FIGURES.....	91

I. INTRODUCTION

Describing future roles of global nuclear energy on a time horizon of 2050 and beyond in one way or another reduces to an exercise in futurology. The main force driving an exercise of this kind is the desire to understand regional long-term impacts of front-end (including reactor) and back-end nuclear fuel-cycle strategies on regional and global market share assumed by nuclear energy. The evolution of these market shares is determined primarily by an interdependent array of economic (*e.g.*, resource, R&D, capital, operating, and environmental costs) and policy (*e.g.*, R&D emphases, energy structuring, nuclear material inventories, security constraints, *etc.*) choices. These choices in turn are influenced primarily by technological, security, and economic drivers that describe and/or determine the state of the country or region.

Studies of the future that do not extend much beyond one generation (*e.g.*, out to ~2020) begin with an understanding of the present state of the world and the forces that shaped that world. Applications of these forces of change much beyond a generational time horizon are subject increasingly to greater uncertainty. Impacts of these uncertainties are codified through the use of “scenario-building” techniques,^{1,2} wherein a range of possible futures is quantified by means of a series of well-defined, simplified, and generally surprise-free assumptions. While an array of alternative futures contributes little to resolving an uncertain future, scenario building offers an improvement to the alternative - the painting of a single and generally biased (either positively or pessimistically) picture of the future.²

The characteristics or attributes of a particular scenario can be expressed in terms of a hierarchical structure, at the top of which are placed demographic variables (*e.g.*, population growth, age structure, workforce size and productivity, and inter-regional migration). Population growth and the striving for improved living conditions for regional populations drive the demand for energy services, which in turn define the demand for secondary (*e.g.*, liquids, gases, solids, and electricity) and primary (*e.g.*, oil, gas, solids, nuclear, solar, and hydroelectric) energies. Most of the attributes that characterize the nuclear energy scenarios adopted in this study fall into the lower echelons of this scenario hierarchy, which is elaborated in Sec. II.A. The impact of key scenario attributes at each level of this hierarchy is examined by a simplified but consistent modeling framework. This framework has as a basis a conceptually transparent and well-documented E³ (energy/economics/

environmental) model³ that has been modified to include material-inventory, economic, and nuclear-proliferation characteristics that are unique to nuclear energy;⁴ this model framework is described in Sec. II.B.

This study searches for answers to the following three generic questions for nuclear energy:

- Growth: To what degree is the market share of nuclear energy determined by top-level scenario attributes like: a) population growth; b) end-use (*e.g.*, residential/commercial, transportation, and industrial sectors) efficiency or energy intensity; c) environmental (*e.g.*, resource-depletion, extraction, carbon-emission) taxes; d) and top-level nuclear-energy (*e.g.*, uranium resource, plant capital, operating, fuel-cycle) costs?
- Fuel Cycle: For a given nuclear energy growth scenario, as defined primarily by answers to the last question, what are: a) the time lines for required nuclear facility and technology developments; b) nuclear material inventory (form, quantity, region) impacts; c) and related economic, environmental, and proliferation risks for a range of fuel-cycle options (*e.g.*, once-through LWRs, plutonium recycle in thermal-spectrum reactors, advance fast-spectrum plutonium burners, breeder reactors)?
- E³ Connectivity: What are the top-level tradeoffs between: a) risks associated with nuclear energy (*e.g.*, proliferation risk); b) environmental impacts of extensive fossil-fuel use (*e.g.*, greenhouse warming); c) and nuclear-energy share fractions (*e.g.*, carbon taxes)?

While these questions pertain primarily to nuclear electric energy, non-electric applications must ultimately be included in explorations related to the first and third questions, particularly in assessing the degree to which nuclear energy can impact long-term environmental, resource, and cost barriers associated with fossil-fuel conversion and burning. After defining and comparing a “basis scenario” in Sec. II.C., key responses too the first “Growth” question are reported in Sec. III.A. The second set of key results address the second “Fuel-Cycle” question in Sec. III.B. The results of a top-level comparison between nuclear proliferation risks and the greenhouse-gas (GHG) mitigating

attributes of nuclear energy are given in Sec. III.C. Discussions of results, interim conclusion, and future work are given in Sec. IV.

II. APPROACH

This scenario-based study of a range of possible global nuclear energy futures conforms to a hierarchy of scenario attributes that are evaluated with a modification⁴ of an established global, multi-regional (13) long-term (~2100), E³ model.³ This section describes both the hierarchy of scenario attributes and the E³ model. The scenarios examined are referenced to a “basis scenario”, which is also reported in this section. The basis scenario should be considered a “point-of-departure” case that is used as a reference for subsequent variations. While not a dramatic departure from a moderately optimistic future, this basis scenario should not be considered in “most-probable” terms; its main purpose is to provide a reference with respect to scenario attribute variations of both upper and lower parts of the scenario-attribute hierarchy.

A. Scenario Hierarchy

1. Background

In presenting alternative images of directions in which the future *could* unfold (*i.e.*, scenarios are *not* predictions or forecasts), each scenario must be defined by a consistent and reproducible set of assumptions. These assumptions form the basis of key driving forces and inter-relationships for change. Scenarios of the kind considered here are generated using formal (mathematical, computer) models. These scenarios can be classified as both “descriptive” and/or “normative”.⁵ A “descriptive” scenario evolves *via* a rule-based model without significant geopolitical, policy/institutional, economic/market, or technology changes. A “normative” scenario allows for (often interactive) modifications of these respective areas. In the context of E³ scenario building, a “business-as-usual” (BAU) scenario generally falls into the “descriptive” class, whereas scenarios that are perturbed relative to the BAU case are infused with “normative” elements. In either case, the scripts that drive a given scenario are relatively “surprise-free”; deep global recessions, globally extended war, medical or food-shortage epidemics, heavy exogenous events (*e.g.*, large meteor impacts, extra-terrestrial invasions), and most strongly nonlinear and evolutionary interactions are not included in the scenario rulebase.

Relatively recent studies by the World Energy Council (WEC)⁶ and by a cooperative effort between the International Institute for Applied Systems Analysis (IIASA) and the WEC⁵ provide excellent examples of scenario characterization. The four WEC study scenarios were generated to illustrate four possible world futures and contain no BAU scenario *per se*; even the Reference or Base Case (Case B) adopted by the WEC study⁶ requires significant improvements (decreases) in historical values of (aggregated) energy intensity: $EI(\text{MJ}/\$) = PE/\text{GDP}$, where $PE(\text{EJ})$ is the annual primary energy demand and $\text{GDP}(\text{T\$})$ is the Gross Domestic (World) Product. Population growth is assumed to be the same for all WEC cases. Also, static *per-capita* energy consumption, and the poverty so implied, continues in some regions, in spite of major increases in world energy consumption. The large decreases in energy intensity, particularly for the WEC⁶ Ecologically Driven Case (Case C), infers massive programs of technology and capital transfers to the REF [Reforming (Eastern Europe and CIS)]⁵ and DEV (Developing) countries. The energy mix that results under all four WEC scenarios is largely based on fossil fuels, even with a moderately increasing contribution from nuclear energy to electricity generation [increasing from 5.5% of total primary-energy demand in 1990 to 5.7% (Case A), 5.9% (Case B), 6.1% (Case B₁), and 6.2% (Case C) in 2020]. Generally, coal would supplant any reduction in nuclear electric generation for reasons based on (driven by) economic, safety, waste, or proliferation concerns.

The follow-on WEC/IIASA study⁵ considered the three WEC cases,⁶ but: a) divided the “High Growth” Case A into three high-growth options; b) re-cast the WEC Base Case (Case B) to function more as a BAU or “Middle-Course” Case; and c) consider two distinctly different options for the “Ecologically Driven” Case (Case C). These scenario distinctions and defining characteristics are summarized in Table I and form the basis for the three nuclear energy variants adopted by the recent IAEA fuel-cycle and reactor strategy study.⁷ Comparisons between this IAEA study with results emerging from the Los Alamos Nuclear Vision Project^{4,8} have been reported;⁹ the present report represents the basis document for the Ref.-9. comparative study.

2. Scenario Attribute Hierarchy

The two examples of scenario creations cited above^{5,6} derived from studies that ostensibly are independent of position on a given approach to providing primary energy [*e.g.*, oil,

gas, solids (coal and biomass), nuclear, solar, and hydroelectric]. When used to examine possible futures from the viewpoint of a particular energy source, a scenario selection and focusing process often (naturally) occurs in order to emphasize specific roles and niches for that energy source. In the case of the recent IAEA examination of nuclear reactor and fuel-cycle strategies,⁷ the IAEA Working Group #2 (Global Energy Outlook) adopted three cases identified as: “High Variant” (HV, WEC/IIASA Case/Scenario A₃); “Medium Variant” (MV, WEC/IIASA Case/Scenario C₂); and “Low Variant” (LV, WEC/IIASA Case/ Scenario C₁), as described in Table I. This selection process is used primarily to examine a range of “nuclear-energy scenarios” and related implications that these scenarios may suggest for nuclear-energy concerns related to uranium resource, fuel-cycle facilities, nuclear-material inventories (location, quantities, and form), and spent-fuel waste. The economics that led to the particular nuclear-energy demand scenarios remains relatively frozen in the assumptions of the original studies. The decoupling that result when an investigation enters the problem far down into a hierarchy of interdependent scenario attributes risks distortions of final results through the loss of pertinent trade offs. A recasting of the procedure used to generate the scenarios definitions (attributes) embodied in the Ref. 5,6 studies into a hierarchal format gives more visibility to this potential problem, in addition to providing both a focus and an intercomparability to related studies. This hierarchy of scenario attributes is ordered in a way that places at the top those scenario rules or definitions that have a reduced likelihood for change, deviation, or connectivity with respect to rules or definitions residing at lower hierarchal rungs. Five hierarchical levels for scenario rule/definition-making are suggested and defined in Table II. Examples derived from the WEC⁶ and WEC/IIASA⁵ investigations are also listed for each of the proposed five levels.

In addressing specific questions related to future demand for nuclear energy and the impacts that specific technologies and policies have on that demand, it is important to understand where in the scenario definitional hierarchy described in Table II one enters the problem. Furthermore, important questions arise in connection with this scenario rule/definitional hierarchy. First and foremost is the extent to which this “reductionist” (Descartian) model can be used to project futures through model-based scenarios, as well as where in the hierarchy is the modeler allowed to enter. The connectivity or “fuzziness” between hierarchal levels presents another concern, particularly at the lower (working) levels. This concern exists, even at the higher levels [*e.g.*, the connectivity between

population growth and *per-capita* GNP(GDP)]. Lastly, issues of both technological and geopolitical dynamics and stability enter with respect to assumptions dealing with:

- regional differences in economic growth;
- limits (if any) to human technological ingenuity;
- metrics needed to assess the level of geopolitical “favorability” needed to assure rapid economic growth rates that form the basis of some scenarios (*e.g.*, the WEC/IIASA “High Growth” Case A, Table II);
- similar metrics used for the assessment of market “favorability”;
- rates of capital-stock turnover for a given energy-service (ES) sector (*e.g.*, residential/commercial, industrial, and transportation) needed to assure the assumed rates of improvements (decreases) in energy intensity, and related dependencies on time and region.

B. Global Economics/Energy/Environmental (E³) Model

1. Overview of ERB Model

The ERB (Edmonds, Reilly, Barns) model³ is based on a behavioral market equilibrium that internally balances energy production and usage. While simplified compared to the Linear-Programming (LP) or hybrid models, the ERB model was judged to target adequately the early needs of the present study, is available to the public, is adaptable to modification, and is generally transparent and well documented.³

The ERB model was developed nearly 25 years ago at the Oak Ridge Associated Universities Institute for Energy Analysis (IEA/ORAU) under contract to the DOE for the CO₂ Research Division and has been adapted to examine CO₂ emissions by several institutions, including EPA, MIT, EPRI, and GRI. Although an earlier version is available electronically through IEA/ORAU, the Battelle Pacific Northwest Laboratory (PNL)¹⁰ supports more recent versions. The recursive ERB model gives a “top-down” economists view of highly aggregated E³ interactions, compared to the “bottom-up” engineering/technologists view,^{11,12} and is comprised of four main parts: supply, demand,

energy balance and GHG emissions (a postprocessor). Supply and demand are determined for six primary energy categories: oil(conventional and nonconventional); gas(conventional and nonconventional); solids (coal and biomass); resource-constrained renewables (hydroelectric and geothermal); nuclear (fission, with fusion being included as a form of solar energy^{3,13}); and solar (excluding biomass, includes solar electric, wind, tidal, ocean thermal, fusion, and advance renewable energy; solar thermal is included as a form of energy conservation). The energy-balance module assures that supply equals demand in each global regions, with primarily electrical energy assumed not to be traded (*e.g.*, assumed to be generated and used within a given global region). Figure 1 gives the structure of the ERB model, as modified for the purposes of the present study (Sec. II.B.2. and Ref. 4). The energy and economic (market-clearing) balances indicated on Fig. 1 are performed for 13 global regions depicted schematically in Fig. 2 (increased from the nine used in the original ERB model³) and for nine 15-year time steps that start in the base year 1975 and moves out to 2095. Energy balance across regions is established by a set of rules³ for choosing the respect prices that are required for supply to equal demand in each energy-service group for each fuel. The specific test of convergence requires that the difference in regional sums of demand and supply for each of the three fossil primary fuels (oil, gas, and solids) be less than a specified value.

The ERB model originally tracked only CO₂ emission, with CH₄ and N₂O being added later. Appropriate carbon coefficients (GtonneC/EJ) are applied at points in the energy flow where carbon is released to the atmosphere; carbon flows at points where oxidation does not occur are also taken into account. Unlike the nuclear model, evaluation of GHGs is made after the main computational sequence is completed and economic equilibrium is achieved at a given time interval. While the GHG emissions are computed after global economic equilibrium and energy balance is achieved for each to the nine 15-year time steps, the nuclear component, as modified for use by the present study,^{4,15} must be evaluated integrally with the iterative approach to economic and energy equilibrium that forms the heart of the ERB model. In some respects, the nuclear-energy part of the modified “top-down” ERB model has “bottom-up” characteristics.

The demand for energy is determined separately for each of the above-mentioned six primary fuels for each of 13 global regions and for each of nine times. Five exogenous inputs (including taxes and tariffs) determine the local energy demand. The base

(exogenous) GNP (labor-force productivity \times population) is used as an indicator of both (regional) economic activity and as an index of regional income. The base GNP is modified through price elasticities to model energy-economy interactions, with $\text{GNP} \propto \text{price}$ for energy-rich regions and $\text{GNP} \propto 1/\text{price}$ for global regions that must import energy. Non-price induced improvements in end-use energy efficiency are expressed in the original ERB model as a time-dependent index of energy productivity that is independent of energy prices and real income. This parameter is similar to the Autonomous Energy Efficiency Improvement (AEEI) used in other more elaborate (inter-temporal) “top-down” models.¹⁴ An option has been incorporated into the ERB model that exogenously forces a specified (non-price-induced) decrease in energy intensity [*e.g.*, ES/GNP] for each global region. Either approach allows scenarios to be examined that span the range from continued improvement to technological stagnation, irrespective of world energy prices and real income. World energy prices for all fossil fuels are established through energy balance, with regional (fossil) fuel prices being determined by local taxes, tariffs, and transport charges. Interregional trade, however, does not occur for solar, nuclear, or hydroelectric power.

The demand for energy services (*e.g.*, residential/commercial, industrial, and transportation) for each of thirteen (Fig. 2) global regions is determined in ERB by: a) the cost of providing these services; b) the level of income (\propto GNP); and c) the regional population. Energy services are fueled by an array of four secondary fuels (liquids, gases, solids, and electricity). The mix of these secondary fuels used to provide a given energy service is determined by a cost-based market-share algorithm,³ as is the demand for fuels used to produce electricity and the share of oil and gas transformed from coal and biomass. The four secondary energy sources are generated from the six primary fuels [*e.g.*, oil, gas, solids (coal and biomass), nuclear, hydro, and solar], with nuclear, hydro, and solar providing only electrical secondary energy; non-electric solar is treated in ERB as a conservation technology to reduce the demand for the three marketed fuels (*e.g.*, oil, gas, and solids). The tracking of PE \rightarrow SE \rightarrow ES transformations is modeled using Leontief-type formulation.¹⁶ A second important function of the energy demand module is to maintain a set of energy flow accounts. As is elaborated in Ref. 15, the nuclear energy module added to ERB, for purposes of the present study, replaces the Leontief equation for

nuclear, which originally³ was based only on a scaled cost of uranium extraction (treated in ERB in this regard like a fossil fuel), with one based on capital, operating and maintenance (O&M), fuel-cycle, and decontamination and decommissioning (D&D) costs. These costs are then fed back to the ERB demand module to determine the respective market-share fraction for nuclear energy as a function of time and region. As noted above, this modification lends a “bottom-up” character to the nuclear energy part of the ERB computation.

The energy supply module estimates: a) the supplies for all regions and fossil fuels forms the basis for the (iterating) world prices; b) the cumulative usage; c) and the cost of recovery (including environmental costs) at a given resource grade. Energy supplies are disaggregated into two categories: a) renewable (hydroelectric, solar, biomass, and nuclear breeder); and b) non-renewable (conventional and unconventional oil, natural gas, coal, and non-breeding nuclear). The use of a graded resource base (for fossil and nuclear) allows the importance of the fuel resource base to be examined. Fuels like oil shale (and possibly fusion) can be considered “backstop” technologies, in that they present a small resource at a low cost, but are transformed into a large resource at high costs. A given resource is active and able to contribute to the demand only if the primary-energy price delivered to the energy supply module exceeds the production cost, and if the resource has not been exhausted. The uranium resource model originally used in ERB,³ for purposes of the present study, has been replaced with that suggested in Ref. 17, as interpreted in Ref. 18; this extended uranium resource model is elaborated in the following section.

2. Additions to ERB Model

The main modifications made to the ERB model for the purposes of the present study are the addition of an improved (higher fidelity) nuclear energy model and the increase in the number of global regions from nine to thirteen. Figure 2 gives a schematic view to the 13-region model presently being used to reflect contemporary geopolitical conditions; the main regional shifts, compared to the original nine-region ERB model,³ include: a) moving Canada out of the OECD-Europe grouping; b) separating Eastern Europe from the FSU; c) dividing Africa into northern and southern regions; d) separating India from of the Southeast Asian region; and e) moving South Korea from the CHINA⁺ region to the OECD-Pacific region. The size of each region on Fig. 2 reflects the respective land mass. In converting from a nine-region to a thirteen- region model, the many demographic,

productivity, resource, and macroeconomic data originally assembled as part of the ERB model³ where scaled without update to match the new regional land masses and populations. The population projections used in the original ERB model were also increased somewhat (~10%) to conform with more recent U.N. projects used by the WEC⁶ and the WEC/IIASA⁵ studies cited above, with the latter providing a basis for even more recent IAEA nuclear fuel-cycle and reactor strategy studies.⁷ Lastly, as subsequently discussed (Sec. III.C.), an analytic greenhouse-warming model was added to allow the CO₂ emission rates reported by the original ERB model to be interpreted in terms of actual GHC atmospheric carbon-dioxide accumulations and attendant average global temperature rise.

The nuclear model developed and operated “under” the ERB model performs three primary functions: a) determines a “top-level” cost estimate in terms of a cost of electricity that is reformed into the Leontief coefficients used to determine costs and market shares, as described above; b) tracks the flow of key nuclear materials throughout the nuclear fuel cycle [*e.g.*, natural uranium, low-enriched uranium, plutonium, and spent fuel] for use in subsequent nuclear-waste and proliferation-risk assessments; and c) performs a multi-attribute utility (MAU) analysis of proliferation risk associated with the civilian nuclear fuel cycle. The costing and material-stream flows are described in Ref. 15, whereas the details of the MAU-based proliferation-risk assessment are elaborated in Ref. 19. Preliminary results of this combined, regionally resolved model are given in Ref. 4, with Sec. III.C. giving a top-level comparison of (increased) proliferation risk with (reduced) global warming attendant to increased use of nuclear energy.

a. Nuclear Energy Model

Before costs, material flows/inventories, or proliferation risks can be estimated, characteristics of the fuel cycle must be specified. The nuclear model reported in Ref. 15 and evaluated herein is based only on the uranium/plutonium cycle, as utilized in each global region at each time interval by an economically determined ratio of LWR and LMR systems. The LWR in a given global region operates along an exogenously enforced MOX recycle trajectory of nominal MOX core fraction, f_{MOX} , *versus* time that exponentially transcends from an initial MOX core fraction to a final MOX core fraction with a specified time constant. These MOX recycle trajectories are specified as a function of region. The LMR system, if economics and technology diffusion time constraints allow, is introduced

with a preassigned breeding ratio. In the present version of the model, plutonium is assumed to flow freely between global regions, where deficits in some regions are assumed to be corrected by flows from regions with excess plutonium, as long as the global plutonium in the form required remains positive. Detailed plutonium balance and control remains for future work²⁰ and more detailed nuclear and costing models. Specifically, inter-regional nuclear materials flow constraints, breeding ratios driven by inventory and need requirements, and/or cost- and/or sanction-based selections of MOX recycle parameters are important areas of future work. Lastly, as described in Appendix A, the economic implications of the use of fast-spectrum neutrons to burn actinides in support of LWRs is also considered (Sec. III.B.4.), with both LMRs and accelerator-based systems being examined; generically, these LWR support systems are called Fast Spectrum Burners (FSBs), and, while not necessarily economic as a stand-alone commercial power station, generate and sell electricity to the grid to help defray expected high capital and O&M costs.

b. Costing

Costing of nuclear energy (both LWRs and LMRs) is based on a “top-level”, highly aggregated algorithm¹⁵ that accounts for annual capital charges, annual plant O&M charges, and annual charges related to a nuclear fuel cycle. The component of the cost of electricity, COE(mill/kWh), related to the plant capital costs is expressed in terms of a fixed charge rate, and a unit total cost, UTC(\$/kWh). The annual O&M charges are expressed as a fraction of the total capital cost of the power plant. Differences in COE for LWR and for LMR are reflected primarily in differences in the respective UTC values and that part of the COE related to the fuel cycle *per se*, as elaborated in Ref. 15. For each global region and time interval, the COE-minimizing fraction of nuclear energy delivered by LWRs (at a given value of MOX recycle fraction, f_{MOX}) is determined, and an LWR-LMR composite nuclear energy price is returned to the ERB demand module for evaluation of the respective market-share fraction for that particular region and (iterated) market-clearing world fossil-fuel price. Before this nuclear energy price is returned for a given LWR fraction, f_{LWR} , however, a simplified technology diffusion model²¹⁻²³ is used to disallow unrealistically large rates of LMR market penetration based solely on economic considerations. Since the global plutonium flow model is presently in a rudimentary form with respect to regional and (reactor) system allocation rules, particularly with respect to the introduction of (high-inventory) LMR. Since most of the nuclear energy demand scenarios considered in this study do not seriously impact known resources (KR)¹⁷ of uranium on

the time scale being considered (~2100), the results presented herein do not allow the economic introduction of the LMR for the UTC_{LMR}/UTC_{LWR} ratios used (≥ 1.5); the LMR as an advanced burner of plutonium in support of an LWR-based nuclear economy, however, is considered (Sec. III.B.4.) as are alterations in scenario attributes that could lead to the introduction of commercial LMR power plants (Sec. III.B.3.).

c. Material Flows

The nuclear fuel cycle can be described²⁴⁻²⁶ in terms of the following sequence of processes, with the attached designators being used in subsequent diagrams and analyses: Mining and Milling of uranium (MM) → Conversion of uranium oxide to the volatile fluoride (CV) → Isotopic Enrichment (ER) → Fuel Fabrication (FF) → fissioning in Reactor (R, REA) → Spent Fuel Cooling and storage (SF) → Reprocessing (RP, REP) → Repository (RS) directly as SF or as separated Fission Products (FP) and Minor Actinides (MA). Figure 3 illustrates a generic fuel cycle that has been constructed from a series of building blocks and represents the above-described processes. The simplified species-resolved mass balances described in Ref. 25 based on the kind of input-output analysis depicted on the bottom of Fig. 3 is used to model material flows in this part of the nuclear model inserted under the ERB model. As described in Ref. 25, unit and operating costs are applied to each of the processes depicted in Fig. 3, from which a fuel-cycle cost for the entire system can be determine; Ref. 15 describes an aggregated version of this method that is used to estimate that part of the COE associated with the fuel cycle. Plutonium flows and accumulations are monitored for each region as a function of time, with reactor plutonium, separated plutonium in reprocessing and fuel fabrication, and accumulated in spent fuel being the four major categories being tracked. The second frame of Fig. 3 elaborates on these (regional) LMR/FSB plutonium flows, with the following inventory designators being used: REA = reactor inventories; ACC = LWR-recyclable (less than N cycles) spent-fuel plutonium; REC = LWR-nonrecyclable (greater than N recycles in LWRs, usable only in FSBs) spent-fuel plutonium; SEP = separated plutonium in reprocessing (REP) and fuel fabrication (FF), with $SEP = REP + FF$. Figure 3B also indicates the regional and temporal values of the MOX core volume fraction and the relevant plutonium concentrations in each region required to approximate a material balance.^{27,28} Sections III.A. and III.B. of Appendix A elaborate on a continuum version of the plutonium balance used in the recursive relationships that advance the ERB computations in time. As is indicated in

Sec. III.B.2., a number of the cycle-time-averaged neutronic parameter assumed to evaluate this model have impact on the computed material flows/inventories. (Figs. 58 and 59). The plutonium inventories indicated on Fig. 3B are used as part of the proliferation-risk assessment associated with each global region as a function of time,^{4,19} for a specified set of exogenous nuclear and ERB parameters.

d. Proliferation Risk

Two independent applications of MAU theory²⁹⁻³¹ to the assessment of proliferation risk from the civilian nuclear fuel cycle have been reported.³²⁻³⁵ References 32 and 33 examined the value or utility to a potential proliferator of obtaining nuclear-explosive materials from specific points within the nuclear fuel cycle depicted on Fig. 3. While treating the nuclear fuel cycle in more aggregated form, the MAU-base studies reported in Refs. 34 and 35 treated both the political-environment (ENV) and nuclear-weapons-aspiration (NWA) levels that set the stage for a national decision on proliferation, as well as treating in more detail the method by which specific proliferation criteria or attributes are described and evaluated. The MAU methodology that results from the joining of the Refs. 32 and 33 and Refs. 34 and 35 approaches to defining and evaluating proliferation-risk metrics for application to the above-described nuclear model is elaborated in Ref. 19.

In evaluating the proliferation-risk model, the ENV and NWA parameters are specified for each global region as a function of time. The ENV and NWA parameters are used, along with attribute or criteria basis (normalization) parameters, to establish the shape of utility and subutility functions posited to describe each of five (proliferator-based) criteria:³⁴ Development Time (DT); Warning Period (WP); Inherent Technical Difficulty associated with Material Processing (ITD_{MP}); Inherent Technical Difficulty associated with Nuclear-Weapons fabrication (ITD_{NW}); and Cost (CST). Once ENV, NWA, and the state of sanctions (SANC) are specified for a given global region and time, and using the $f_{MOX}-f_{LWR}$ mix as a proxy for describing the k^{th} fuel cycle, the above-described $j = 5$ attributes are applied to each of $i = 4$ (HEU, SPU, MOX, and SFT) nuclear material streams. The fraction of all nuclear energy generation from LWRs is $f_{LWR} = 1 - f_{LMR}$. Plutonium undergoing fissioning in reactors, RPU, is not included at this point in the proliferation-risk assessment, under the assumption the reactor plutonium that is actively undergoing fission is “safe and secure”.

Using weights generated from pairwise comparison techniques^{25,32,36} weighted utilities for each material stream are generated as a function of time for each global region. These material-stream utilities are then time-weighted (discounted) and summed to give a Proliferation-Risk Index,^{25,32} PRI_{ilm} , for stream i , region l , and time m , for the k^{th} fuel cycle. This PRI value represents a weighted average of the particular LWR/LMR mix, as determined by the cost-minimized, market-penetration-rate-constrained value of f_{LWR} . The material stream with the maximum PRI is selected as the index to be monitored, $PRI_{lm} = \text{MAX}\{PRI_{ilm}\}$. Lastly, pairwise comparison techniques³⁶ are again use to weigh the importance of region l compared to a reference region l' in terms of importance of the respective value PRI_{lm} and used to generate a global proliferation-risk index, PRI_m , relative to a reference region at time m . It is this latter, highly aggregated metric that is used in subsequent comparisons (Sec. III.C.), with the reference (perspective) region being taken as USA.

C. Basis Scenario

The primary function of the “basis scenario” is to provide a point-of-departure to which changes/shifts from top-level or lower-level hierarchal variations can be referenced. While the utility of the basis scenario is best served if it reflects a “most probable future”, the uncertainties associated with identifying a most probable future, particularly for the multi-generational time scale being considered, are too great to identify the basis scenario with one that would most likely happen. Huge uncertainties in regional demographics and wealth generation couple with long-term shifts in cultural attributes and value systems to drive these uncertainties. While population projections *per se* have proven to be robust,² the “fine structure” that defines the demographics of that growth is largely unresolvable on a multi-generational time scale (*e.g.*, evolving aging distribution, impacts of majority needs on the political systems and the policies they generate, shifts from industrial economies to service economies, societal needs and problems related to age and gender shifts in the work force, evolving differences in priorities that drive “younger” societies *versus* “older” societies, shifts in worker productivities, *etc.*)².

Major forces behind total primary energy demand are: a) population growth; b) workforce makeup (fraction of population, age) and productivity as it drives GNP growth; c) and the

efficiency with which primary energy is converted to secondary energy and ultimately to provide energy services. These top-level scenario attributes are inter-related in a way that is not captured by most long-term E³ models. While these top-level scenario attributes strongly impact energy demand, that part of the demand potentially served by nuclear energy is determined in competition with alternative sources through economic, environmental, and policy choices made further down the hierarchy described in Sec. II.A. and Table II.

1. Description of Basis Scenario

The top-level scenario attributes used to define the basis scenario derive with some modification from the data base used to define a “business-as-usual” (BAU) case for the ERB model, as that model was applied to understanding the economics of carbon-dioxide emission control.^{3,37-39} As summarized in Table II, the basis scenario is defined by four top-level attributes (population, GNP, energy intensity, and energy resource), a mid-level attribute (taxes and tariffs), and lower level attributes related primarily to internal drivers for nuclear energy (resource, capital, operating, and fuel-cycle costs). The population data base originally used in ERB was shifted upward (~10%) in this study to reflect recent U.N. projections.^{5,6} The GNP projections used in ERB begin with base-year (1975) values, and then scale subsequent years according to population growths, workforce productivity increases and energy service prices. The population growth was modified as noted above, and the exogenously determined productivity increases were left unaltered from the data base originally used in ERB. Energy intensity is specified indirectly in ERB through improvements in efficiencies that relate energy service (ES) demands to the amounts of secondary energy (SE) needed to meet these demands; again, the ~1%/yr decrease in the ratio ES/SE used in ERB for most of the regions is also used in this study to define the basis scenario. The relationship between cost and grade for fossil fuels used in ERB was also used without modification in this study, but the uranium resource cost *versus* grade relationship given in Ref. 17, however, replaces that originally used in ERB. Taxes and tariffs as reported in the ERB model remain unchanged, but, as discussed in Sec. II.B.2, the model for determining nuclear energy costs for use by ERB to estimate market-share fractions is that reported in Ref. 19. As is indicated on the Table-III summary of upper-hierarchical scenario attribute variations, the main taxation variation was that applied at the fossil-fuel consumption level (*versus* the level of resource severance) to stem carbon emissions; for the basis scenario, this carbon tax is zero. Table IV lists key nuclear energy

parameters used to generate Leontief coefficients for that part of the ERB model that determines market-share fractions for the basis scenario and the subsequent Table-III scenario variations.

Figure 4 gives the exogenous population growth used to drive the ERB model for the basis scenario conditions described above. To simplify data displays, the 13 regions have been aggregated into three macro-regions in accordance to the procedure adopted in the Ref.-5 study: industrialized countries, OECD = USA + CAN + OECD-E + OECD-P; reforming economies, REF = EEU + FSU; and developing countries, DEV = CHINA + ME + NAFR + SAFR + LA + IND + SEA (Fig. 2). The basis scenario characteristics that result from this population growth are presented with little additional comment, although comparisons with the Ref.-5 and 7 results are given in Sec. II.C.2. Figures 5-16 give the basis scenario E^3 parameters and respective growth rates that result: GNP (Fig. 5); primary energy intensity (Fig. 6); global primary energy mix (Fig. 7); total primary energy, along with a comparison with scenarios used in Ref.-7 (Fig. 8); a summary of global growth rates of population, GNP, total primary energy, and primary energy intensity (Fig. 9); nuclear energy growth at both the aggregated and 13-region levels, along with a comparison with the Ref.-7 scenarios (Fig. 10); *per-capita* primary energy demand (Fig. 11) and *per-capita* GNP (Fig. 12); a correlation between primary energy intensity and *per-capita* GNP for three aggregated regions (Fig. 13A), as well as for each of the 13 regions (Fig. 13B); electricity fractions (Fig. 14); evolution of global economic distributions (Fig. 15); and a summary of global and regional CO₂ emissions (carbon mass, Fig. 16). A subset of these basis scenario results is used for a more in-depth comparison with the Ref.-5,7 results in the following subsection.

2. Comparisons with Other Studies

Although no special effort was made to “force” the basis scenario reported herein to track recent, more detail studies,^{5,6} a comparison of key higher-level scenario attributes with other work is useful. Comparisons of total primary energy and total nuclear energy projections with the WEC results^{5,6} *vis à vis* the Ref.-7 IAEA study have been already been reported in Figs. 8 and 10, respectively. Both studies use U.N. projections for population growth, albeit some regional differences exist because of the analytic algorithm introduced into the ERB model to facilitate (eventual) parametric investigations of GNP-population feedback effects. A comparison of the rates of GNP growth (specified in the WEC studies,

computed in ERB) is given in Fig. 17 at both total (world) and aggregated (macro-regional) levels. A similar comparison of total primary energy demand growth and the rates of energy-intensity decrease are given in Figs. 18 and 19, respectively. Lastly, Fig. 20 compares the global conversion of primary energy to secondary energy, in the case of ERB results, and “final energy”, in the case of the WEC/IIASA results.⁵ For the ERB model the improvement in use of secondary energy to provide given energy services is of the order $\epsilon_{jk} \sim 0.01$ 1/yr for all but the first two time periods and for all regions (k = end-use energy service, j = secondary energy fuel); the impact of linearly decreasing $\epsilon_k \equiv \epsilon_{jk}$ from 0.01 in 2005 to zero in 2095 is also shown in Fig. 20.

Generally, while differences exist between the recursive, “top-down” ERB model and the more detailed (*e.g.*, inter-temporal, combined top-down/bottom-up) models⁴⁰ used in the WEC/IIASA studies,⁵ these differences are not large. Furthermore, fine-tuning of exogenous input to the ERB model can bring better “agreement”, although the utility of this kind of exercise is questionable - both models are limited by a common uncertainty in attempting to project trends onto multi-generational time scales. For the purposes of the present study, the benchmarking results reported herein yield adequate comparisons. The results presented in the following section are based on departures from the basis scenario that are associated with: a) external drivers (variations in upper-level parts of the scenario attribute hierarchy); and b) internal drivers (variations in attributes that reside at the lower rungs of the hierarchy).

III. RESULTS

Demand for nuclear (electric) energy in the basis scenario (Sec. II.C.) is determined primarily by the upper-level hierarchal attributes (Sec. II.A., Table II). Table III lists in descending hierarchal order key scenario attributes identified for the nuclear energy demand variations of interest to this study. The upper-level attributes define “external drivers” that ultimately determine the nuclear-energy demand for the basis scenario. Departures from the basis-scenario nuclear-energy demand are caused by changes in these upper-level attributes. The following subsection reports the sensitivities of demand to these upper-level attributes. A range of “departure scenarios” result from variations in these external drivers. The impacts of drivers that are internal to nuclear energy (*i.e.*, scenario attributes that are lower in the scenario-attribute hierarchy) on the choice of optimal nuclear fuel-cycle strategies and the relationship of these choices to the external drivers are examined for both the basis scenario and for a range of departure scenarios. The impacts of drivers that are internal to nuclear energy (*e.g.*, once-through *versus* plutonium recycle in thermal-spectrum reactors, advanced reactors and plutonium burning, fuel-cycle dependent inventories of nuclear materials and related cost, environmental, and proliferation impacts, *etc.*) are reported in the subsequent Secs. III.B. and III.C.

A. Top-Level Hierarchal Variations: Impacts of External Drivers

The five external drivers (population, GNP, energy intensity, and taxes) are combined with the top-level economic parameters [capital and (uranium) resource costs] in Table III to define the main “external drivers” that are varied to explore possible nuclear energy demand scenarios. For the purposes of this study, which emphasizes intrinsic fuel-cycle issues in identifying the main “internal drivers”, the capital and resource costs of nuclear energy are characterized as external drivers. All upper-hierarchal variations are single-point perturbations about the basis scenario, as defined in Tables III and IV and elaborated in Sec. II.C.; this basis scenario corresponds to a once-through LWR fuel cycle, with variations thereon being reported as part of the internally driven scenarios reported in Sec. III.B. Nuclear material flows and inventories for the basis scenario are reported in Sec. III.B.1.

1. Population

The basis scenario and most of the related departure scenarios follow the U.N. population project that projects nearly 12 billion persons on earth by the year 2100. As noted in Sec. II.B.2., matching of the population growth originally used in the ERB model³ with the U.N. projections required an overall ~10% increase in world population. This matching was accomplished by assuming a linear growth rate between 15-year ERB time intervals, matching that linear growth with population growth over the first ERB time interval (1975-1990), and then forcing an exponential decrease in the linear growth for subsequent time periods such that each of the thirteen regions achieved a specified asymptotic population relative to the population in 1990. The regional asymptotic population level and the associated decay rate of the inter-temporal linear growth are two variables that can be used conveniently to specify an endstate (2100) population, while providing a means to feedback key regional economic parameters (*e.g.*, GNP) on the population growth. Adjusting this asymptotic population in a way that gives $\sim\pm 17\%$ variations in world populations in 2100 relative to the U.N. projections results in the shifts in primary- and nuclear-energy demands given in Figs. 21 and 22, respectively. The respective demand curves for the high, medium, and low (nuclear energy) variants used in the Ref.-7 study are also displayed. These single-point population variation were made without adjustments to the base (1975) GNP used in the ERB model.

2. Workforce Productivity (GNP)

As is indicated in Sec. II.B.1., the ERB model modifies a base regional GNP in time for: a) population increase; b) an aggregated price for energy services using a region-dependent price elasticity; and c) an increase in workforce productivity, which is expressed as a region- and time-dependent annual productivity enhancement rate. Given the base (1975) GNP and population growth as fixed input, the impact of GNP variations was examined by means of the latter productivity factor. Figure 23 gives the impact of region-independent increase and decrease in productivity by $\pm 20\%$ for both the world and for the three aggregated macro-regions (OECD, DEV, and REF). The time at which GNPs for OECD and DEV macro-regions are equal is pushed into the future at a rate of ~ 0.25 yr per percent (region-independent) decrease in workforce productivity; this productivity reflects evolving workforce percentage (of total population), age distribution, and skill levels, all of which are expected to show a strong region dependence. The impacts of these GNP variations

vis à vis the highly aggregated workforce productivity enhancement rate on primary- and nuclear-energy demand is shown on Figs. 24 and 25, respectively. Comparisons with the Ref.-7 high, medium, and low (nuclear-energy) variants are also given. The impact of GNP on energy demand, for the income elasticities used in the ERB model, are much greater than that for single-point (*e.g.*, base GNP values not adjusted) population variations (Figs. 21 and 22) alone.

3. Energy Intensity (End-Use Efficiency)

The ERB model varies (primary- or secondary-energy) energy intensity indirectly through a technology improvement rate that relates an ever decreasing secondary-energy (SE) requirement needed to satisfy a given energy service (ES) demand. The basis scenario uses a regionally depended technology improvement rate of $\epsilon_k = 0.01$ 1/yr after 1990, which is unchanged from that in the original ERB data base.³ As noted in Sec. II.B.2., this technology improvement rate, is associated with non-price efficiency enhancements and is related to the Autonomous Energy Efficiency Improvement (AEEI) of Ref. 14. The resulting ratio of second energy to primary energy for the basis scenario was compared to the WEC/IIASA results⁵ in Sec. II.C.2. on Fig. 20. The variation and impact of this region- and time-dependent technology improvement rate are elaborated on Fig. 26. Generally, the decrease in the PE \rightarrow SE transformation/conversion efficiency as time unfolds is a result of regional populations (some more than others) demanding higher forms of energy (*i.e.*, liquids and electricity) to provide the energy service demands of a growing population that has more wealth. The *per-capita* GNP increase was shown in Fig. 12, albeit, the *per-capita* GNP is far from achieving full equipartition on a global basis, as is indicated on Fig. 15. Serious problems are associated with the use of *per-capita* GNP as an index of human welfare, however.⁴¹

The impacts of increases and decreases of the technology improvement rate on the rate of energy-intensity decrease is depicted on Fig. 27, with technology improvement rates much below $\sim 0.1\%/yr$ actually reversing the desired decrease in global energy intensity. Lastly, the impacts of a range of technology improvement rates on both primary- and nuclear-energy demand are shown in comparison with the Ref.-7 demand scenarios on Figs. 28 and 29, respectively. A technology improvement rate as high as $\sim 1.5\text{-}2.0\%/yr$ closely track the “Ecologically Driven” Low-Variant scenario of Ref. 7, whereas the technology

improvement rate must fall to ~0.5%/yr (or linearly decreased from 1.0%/yr to zero over the period 2005 to 2095) to reproduce the “gluttonous” High-Variant case of Ref. 7.

4. Carbon Tax

Increasing population, increasing GNP, or decreasing technology improvement rates are not the only means to increase the demand for nuclear energy. In fact, these upper-hierarchy (external) drivers have the obvious disadvantage of riding on a wave of increase energy use in general, and this increased usage has implications for resource depletion and environmental degradation. The imposition of a carbon tax has the effect of increasing the cost of fossil fuels (particularly coal), decreasing total energy use and (somewhat) GNP, while increasing the market share for reduced- or zero-carbon energy sources. The impact of applying a strong carbon tax rate (40 \$/tonneC/15yr) on the global energy mix is shown in Fig. 30; the counterpart (energy-mix) information for the basis scenario is given in Fig. 7. Imposition of these (increasing) carbon taxes begins in 2005. The impact of carbon taxes on primary- and nuclear-energy demand, along with the Ref-7 high-, medium- and low-variant scenarios, are depicted on Figs. 31 and 32, respectively. Lastly, the impacts of the two (20 and 40 \$/tonneC/15yr) carbon tax rates on global emission of carbon (*vis à vis* carbon dioxide only) into the atmosphere is shown on Fig. 33. The decrease in the carbon intensity (carbon emission per unity of total primary energy) shown in Fig. 33 reflects the increase use of nuclear and solar energies (and to a lesser extent hydroelectric), and the significant decrease in the use of carbon-intensive coal. For these and the basis scenarios, biomass is priced high and does not become a major contributor to the primary energy demand.

Although the ERB model can be used to assess economic impacts and trade offs of a range to “top-down” CO₂ mitigation schemes, the model was limited to projecting climatic impacts base solely on emission rates. Preliminary work using the ERB model is underway to implement CO₂ accumulation and atmospheric temperature-rise models^{12,42} to assess better the relative costs and risks associated with greenhouse warming *versus* increased use of nuclear energy; preliminary results in this regard are reported in Sec. III.C., which elaborate Figs. 30-33 for a $f_{\text{MOX}}^f = 0.3$ LWR scenario.

5. Nuclear Economics

Although the details of nuclear energy cost logically should be treated as an “internal driver”, in the context of the discussion given in Sec. II.A.2., and for the purposes of this study and the focus given to nuclear fuel-cycle issues, the capital and resource costs associated with nuclear energy are included here as a “borderline external driver”.

a. Capital Cost

For the uranium resource model used^{17,18} and the unit costs associated with the once-through LWR fuel cycle (OT/LWR) adopted for the basis scenario (Table IV), the capital costs assumed for nuclear energy is the main determinant of COE for nuclear power and the market share returned by the ERB model. The capital cost is embodied in a single variable - the unit total cost, UTC(\$/We). The basis scenario adjusted UTC(\$/We) for the first two time steps (1975 and 1990) for each region so that ERB returned a nuclear energy generation for each region that approximated historical values; these UTC(\$/We) values typically are in the range 1.5-2.0 \$/We. The basis case then increased UTC over the period 2005-2095 to achieve an asymptote of 2.4 \$/We. The impacts of increasing and decreasing this asymptote to 3.0 and 2.0 \$/We, respectively, are shown on Fig. 34. All regions were treated equally for times greater than 2005. The comparison with the Ref.-7 high-, medium-, and low-variant cases given on Fig. 34 indicates that the range of this UTC variation is sufficient to cover the scenarios suggested in Ref. 7. The impact of these UTC variations on atmospheric carbon emissions is illustrated on Fig. 35. Comparing these results with those of the previous section on carbon taxes (Fig. 33) indicates that while carbon taxes creates a favorable environment for nuclear energy growth with reductions in GHG emissions, the cost-driven increase or decrease in nuclear energy demand, as indicated by the forced market equilibrium model of ERB, alone has little impact on GHG emissions.

b. Uranium Resource

The relationship between uranium resource grade, resource amount, and cost,¹⁷ as summarized in Ref. 18, is depicted in Fig. 36A. Aggregating into the Conventional Resource (CR), Known Resource (KR), and Total Resource (TR) categories, as defined in the caption to Fig. 36A, Fig. 36B gives a range of unit cost scaling that results. The basis scenario assumes a relationship between uranium resource depletion and mined/milled

uranium ore costs under the assumption that the KR case describes reality. If uranium resources are limited to the CR category, a higher unit cost of mined/milled (MM) uranium ore results, whereas lower costs result if Total Resources (TR) are used. For either case, the weight fraction of ^{235}U in tailings, x_t , is determined by the minimum (optimum) cost conditions^{24,25} for the relative values of mined/milled uranium unit cost, $UC_{\text{MM}}(\$/\text{kgU})$, as given in Fig. 36B for the respective uranium resource model (*e.g.*, CR, KR, or TR) and the unit cost of enrichment, $UC_{\text{SW}}(\$/\text{kgSWU})$, given in Table IV. While the time line of this study should permit the development and introduction of technologies that reduce $UC_{\text{SW}}(\$/\text{kgSWU})$, such reductions are not included in the present results. As is indicated on Table IV and Fig. 36B, UC_{MM} is given by the expression $U_{\text{MM}} = U_1 M_{\text{U}}^v$, where M_{U} is the accumulated (global) use of uranium, and the constants U_1 and v are dependent on the uranium resource assumption (*e.g.*, CR, KR, or TR). A minimum price of $UC_{\text{MM}}^0 = 100 \text{ } \$/\text{kgU}$ is enforced, however, for all resource categories, and the optimum-cost tailings fraction, x_t , is used in all cases.

The dependence of M_{U} , UC_{MM} , and x_t on time and uranium resource assumption (again, KR describes the basis scenario) is given in Fig. 37. For both KR and TR uranium resource assumptions, uranium costs remain at the threshold price for the basis scenario nuclear-energy demand, although departure for the threshold price in the last time step for the KR case is indicated. The conservative CR case, however, shows an increase in uranium prices after the year 2050 for the basis scenario nuclear-energy demand, with these increased uranium prices resulting in a decreased nuclear-energy demand and reduced uranium consumption. This slightly reduced uranium consumption and nuclear-energy demand are shown on Figs. 37 and 38. These decreases are small and occur only after 2070, which is outside the timeframe considered by the Ref.-7 study.

Earlier studies of this kind using the ERB model⁴ were based on a resource depletion model²⁵ that is even more conservative than the CR case depicted on Fig. 36B. Higher uranium prices resulted in higher overall fuel cycle costs earlier than those indicated in Fig. 37.

The introduction of a carbon tax (Sec. III.A.4.) and the resulting increase in nuclear energy demand also increases the rate of uranium resource depletion and the unit cost of uranium

fuel; the impact of a 40 \$/tonne/15yr carbon tax rate (Sec. III.A.4.) on uranium depletion and the unit costs that result are also included on Fig. 37. As will be shown in Sec. III.B.3. introduction of a CO₂-mitigating carbon tax increases the market share for nuclear energy (Fig. 30 *versus* Fig. 7), depletes a given uranium resource, and, under some circumstance, accelerates the economic introduction of the breeder reactor.

6. Composite Impacts of External Drivers

The results of these upper-hierarchical variations indicate that the demand for nuclear power can be influenced significantly by a number of global variables that are far removed from nuclear energy *per se*. The impacts of these “external drivers” on the demand for nuclear power are shown in (selected) composite on Fig. 39, which also includes the high-medium- and low-variants considered in Ref. 7. Whether the nuclear energy demand scenario is driven by GNP (workforce productivity), energy intensity (demand-side driver through energy-service technology improvements), carbon taxes (supply-side driver), or top-level nuclear economic considerations (*e.g.*, UTC, supply-side driver), the impacts on parts of the global environment that fall outside of areas related to nuclear materials and fuel cycles *per se* can be important. For example, Fig. 40 illustrates the range of atmospheric carbon emissions for some of the externally driven departure scenarios being considered. For reasons of consistency of impact and assumption, the high and low nuclear energy demand variants relative to the basis scenario are generated from assumptions of low and high rates of SE → PE transformation technology improvements, ϵ_k (1/yr). Figure 41 gives the nuclear energy demand for the variants that result, as well as comparisons with related variants reported in Ref. 7. The low-demand/high- ϵ_k variant is equivalent to the “Ecologically Driven” Case C of Ref. 5 (Table II), whereas the high-demand/low- ϵ_k variant given on Fig. 41 is similar to the “High-Growth” Case A.

B. Lower-Level Hierarchical Variations: Impacts of Internal Drivers

This subsection examines the impacts of lower-level scenario attributes (Table III) on the demand for nuclear energy. These lower-level attributes constitute “internal drivers” and include: a) degree of plutonium recycle in LWRs; b) breeding of plutonium in commercial LMRs; and c) the use of Fast-Spectrum Burners (FSBs) in consort with either once-through or plutonium-recycling LWRs.

1. Once-through LWRs

a. Nuclear Material Inventories

Except for the generation, flows, and inventories of nuclear materials, the once-through LWR scenario is described by the basis scenario (Sec. II.C.). Key global mass flows and inventories are shown as a function of time for the basis scenario on Fig. 42. The majority of the plutonium resides in unrecycled spent-fuel form (SF = ACC). Since the basis scenario has negligible plutonium recycle, inventories of separated (SEP) and fully recycled (REC) plutonium are nil. The integrated emission of CO₂ to the atmosphere, as well as preliminary estimates of proliferation utility, $\langle u \rangle$, and risk index, PRI, are also included on Fig. 42. The atmospheric response model described in Sec. III.C. is used to relate these integrated emissions, M_{CO_2} (GtonneC, since 1975), to growing atmospheric inventories, W (GtonneC), and attendant temperature rise, ΔTK . The proliferation utility is evaluated (weighted) relative the USA and uses input^{4,19} (*e.g.*, ENV, NWA, and related proliferation utility parameters) that reflects a relatively homogeneous world. A regional breakout of the total plutonium inventory curve is given in Fig. 43, with Fig. 43A displaying the thirteen regions and Fig. 43B. aggregating these regions into OECD, REF, DEV. Most notably from this figure is the shift in plutonium accumulations for the basis scenario (*e.g.*, OT/LWR) towards the developing regions, in spite of the large “head start” for the OECD countries. Lastly, the global “concentration” (refer to Fig. 15 captions for description) of plutonium in its various forms is depicted in Fig. 44. While the global distribution of total plutonium (mainly in LWR-recyclable spent-fuel form, ACC) appears to move towards uniformity, plutonium contained in reactors (REA) initially becomes more uniform on a regional basis, but the large growth in developing regions (mainly CHINA⁺) shifts global REA plutonium concentration upward at later times.

b. Demand Variants

Total global plutonium accumulations for the high- medium(basis-scenario)-, and low-demand scenarios (Fig. 41; $\epsilon_k = 0.005, 0.01, \text{ and } 0.015$ 1/yr, respectively) are shown in Fig. 45, which includes the total plutonium accumulations reported from the Ref.-7 study for comparison. Figure 46 gives the uranium requirements for these three (high, low, and basis) scenarios, along with comparisons with the Ref.-7 projections. In these figures the

HV($\epsilon_k = 0.005$ 1/yr), MV($\epsilon_k = 0.010$ 1/yr), and LV($\epsilon_k = 0.015$ 1/yr) designators are used to indicate High, Medium, and Low Variants that are counterpart to the present study because of the close agreement of the respective nuclear-energy demand curves with those of Ref.-7 (*e.g.*, Fig. 41).

c. Basis Scenario Realignment

Prior to examining global plutonium inventory responses to plutonium recycle in LWRs, LMR operation, and the implementation of Fast Spectrum Burners (FSBs), refinements in the “top-level” nuclear materials balance (Fig. 3B) were made. These refinements resulted in slight shifts in the time evolution of the material inventories reported for the OT/LWR basis scenario (*e.g.*, Figs. 42, 43, and 44). These three sets of figures are repeated for the refined model in Fig. 47 (Fig. 43), Fig. 48 (Fig. 42), and Fig. 49 (Fig. 44). Additionally, Fig. 48A gives a regional breakout of reactor plutonium (REA) inventories of this realigned OT/LWR basis scenario.

2. Plutonium Recycle in Light-Water Reactors (LWRs)

For each global region, the LWR recycle model forces the (volume) fraction of the LWR core that is operated on MOX, f_{MOX} , to follow a specific trajectory; the model in its present form does not make the choice of f_{MOX} based on economic grounds. A range of functions are used to drive f_{MOX} , all of which are characterized by: a) the initial MOX core fraction, $f_{\text{MOX}}^{\text{o}}$; b) the final MOX core fraction, $f_{\text{MOX}}^{\text{f}}$; c) the time at which the MOX trajectory is initiated, t_{MOXo} ; and d) a nominal doubling time, T_{MOX} , used to determine the rate, λ_{MOX} , at which f_{MOX} approaches $f_{\text{MOX}}^{\text{f}}$. Figure 50 gives f_{MOX} trajectories for the $\tanh(\lambda_{\text{MOX}} t)$ driving function used in this study ($t_{\text{MOXo}} = 2005$ and $T_{\text{MOX}} = 10$. yr; Table IV lists other relevant parameters), for a range of final MOX core volume fractions, $f_{\text{MOX}}^{\text{f}}$, considered in this study. Most results are reported for $f_{\text{MOX}}^{\text{f}} = 0.30$.

Another model limitation is the absence of an inter-regional plutonium allocation model. For each global region, the amount of plutonium residing in reactors (REA), in processing or fuel fabrication as a separated form (SEP = FF + RP), or accumulated in spent fuel as either recyclable to LWRs (ACC) or fully recycled and of marginal use in a thermal-

spectrum reactor (REC), is determined by the evolving (regional) demand for nuclear power. Depending on that demand and the level of plutonium recycle desired, as well as initial accumulated inventories, the accumulated LWR-recyclable plutonium inventory, ACC, may or may not be sufficient to meet regional demands. In the case where ACC is insufficient to meet demand, a negative inventory is recorded that reflects plutonium being used in those regional reactors that originate from outside that region. Since a rule-based plutonium “clearinghouse” model is not fully developed,²⁰ the tracking of regional total plutonium inventories, $TOTAL = SEP + REA + ACC + REC$, includes only positive inventories, under the presumption that negative values of ACC would be met from regions with surpluses through a set of yet-to-be-determined allocation rules. Whenever regional totals are presented, they reflect an inflation related to these unresolved “contributions” from regions with surpluses in order to resolve deficits in other regions. These deficits are resolved on a global basis, however, when total plutonium inventories are reported as TOTAL(NET) values, rather than as TOTAL(GROSS) values. In essence, regions that operate with negative ACC inventories are allowed to push forward with the growth in nuclear energy demand and increased use of MOX cores, but the required subtractions from regions with positive ACC inventories are made only at the global level, and not at the regional level. When the world runs out of recyclable plutonium (*e.g.*, global ACC goes to zero), the results become invalid, with or without a plutonium allocation model, unless the exogenously driven f_{MOX} is reduced;^{27,28} the ERB model in its present form does not incorporate this kind of feedback response.

Evolution of total plutonium inventories for the thirteen regions and the three macro-regions (OECD, REF, and DEV), along with world totals, are shown for $f_{MOX}^f = 0.30$ in Fig. 51. The world totals from the (realigned) OT/LWR basis scenario are also included for comparison. Both the TOTAL(GROSS) and the TOTAL(NET) inventories are shown, but the allocations of surplus plutonium from OECD regions to meet deficits arising in DEV or REF regions (if any) are not reflected in the macro-regional curves on Fig. 51B. Each regional curve of TOTAL inventory (Fig. 51A) has not resolved regional plutonium deficits, where they exist, through ACC inventory reductions in regions with surpluses; these are “unallocated” curves. Generally, the (regionally uniform) “turning on” of the MOX option in year 2005 results in an initial decrease in accumulated (ACC, and TOTAL) plutonium in those regions (mainly OECD) where surpluses exist, as these stocks are depleted to supply MOX needs in both refitted existing LWRs and in supplying new ones that come on line. Depending on the regional ensemble of relative growth rates in nuclear

energy and MOX implementation, global plutonium inventories continue to decrease or can increase again in later years.

The evolution of the global plutonium inventories according to form (ACC, REC, REA, and SEP, as defined in the caption) is displayed in Fig. 52 at both global and regional levels for $f_{\text{MOX}}^f = 0.30$. Most notably is the dip of the world ACC inventory around the period 2030-40, which is followed by a brief recovery. Ultimately the global ACC inventory is turned around when the strong nuclear energy demand from CHINA⁺ is manifested, in accordance with the top-level attributes that define the basis scenario. The buildup in REC (fully recycled for $N = 4$) and SEP (FF + RP) inventories is noted. For all cases, the world is treated uniformly insofar as the desire for and level of plutonium recycling in each region is concerned. The regional structure responsible for the global ACC inventories ultimately going to zero for this exogenously imposed MOX demand scenario (for all regions, $f_{\text{MOX}}^f = 0.30$, $t_{\text{MOX}o} = 2005$, $T_{\text{MOX}} = 10$ yr) after ~2080 is given in Fig. 52B, which also gives the global ACC inventory for the (OT/LWR) basis scenario. Other frames in Fig. 52 give the time dependence of fully recycled (REC, $N \geq 4$), reactor (REA), and separated (SEP = FF + RP) plutonium. Apart from plutonium actively undergoing fissioning in reactors, which generally can be considered to be “safe and secure”, the major component of global plutonium inventories is in the multiply recycled form (REC, deemed no longer usable by thermal spectrum reactor), and, until CHINA⁺ under the basis scenario conditions enters the nuclear energy market after ~2050, most of the REC inventory resides in OECD countries (Fig. 52C); a similar statement applies to plutonium in the SEP form (Fig. 52D.). Lastly, evolution of the global concentration of plutonium in the ACC, REC, REA, SEP, and TOTAL forms is shown in Fig. 53, with strong localization in the ACC and REC forms being indicated.

Generally, the trajectories illustrated in Fig. 52 depend on regional “fine structure”, as determined by technical motivation and capability, economic status, and state of international controls or sanctions. The global ACC inventory that supports the MOX expansion for the conditions simulated is depleted somewhat by ~2035, rebounds because of USA and OECD-E contributions to the “pool”, then in ~2080 goes irrevocably negative; unless the REC pool can be tapped for further LWR plutonium, a major user like CHINA⁺ would have to pull back on plutonium recycle to LWRs, or introduce fast-spectrum plutonium burners. One scenario examined attempts to accommodate aversion to

reprocessing in the USA with the growing needs of CHINA⁺ after 2050 by not recycling in the former and shipping the increased ACC inventories to the latter, as the need arises. While this USA → CHINA⁺ scenario gives interim relief to the world ACC demand, the long-term difference in nuclear energy demand between USA and CHINA⁺ regions is too large for the USA to eliminated out-year plutonium deficits in the CHINA⁺ region.

Decreasing the nominal value of f_{MOX}^f is another way to achieve a small but sustainable ACC inventory. Figure 54 shows the impact on total global plutonium inventories of decreasing the final (nominal) MOX fractions in this regard. Figure 55 gives the dependence of the (LWR-recyclable, $N \leq 4$) ACC plutonium inventories on f_{MOX}^f , again assuming a “uniform” world with regard to plutonium recycle in LWRs Lastly, the comparison chart on Fig. 56 indicates respective impacts on (global) uranium requirement and price *versus* time as f_{MOX}^f is varied; a comparison with the basis (once-through LWR) scenario is also shown. Although the unit fuel cycle costs shown on Fig. 56, $UC_{\text{F:LWR,LMR}}(\$/\text{kgHM})$, are moderate without plutonium recycle, with recycle these costs can experience an initial doubling upon recycling, which diminish in the out years as enriched uranium requirements decrease; these changing fuel-cycle costs enter into the overall energy costs for nuclear that are fed to the ERB model and used to determine market shares. Figure 57 shows the impact of increased fuel-cycle costs on the aggregate demand for nuclear energy. Interestingly, as will be shown in Sec. III.C. increasing f_{MOX}^f and the attendant (slight) decrease in nuclear-energy demand, without a carbon tax, leads to slightly increased use of fossil fuel and atmospheric GHG inventories.

The “top-level” neutronics model (Fig. 3B) requires a number of highly aggregated and time-averaged (over the fueling cycle) parameters to be specified. Most of the parameters listed in Table IV are held fixed throughout this study. Two reactor-core parameters to which the overall nuclear materials balance and inventories are particularly sensitive are: a) the beginning-of-life plutonium loading in the MOX part of the LWR core, $x_{\text{Pu}}^{\text{BOL}}$; and b) the fraction f_{49} of all fissions in the MOX part of the LWR core that occur in the “virgin” plutonium (*versus* MOX fissions occurring in bred plutonium). These parameters are sensitive to burnup, BU(MWd/kgHM); MOX core volume fraction, f_{MOX} ; level of recycle, N ; *etc.* Figures 58 and 59 show the sensitivity of total (world) plutonium

inventories and the inventories of LWR-recyclable plutonium, respectively, as both $x_{\text{Pu}}^{\text{BOL}}$ and f_{49} are varied for $f_{\text{MOX}}^f = 0.30$; the parameter f_{49} seems to be the most sensitive in extending ACC plutonium resources.

The LWR plutonium recycle results presented in Ref. 9 are based on $f_{49} = 0.5$ and $x_{\text{Pu}}^{\text{BOL}} = 0.03$. The time evolution of the global plutonium inventories TOTAL(NET), ACC, REC, SEP, and REA for these conditions is shown on Fig. 60 in comparison to the (realigned) OT/LWR basis scenario (Fig. 48). Comparisons are also given on Fig. 60 with the Ref.-7 High \rightarrow Low Variant cases that each consider the once-through (OT) and the $f_{\text{MOX}}^f = 0.30$ MOX recycle cases.

The main point derived from Figs. 54-57 are: a) plutonium recycle for the basis scenario conditions (other than the non-zero f_{MOX}^f) can reduce global plutonium inventories by factors of 2-3 - this result is in agreement with the Ref.-7 study (Fig. 60); b) aside from “safe-and-secure” reactor plutonium (REA), the main long-term plutonium inventories can be made to reside in the LWR-unusable REC category (for $N = 4$) by judicious temporal and regional choices of MOX recycle parameters (*i.e.*, f_{MOX}^f , $t_{\text{MOX}o}$, and T_{MOX}) - for the Ref.-9 conditions REC slightly exceeds ACC by the year 2095, but shifts in key neutronics parameters (Fig. 59) can lead to the LWR-nonrecyclable form (REC) being dominant; c) the long-term impact of plutonium use in LWRs on the uranium resource (and cost) for basis scenario assumptions (KR) is small, but not negligible (Fig. 56) - this observation, however, is sensitive to the uranium resource category that is adopted as reality (Fig. 36B, the basis scenario is based on KR); d) continued and growing use of LWRs on a global scale at levels dictated by the nominal basis scenario attributes leads to a continued and growing inventory of plutonium in the REC category (Fig. 52A), even for the neutronics parameters used for the Ref.-9 study (Fig. 60); e) increased fuel cycle costs associated with plutonium recycle in LWRs can have an (small) impact on the demand (market share) for nuclear energy, as determined by the ERB logit-based algorithms (Fig. 57); and f) the “top-level” material balance model used herein gives results that are sensitive to the choice of aggregate reactor-core neutronics parameters used, particularly the “virgin” (plutonium) fission factor, f_{49} , and the beginning-of-life plutonium loading in the MOX, $x_{\text{Pu}}^{\text{BOL}}$ - the

inter-dependence of these crucial (flux) time-averaged quantities on BU, N, and f_{MOX} requires more attention in the context of the nuclear materials model used herein.

3. Liquid-Metal Breeder Reactors (LMRs)

The use of fast-spectrum burners (FSBs) to fission more completely all isotopes of plutonium and the minor actinides (*e.g.*, neptunium, americium, and curium) is examined in the following section. Recent studies of the use of fast-spectrum reactors to burn plutonium and the minor actinides have been reported.⁴⁴ Before the economics of FSBs is examined, this section reports on the resource/economic condition necessary for the introduction of the commercial LMRs, using the nominal nuclear and economic parameters listed in Table IV. It is emphasized that the short-comings of the inter-regional plutonium supply-and-demand model discussed above are magnified when the startup demands of commercial LMRs are considered. Furthermore, the integration of LMR breeding-ratio/doubling-time scenarios with the economics of LWR displacement requires considerable model development beyond that presently used in ERB.

As described in Ref. 15, the cost of energy derived from nuclear resources used by the ERB model to generate regional share fractions is determined by means of an optimization procedure applied at each of the nine times separated by 15-year intervals. This procedure essentially examines a full range of LWR/LMR mixes on a COE basis to determine the fraction $f_{\text{LWR}} = 1 - f_{\text{LMR}}$ of all nuclear power for a given region and time that would minimize the overall cost of nuclear energy presented to the ERB market-share algorithm. For low uranium resource depletion (*e.g.*, low uranium costs), higher LMR capital and fuel-cycle costs, and without imposing added external costs for LWR-derivative plutonium and waste accumulations, addition of LMRs at any non-zero value of f_{LMR} generally increases the composite cost of nuclear energy transmitted to the ERB market-share algorithms, for the nuclear and economic parameters used (Table IV). For scenario attributes where non-zero f_{LMR} values reduce the overall cost of nuclear energy, the rate at which LMRs were introduced into a given region is limited by a technology diffusion time;²¹ both the economic and the technology-driven LMR introductions are reported.

For all previously presented results, an LMR having a unit direct cost relative to LWRs $\text{UTC}_{\text{LMR}}/\text{UTC}_{\text{LWR}} \gtrsim 1.5$ would not be economically competitive with LWRs under the basis demand scenario or uranium resource costs that follow a Known Resource (KR)

scaling (Fig. 36). Within the context of the ERB model, three scenario attributes were modified to stimulate the introduction of LMRs:

- use of the more conservative CR uranium resource model (Fig. 36);
- reduce the relative cost of the LMR, $f_{UTC} = UTC_{LMR}/UTC_{LWR} - 1$;
- stimulate overall demand for nuclear energy:
 - impose carbon taxes (Fig. 39);
 - reduce the overall cost of nuclear energy (Fig. 39).

Time dependencies of economics- and technology-driven introduction of LMRs on a range of scenario attributes that are favorable to LMRs are illustrated on Fig. 61, where the fraction of all nuclear energy generated from LWRs is determined under the assumption of a homogeneous world (*i.e.*, all factors determining the time-dependence of f_{LWR} are independent of region). All cases examined use: a) the once-through ($f_{MOX} \sim 0.0$) LWR basis scenario; and b) scaled uranium cost according to the more conservative CR resource scenario (Fig. 36). The latter scenario attribute seems essential for LMR introduction under realistic variations of the other attributes listed above. Under these assumptions, economic entry of the LMR occurs within the ~ 100 -yr time frame of this computation only for $f_{UTC} \lesssim 0.1$. Increasing the demand for nuclear energy (and uranium resources under the CR scenario) by imposing a worldwide carbon tax both decreases the introduction date for LMRs and/or increases the cost threshold as manifested through f_{UTC} (Cases B and C, Fig. 61). Increasing the share fraction of nuclear energy by decreasing overall cost (*e.g.*, the asymptotic value of UTC_{LWR} is decreased from the basis scenario value of 2.4 \$/We to 2.0 \$/We, Fig. 39) has a similar impact on LMR introduction as does the imposition of a carbon tax (*e.g.*, Cases C *versus* D on Fig. 61, both for $f_{UTC} = 0.1$). Lastly, re-imposing the basis scenario resource attribute (KR scaling, Fig. 37) for the Case D conditions (Fig. 61, $f_{UTC} = 0.1$, $UTC = 2.0$ \$/We) pushes LMR introduction to beyond the ~ 2100 time frame of this computation.

The main plutonium-inventory impact for scenario attributes that allows the economic introduction of commercial, plutonium-burning LMRs is that plutonium accumulated (ACC) from previous (once-through) LWR operations is transferred to the operational bowels of the displacing LMRs. For the Table-IV parameters, in fact, full global

implementation of LMRs under the Case D (Fig. 61) scenario attributes is insufficient to meet new-reactor- inventory demand, as is indicated on Fig. 62. This figure shows the time dependence of global plutonium inventories for a range of forms: ACC = accumulated (REC = plutonium that has been fully recycled in LWRs, and is zero for the basis scenario once-through fuel-cycle option used); REA = actively fissioning reactor inventories; and SEP = non-LMR reprocessing and LMR fuel fabrication associate with plutonium having LWR origins. Increasing the LMR breeding ratio from unity to 1.2-1.3 has little impact on the plutonium deficit indicated on Fig. 62; the demand by new LMRs exceed any breeding capacity on the time scales being considered. In addition to showing the basis scenario (once-through LWR, but at reduced cost to facilitate comparison), a case where LMRs are implemented globally only in OECD countries is also shown on Fig. 62; non-OECD regions are excluded from implementing LMRs in this analysis by imposing higher UTC_{LMR} values.

4. Fast-Spectrum Plutonium Burners (FSBs)

a. Approach

The previous section constrained the introduction of LMRs on the basis of competitiveness with LWRs and was driven primarily by considerations of uranium resources and basic unit costs (differentials). Generally, it was found for the limited circumstances (*e.g.*, scenario attributes) examined that fairly unusual or stringent conditions must exist before a competitive LMR would make its debut before the year 2100. An alternative approach to dealing with the plutonium inventories accumulating from LWRs, with or without high-N recycle, is to fission this once-through and/or high-recycle material in a fast-spectrum burner (FSB). The use of FSBs, like the LMR/IFR^{44,45} or accelerator-based (ATW)^{46,47} systems, as plutonium-management elements would be pursued at some cost penalty, in that these FSB systems are expected to have capital and O&M charges that would force the sale of (net) electrical power generated therefrom to be made at a higher cost than from LWRs that are allowed to accumulate plutonium at low to moderate charges.

The primary questions addressed in this section are:

- To what extent must COE be incremented for a LWR-based nuclear economy that is supported by LMR- or ATW-based FSBs, where the fraction f_{FSB} of the total regional

nuclear energy capacity is provided by the FSB system [*i.e.*, support ratio is $SR_{FBS} = (1 - f_{FSB})/f_{FSB}$]?

- What is the (cost) impact on regional and world nuclear energy demand if the FSB route to dealing with LWR generated plutonium is taken?
- To what extent and on what time scale are accumulated plutonium inventories diminished by specific FSB approaches, and to what extent is plutonium inventory actually destroyed *versus* merely shifted (*e.g.*, from accumulated LWR spent fuel to active reactor inventories in FSBs)?
- Do significant “top-level” differences exist for ATW *versus* LMR approaches to plutonium management *vis à vis* FSBs? With respect to this question, the following issues must be considered:
 - While generally efficient in terms of the fraction $\eta_p = \eta_{TH}(1 - 1/Q_E)$ of total thermal power that appears for sale on the electrical grid, the LMR requires non-zero conversion ratios⁴⁴ for reasons of neutronic stability and, hence, a non-zero internal “circulation” of plutonium and a corresponding diminution of capacity to serve LWR client reactors; additionally, LMRs operate with high(er) intrinsic plutonium inventories, which can be viewed either as an advantage or a disadvantage, depending on degree to which such in-reactor material (including material circulating as part of any integral processing scheme) can be viewed as “safe-and-secure”.
 - Although the accelerator-based (ATW) approach to FSBs has no intrinsic, safety-driven need to “recirculate” plutonium, and intrinsic inventories can be considerably below that of the LMR, the ATW has a higher recirculating power requirement (*e.g.*, lower Q_E and a lower η_p) and a higher capital cost, both being burdens associated with the accelerator needed to drive subcritical (proton \rightarrow neutron)target/blanket system. A somewhat “relaxed” neutron economy may also allow the more complete burning of minor actinides and long-lived fission products, but flexibility is exercised at a price (accelerator neutrons are expensive, amounting to ≥ 500 k\$/mole⁴⁶).

To begin addressing these questions, the simplified model described in Sec. III.C.2. of Appendix A was implemented as part of the ERB model, wherein the factor f_{COE} by which

the cost of LWR-base nuclear energy would be increased was used to reflect the economic penalty associated with a particular FSB scheme back to the ERB market-share determination. The factor f_{COE} is given by Eq. (A-21) in Appendix A and is a function of the share ratio, $\text{SR}_{\text{FBS}} = (1 - f_{\text{FSB}})/f_{\text{FSB}}$, where f_{FSB} is the fraction of the total nuclear capacity provided by the FSBs in a given global region at a given time. The share ratio is determined by an exogenously specified “prescription” that gives the rate R_{Pu} (kgPu/yr) at which accumulated plutonium (in either ACC or REC forms) should or could be reduced. Additionally, the (maximum) magnitude and deployment rate of FBS capacity, $P_{\text{E}}^{\text{FSB}}$ and $\epsilon_{\text{FSB}} P_{\text{E}}^{\text{FSB}}$, respectively, must be constrained, where ϵ_{FSB} (1/yr) is a linear rate of implementation.

If the regional plutonium inventory at a given time, $I_{\text{ACC}} + I_{\text{REC}}$, is to be reduced by some factor f_{FSB} in time interval Δt , then on average $R_{\text{Pu}} = f_{\text{FSB}} (I_{\text{ACC}} + I_{\text{REC}})/\Delta t$. For an FSB system having (requiring) a conversion ratio CR, a specific inventory SI(kgHM/MWt), and an effective concentration of active plutonium (including low-inventory integral processing) $x_{\text{Pu}}^{\text{FSB}}$, a nominal material balance reflects the following

$$R_{\text{Pu}}(\text{kgPu}/\text{yr}) = \left(\langle P_{\text{E}}^{\text{FSB}} \rangle / \eta_{\text{p}}^{\text{FSB}} \right) \left[\alpha p_{\text{f}} (1 - \text{CR}) + \epsilon x_{\text{Pu}}^{\text{FSB}} \text{SI}_{\text{FSB}} \right], \quad (1)$$

where $\langle P_{\text{E}}^{\text{FSB}} \rangle$ is the average power required over the time increment Δt and $\alpha = 0.39$ kgPu/MWt/yr is defined in the Nomenclature. Since $\langle P_{\text{E}}^{\text{FSB}} \rangle \sim P_{\text{E}}^{\text{FSB}} (1 + \epsilon_{\text{FSB}} \Delta t/2)$, where $P_{\text{E}}^{\text{FSB}}$ is the FSB capacity at the beginning of the time increment, Eq. (1) can be arranged to solve for the growth rate, ϵ_{FSB} required to meet the exogenously specified average plutonium removal rate; the required expression for $y = \epsilon x_{\text{Pu}}^{\text{FSB}} \Delta t/2$ is given as follows:

$$y^2 + (1 + \Delta f / \tau_{\text{FSB}})y + \Delta t(1/\tau_{\text{FSB}} - 1/4\tau_{\text{SYS}}) = 0, \quad (2)$$

where,

$$\tau_{\text{FSB}}(\text{yr}) = 2SI_{\text{FSB}} x_{\text{Pu}}^{\text{FSB}} / [\alpha (1 - \text{CR})p_f] , \quad (3)$$

$$\tau_{\text{SYS}}(\text{yr}) = P_{\text{E}}^{\text{PSB}} SI x_{\text{Pu}}^{\text{FSB}} / (2 \eta_{\text{p}}^{\text{FSB}} R_{\text{Pu}}) . \quad (4)$$

The parameters used to evaluate Eq. (2) within the ERB model at each time step starting at the year 2005 are listed in Tables IV and A-III (Appendix A). The following constraints are applied for each global region at each time:

- The value of implementation/deployment rate $\epsilon_{\text{Pu}}^{\text{FSB}}$ returned by Eq. (2) is subjected to an exogenously determined upper limit;
- The FBS capacity $\langle P_{\text{E}}^{\text{FSB}} \rangle$ implemented on average over a given time increment Δt is limited to a specified fraction of the LWR capacity, $P_{\text{E}}^{\text{LWR}}$, for each region at each time;
- To avoid a “surge” in FSB demand upon first implementation (in year 2005), when the LWR-generated plutonium inventories are the largest, only a fraction of that inventory is allowed to be processed through FSBs at that time.

These constraints and other parameters used in the preliminary evaluation of the impact of FSBs are listed in Tables IV and A-III (Appendix A).

b. Results

The limited results presented herein are based on departures from the once-through LWR basis scenario. More comprehensive analysis of optimal ways to manage civilian plutonium must balance the costs of LWR recycle as a front-end burner compared to more expensive FBS systems having as a main attribute the ability to deal with plutonium forms that cannot be fissioned efficiently in LWRs. Generally, the results of the constrained implementation algorithm described above for any given region depend on the growth of nuclear power and plutonium inventories in that region, and on the magnitude of the constraints imposed on FSB deployment rates and magnitudes (relative to LWRs). Figure 63 gives the regional and temporal behavior of the FBS fraction. Regions (OECD) with a history of nuclear power and accumulated plutonium begin at the constrained FBS capacity, and depending on subsequent growths in nuclear energy, fall below that limit. The FSU and EEU regions are

intermediate in reaching for that limit, and the developing regions do not approach the FSB capacity limit. Canada, with the relatively low nuclear capacity and moderate initial inventories is always working at the imposed limit of $f_{\text{FSB}} < 0.33$ ($\text{SR}_{\text{FSB}} > 2$). For all cases, Eq. (2) reported an implementation rate that exceeded (by ~2-3) the maximum of $\epsilon_{\text{FSB}} = 0.04$ 1/yr.

The economic impact on COE, as determined by Eq. (A-21), is reported for each region as a function of time in the form of $1 - f_{\text{COE}}$ on Fig. 64 for the LMR(CR = 0.6) FSB scenario. For the LWR *versus* LMR financial and costing parameters used (Tables IV and A-III), the early deployment of LMR-based FSBs, when the demand is high and the support ratio is at the (constrained, *i.e.*, it would go lower if allowed) low value, the cost impact for this case is a significant ~30% for the OECD “heavy users”. Later in time, when LWR-accumulated plutonium has diminished (*e.g.*, either burned or deployed in the high-inventory FSBs), the cost impact approach the 10-15% level. Generally, the $1 - f_{\text{COE}}$ dependencies depicted on Fig. 64 are direct reflections of those for f_{FSB} in Fig. 63. Shifting key FSB parameters in Eq. (A-21) will corresponding shift these results.

The nuclear energy costs passed back to the determine market shares have been increased for each region at each time by the factor f_{COE} given in Fig. 64. The impact of these increased costs on overall demand for nuclear energy is shown in Fig. 65, which also compares the impacts of three FSB scenarios with the demand that characterizes the basis scenario, as well as the IAEA High/Medium/Low-Variant nuclear-energy demand scenarios.⁷ Also shown on Fig. 65 is the impact of reducing the unit-capital-cost ratio $\text{UTC}_{\text{FSB}}/\text{UTC}_{\text{LWR}}$ form 1.5 to 1.1 The three FBS scenarios are: LMR with CR = 0.6; LMR with CR = 0.2; and ATW [CR = 0.0, but reduced intrinsic plutonium inventory ($\text{SI}_{\text{ATW}} \times \text{Pu}^{\text{ATW}}$), reduced engineering gain (Q_E), and increased unit total cost (UTC_{ATW})]. Within the uncertainty of this highly aggregated costing model, the LMR/FSB and the ATW/FSB appear to trade internally recirculated plutonium for internally recirculated power to give nominally the same (low) support ratio and elevated values of f_{COE} ; this result is in agreement with the simple analytical results discussed in Sec. III.C.2. of Appendix A. Generally, implementation of any of the FSB schemes considered here provide a good match to the IAEA Low-Variant case.⁷

The temporal and regional impacts on LWR-accumulated plutonium inventories for the LMR(CR = 0.6) FSB scenario are illustrated on Fig. 66, which presents comparison frames with results from the basis scenario (once-through LWRs). As indicated above, for all cases the constrained limit on deployment rate, ϵ_{FSB} , was encountered for all regions at all times. According to Fig. 66B, the constrained implementation rate is insufficient to hold down the growth of accumulated plutonium in the CHINA⁺ region. While the decreases in LWR-accumulated plutonium are significant, a large part of this plutonium is used to start up the high-inventory LMR/FSBs, as is indicated by the inventories of global plutonium expressed on Fig. 67 as a function of time and form [mainly REA = reactors (both LWRs and FSBs), and LWR-accumulated spent fuel; REC = fully recycled and SEP = separated (*e.g.*, fuel fabrication and reprocessing) do not appear for this once-through LWR case, where the FSBs are assumed to invoke integral processing]. It should be noted that the comparison between the basis scenario and the FSB scenario must accommodate the significant differences in demand for nuclear energy brought about by the expense of the FSB scheme adopted here.

C. Integrated Risk Comparison: Nuclear Proliferation *versus* Global Warming

1. Approach

Section III.A. reports the results of single-point variations of the upper-level hierarchal attributes (*e.g.*, external drivers of nuclear-energy demand), and Sec. III.B. deals primarily the lower-level attributes (*e.g.*, internal drivers of nuclear-energy demand). This section investigates the potential of nuclear energy as a means to mitigate greenhouse warming and compares this potential with accompanying risks associated with nuclear proliferation. Specifically, this relationship between proliferation risk and supply-side GHG abatement is examined using: a) the MAU-based Proliferation Risk Index (PRI) described in Sec. II.B.2.d. and Refs. 4 and 19; and b) the global-warming model elaborated in Ref. 12. The PRI model is a combination and extension of MAU analyses described in Refs. 32-35, and the global-warming model is that reported in Ref. 42. The latter is a linear integral-response model that uses GHC concentration and temperature impulse-response functions that have been calibrated against computational results from coupled ocean-atmosphere circulation models.⁴⁹

A range of (supply-side) scenarios are generated through the application of carbon taxes at varying rates (\$/tonneC/15yr) to examine the relationship between (reduced) global warming and (increased) PRI as the forced market-equilibrium and related energy share fractions adjust (*vis à vis* the ERB algorithms) under the imposition of this consumer-based carbon tax. The primary “risk” variables being compared are PRI and the long-term increase in average atmospheric temperature, $\Delta T(K)$. In terms of consequences (economic or otherwise), both PRI and $\Delta T(K)$ are relative measures; for both, actual consequences remain to be measured and assessed. Hence, at the present level of analysis, no economic connection or assessment is made between PRI, $\Delta T(K)$, and the consequences on regional and world economies of both the disposition of an energy tax and the (market-determined) use of otherwise more expensive reduced- or non-carbon (NC) energy sources. The PRI/ $\Delta T(K)$ /GWP (at the level of the ERB model) trade offs examined herein through the carbon-taxation route are limited primarily to the supply side of the energy equation; the impacts of demand reduction (Sec. III.A.3.), in the context of the present model, remain as future work,⁵⁰ although preliminary parametric results in this regard are reported from a highly simplified and aggregated model reported in Ref. 12.

2. Comparative Results

The point-of-departure scenario used to generate carbon-tax-driven scenarios for uncovering explicit PRI/ $\Delta T(K)$ /GWP relationships is that reported in Ref. 9 (Figs. 58-60, with $f_{MOX}^f = 0.30$, $f_{49} = 0.50$, $x_{Pu} = 0.03$, and $N = 4$). Figure 68 gives the global and regional CO₂ (carbon) emission rates, R_{CO_2} , as a function of time. Figure 68A also shows the impact of ever-increasing rates of carbon-tax impositions (\$/tonneC/15yr) on R_{CO_2} (GtonneC/yr); for all cases, application of this consumer-based carbon tax begins in 2005 and linearly increases at the indicated rate. Also shown for the zero-carbon-tax case are the CO₂ (carbon) emission rates expressed on *per-capita* and *per-primary-energy* usage bases; the decrease in the latter ratio (kgC/GJ) reflects increased primary-energy efficiency [decreased energy intensity, EI(MJ/\$)], but the *per-capita* use of fossil fuels is initially constant or falling, followed by an increase, as more-convenient, higher fuel forms are used by an aggregated society that experiences a rising *per-capita* GNP. Most notable from

Fig. 68B is the rapid rise and eventual dominance of the CHINA⁺ region for this zero-carbon-tax case: CHINA⁺ surpasses the USA region after the year 2020.

The impact of the no-carbon-tax CO₂ (carbon) emission rate on integrated emissions, W_o (GtonneC), accumulated atmospheric CO₂ (carbon), W (GtonneC), and average global temperature rise, ΔT (K), is shown on Fig. 69 (W_{IRV} is the atmospheric carbon inventory at the start of the industrial revolution, $t_{IRV} = 1800$). The relatively slow increase of the ratio $\Delta T/(W/W_{IRV})$, as determined from the linear integral-response model used,⁴² is also shown. A recapitulation of the time evolution of global plutonium inventories in a range of forms is shown on Fig. 70, along with the proliferation-risk (“grand”¹⁹) utility function and the related index, PRI, and the integrated CO₂ (carbon) emissions, W_o . Figure 71 correlates these global plutonium inventories with relative CO₂ (carbon) accumulation, W/W_{IRV} , or the temperature rise, ΔT (K), that results; the latter is computed from the year t_{IRV} . The correlations depicted on Fig. 71 are central to subsequent comparisons of global-climate-change (GCC), nuclear-proliferation (PRI), and economic (ΔGWP) impacts. These graphs describe an “operating curve” that reflects increased inventories of nuclear materials (if nuclear energy is to play any role in providing energy and mitigating GHC emissions) and increased atmospheric carbon inventories that inevitably accompany a world population that is expanding both in numbers and in *per-capita* energy use.

The risks associated with increased global inventories of plutonium and GHGs are expressed in terms of the PRI and ΔT parameters, and are correlated in the form of a reduced “operating curve” for the no-carbon-tax case in Fig. 72. As important as is the need to translate both PRI and ΔT into economic and social consequences, the present study does not advance beyond the correlation shown given in Fig. 72. This “operating curve” *per se* is not as important to understanding proliferation-risk/GCC/GWP connectivities as is the shifts in the slopes and magnitudes at a given time as key scenario drivers (*e.g.*, carbon tax rates) are changed. Figure 72 also compares the PRI impacts (for the no-carbon-tax case) of plutonium recycle ($f_{MOX}^f = 0.30$) and the use of the once-through (LWR) fuel cycle. Plutonium recycle increases the PRI by ~10% while have little impact on reducing GCC impacts (*e.g.*, ΔT). Actually the lines of constant time (an

isochrone for 2095 is shown on Fig. 72) are almost vertical, with a slight off-vertical orientation indicating that the small added cost associated with the $f_{\text{MOX}}^f = 0.0 \rightarrow 0.3$ transition reducing slightly the demand for nuclear energy, resulting in a small increase in fossil-fuel use, and leading to slightly larger values of ΔT ($\lesssim 0.05$ K) for the $f_{\text{MOX}}^f = 0.30$ case. Significantly larger impacts are computed for (carbon-tax) enhanced use of nuclear energy (and other reduced- or non-carbon energy sources) forced by imposing carbon taxes, however.

Based on the relatively transparent and empirical market-equilibrium (clearing) algorithms that form the basis of the ERB model, the reduced CO_2 emission rates depicted on Fig. 68A as the carbon-tax rate is increased results from: a) a reduction in the demand for (more expensive) primary energy; and b) a shift in the mix of primary energy sources towards reduce- or non-carbon suppliers. More elaborate (long-term) models would also reflect endogenous increases in either autonomous energy efficiency improvement (AEEI¹⁴), if this concept is used, or induce reallocations of resources among key sectors in each of the world economies as non-energy sectors adjust to increased energy prices.⁵¹ The ERB model is capable only of exogenous changes in the AEEI-like parameter, ϵ_k (Sec. III.A.3.), and for the present series of carbon-tax-rate variations, these demand-side parameters are held fixed.

With these limitations recognized, Fig. 73 gives the impact of carbon tax rate on global primary energy demand; for the limiting case of 50 \$/tonneC/15yr, (leading to a 300 \$/tonneC tax by 2095) a 25% reduction in PE is reported in the year 2095 relative to the no-carbon-tax case. The economic impacts (*e.g.*, reduced GWP) of these carbon taxes are address subsequently. The shift in the mix of primary energy sources [oil, gas, solids(coal + biomass), nuclear, hydroelectric, and solar] that occurs when the carbon tax rate is increased from zero to 50 \$/tonneC/15yr is shown on Fig. 74. The strong decrease in market share for heavily taxed coal is accommodated in part by strong increases in nuclear and solar energies; the limited resources for hydroelectric limit its contribution, and the initial decrease in the market share for gas (which includes syngas from coal, as does oil include synoil³) as carbon taxes are imposed is overcome (relative to the no-carbon-tax case) in the out years for this less carbon-intensive fuel. The shifts in market shares depicted in Fig. 74, however, must be viewed in the context of diminished overall primary-

energy demand (Fig. 73). Increased use of nuclear and solar energies, which in the context of the ERB model are both suppliers of electricity (solar thermal in ERB is treated as a form of energy conservation³), translates into a greater fraction of total primary energy delivered as secondary energy (and eventually to meet specific, income-dependent energy-service demands) in the form of electricity. The fraction of primary energy used as electricity is shown as function of time and carbon tax rate on Fig. 75. When expressed on a common (thermal) basis, the fraction of primary energy used to generate electricity increases from ~40% to $\geq 60\%$ for the high-tax (HT) case in the out years. Lastly, the impact on a nuclear energy of increased carbon taxation is shown on Fig. 76; for the HT case and a nominal capacity factor of $p_f = 0.8$ (Fig. 76 displays annual nuclear electrical energy demand, not capacity), a capacity build rate of ~80 GWe/yr would be required after the year ~2050.

A comparison of key GCC parameters for the no-carbon-tax (NT) and the high-carbon-tax (HT, 50 \$/tonneC/15yr) cases is given on Fig. 77. Carbon taxes imposed at the HT rate, while reducing ΔT in 2095 to ~1.3 K from the ~2.5 K for the NT case, does not stem global warming; the rate of warming at the end of the computational period (2095) amounts to ~0.5 K/100yr (compared to ~2.8 K/100yr in year 2095 for the NT case). As seen from Fig. 77, atmospheric CO₂ (carbon) in 2095 continues to accumulate at a rate of ~1.6 Gtonne/yr (~1/3 times present global emission rate). The impact of carbon tax rate on global temperature rise is shown on Fig. 78.

The imposition of an increasing rate of carbon taxation both reduces (Fig. 73) and shifts (Fig. 74) primary energy usage, while increasing the use of non-carbon energy sources like nuclear and solar energy. For the unit cost parameters used, the role of biomass grows with time, but remains relatively small. The economics model used in ERB does not re-inject the carbon taxes into the economies that are responsible for their generation. The only direct economic impact of higher energy prices is to reduce global and regional productivity as measured through GDP(GNP). Figure 79 gives the decrease in world GNP as a function of the rate of carbon taxation. These GWP percentage decreases are expressed in two forms: a) the percent decrease in the last-year (2095) GWP with and without a carbon tax imposed at a given rate; and b) the percent decrease in the present worth of all GWPs over the period 1990-2095, using a constant pure discount rate of $DR = 0.04$ 1/yr; the former gives $(\Delta GWP/GWP)_{2095} = -4\%$, and the latter gives $(\Delta GWP/GWP)_{PV} = -0.7\%$. The ratio of the present value of incremental GWP to the present value of all carbon taxes

collected over the computation period, again using $DR = 0.04$ 1/yr, is nominally constant in the range 0.6-0.7; the present value of all carbon taxes collected over the computation period is about twice the present value of the GWP decrement.

Also shown on Fig. 79A is the decrease in atmospheric CO_2 accumulation (again, $W_{IRV} = 594$ Gtonne is the atmospheric carbon inventory for $t_{IRV} = 1800$). This reduction in global warming might be considered a benefit against which the decreased GWP balances, albeit, a more careful and consistent accounting of the collected carbon taxes could reduce or reverse the GWP decrements computed from the present model. Lastly, the percentage increase in proliferation risk evaluated in the last year, $(\Delta PRI/PRI)_{2095}$, associated with the increased implementation of nuclear energy is also shown on Fig. 79A. While ΔPRI is small relative to PRI, no quantitative statement can be made with respect to this increased proliferation risk attendant to increased use of nuclear energy to abatement GHG accumulation until the consequences of PRI without carbon taxes are assessed. Lastly, the second frame in Fig. 79 eliminates the carbon tax rate *per se* and plots directly the “benefits” (*e.g.*, reduce ΔT or reduced W/W_{IRV}) against the “costs” (*e.g.*, decreased GWP and increased PRI). This (relative) “benefit-to-cost” assessment, however, remains qualitative until these PRI, GWP, and temperature increments can be related to quantitative social and economic consequences.

At the level of this analysis, the culmination of the comparative risk assessment is the PRI *versus* ΔT relationship for this special set of carbon-tax-driven (supply-side) scenarios. Resolution of the economic implications of this particular set of drivers, as monitored through GWP impacts, remains as future work⁵⁰ that must ultimately relate abatement costs to achieve a given reduction in ΔT to damage costs associated with accommodation to GCC impacts; these costs are generally expressed as percentages of GNP.⁵² In the context of the present study, however, the evolution of the PRI *versus* ΔT “operating curves” depicted on Fig. 80 represents the final result. As discussed above, with or without a GHC-abating carbon tax, both PRI and ΔT will increase with time as populations in number and living standard develop. The first frame of Fig. 80 gives this PRI *versus* ΔT evolution with increasing carbon tax rates, whereas the second frame stresses more the increased nuclear-

energy share under imposition of carbon taxation by giving the fractional increase in PRI relative to the zero-tax case as a function of ΔT . The added sensitivity of plotting $\Delta \text{PRI}/\text{PRI}_0$ reveals that for a given taxation rate ($\$/\text{tonneC}/15\text{yr}$), the fractional increase in PRI shows a maximum at ~ 2065 that is independent of the rate at which the carbon tax is applied. Generally, increased use of nuclear energy through the imposition of a carbon tax slows the rate of global warming while increasing proliferation risk a few percent relative to the zero-carbon-tax case.

Finally, to show explicitly the impact of carbon-tax-stimulated implementation of nuclear energy on reducing global warming in the year 2095, the end points on each curve in Fig. 76 have been correlated with the resulting value of ΔT (end points on Fig. 78) to give ΔT *versus* nuclear-energy demand in Fig. 81. Also shown is the percentage increase in PRI (relative to the zero-carbon-tax case Fig. 80B) that accompanies this increased use of nuclear energy, as is the percentage decrease in GWP (both in 2095 and present-value terms) caused by the higher fossil energy prices. Figure 81 also shows the (demand-side) impact of increasing the AEEI-like parameter, ϵ_k , from the basis scenario value of $\epsilon_k = 0.0100$ 1/yr to 0.0125 1/yr. Ongoing work⁵⁰ is examining these supply-side *versus* demand-side approaches to mitigating GHG emissions.

IV. SUMMARY AND CONCLUSIONS

A range of long-term futures for nuclear energy have been examined by building “surprise-free” scenarios using a consistent, but simplified, modeling tool. Defining scenario attributes are placed in a hierarchy that divides determinants of nuclear-energy futures into external forces and forces that originate from within nuclear energy *per se*. By varying the former upper-level scenario attributes (*e.g.*, population, workforce productivity, energy intensity or end-use transformation efficiency, energy taxes), a wide range of nuclear energy demand scenarios can be generated. Although these scenarios represent only possibilities, and are not predictions, they nevertheless provide a quantitative basis and connectivity for examining impacts of the lower-level internal drivers that influence directly the economic and operation character of nuclear power. Furthermore, the upper-level scenario attributes that lead to a given demand for nuclear energy have economic and environmental consequences into which subsequent lower-level scenarios are embedded and ultimately must consider.

The internal drivers on which the Los Alamos Nuclear Vision Project is focusing center on both the front-end (uranium resource, ready fuel inventories) and the back-end (plutonium inventories in a range of spent-fuel forms, processing, waste disposal) parts of the fuel cycle. Estimates of the (13) regional and (long-term, ~2100) temporal evolution of plutonium inventories, both in form and in magnitude, along with attendant, proliferation risks, has been the main goal of work performed to date. Three nuclear scenarios base on variations in the lower parts of the attribute hierarchy were examined within the above-described context: a) once-through and MOX-recycling LWRs; b) economically competitive LMRs; c) and once-through LWRs being supported by plutonium burning (and storing) FSBs. Synoptic interim conclusions derived from each level of this analysis include:

- *Upper-Level Hierarchal Variations:* Nearly identical high, medium, and low nuclear-energy variants⁷ can be generated from a wide range of external (demographic, economic, policy, market) drivers; decisions made at the lower hierarchal levels on drivers that are internal to nuclear energy should be cognizant of the external conditions that create the demand or anti-demand to which nuclear power is responding.
- *Lower-Level Hierarchal Variations:* These variations and the scenarios that result generally focus on the forms and quantities of plutonium accumulations that accompany

a given upper-level hierarchical demand scenario. Interim conclusions for the three lower-level scenarios examined include:

- *Once-Through or MOX-Recycle LWRs*: With growth in nuclear energy, so grows plutonium inventories; depending on regional and temporal details of this lower-level scenario, and the local demand generated by upper-level scenario attributes, the places where this plutonium resides shift (*e.g.*, ACC, REC, REA, SEP) over time and region; a better understanding of these inter-regional plutonium generations and flows is needed;
- *Economically Competitive LMRs*: based solely on economic considerations *vis à vis* competition with once-through or MOX-recycle LWRs, LMRs appear in the marketplace only if: a) conservative uranium-resource assumptions (*e.g.*, CR scaling, Fig. 36B) are invoked; b) relatively low capital cost are possible (*e.g.*, $UTC_{LMR} / UTC_{LWR} \lesssim 1.1$); and/or c) significant costs for fossil fuel beyond the resource-depletion algorithms used in the ERB model arise (*e.g.*, strong carbon taxes globally applied, Fig. 32). Generally, less-expensive nuclear (electric) power does little for GHG accumulations, but strong carbon taxes both reduce GHG emissions and widen the economic niche of nuclear energy, while moderately decreasing overall primary energy demand and GNP.
- *Fast-Spectrum Burners (FSBs)*: for the parameters used, FSBs based either on LMRs or accelerator-driven subcritical systems (ATWs), even when limited in (minimum) support ratio ($SR_{FSB} = P_E^{LWR} / P_E^{FSB}$) and deployment rate (relative to requirements to reduce accumulated plutonium), have significant impacts on nuclear energy cost and demand [~ 20 - 30% increase upon initial (~ 2005 - 2020) deployment, decreasing to 10 - 15% in the outyears (Fig. 64). If the LMR-based FSB requires a minimum conversion ratio (CR ~ 0.6), this approach to dealing the LWR-accumulating plutonium would have a large internal recirculation of plutonium, thereby forcing down SR_{FSB} and increasing the cost of the LWR/FSB synergy. The ATW in this regard offers an advantage, but operation with a moderately multiplying blanket ($k_{eff} \leq 0.95$) reduces the engineering gain relative to the LMR, and the power-recirculating ATW-based FSB for other reasons is forced to low- SR_{FSB} operations, with high cost impact on the LWR/FSB synergy. While both FSB approaches may have higher unit capital cost than the LWR client, the accelerator can add 15 - 20% to this cost relative to

the LMR. At the level of the present analysis, these contravening economic/operational impacts lead to indistinguishably poor economic performance for both FSB approaches (Fig. 65). Also, for both approaches, much of the decrease in LWR-accumulated plutonium appears as increase in active FSB inventories (Fig. 67).

Using the proliferation risk index (PRI) and the estimate of global warming generated from a linear integral-response model that relates GHG emission rates to global temperature rise,⁴² ΔT , a range of carbon-tax-driven scenarios were created to examine relative tradeoffs between increased PRI associated with increased use of nuclear energy, decreased global warming, and reduced GWP caused by increased (fossil) energy prices. It was found that while high carbon taxes rates (40-50 \$/tonneC/15 yr) can return CO₂ emission rates in ~2100 to present levels, the rate of global temperature rise, while diminished, remains positive (~0.5 K/100yr, compared to 2.8 K/100 yr for the case of no carbon taxes). In the 2100 time frame, the GWP would be reduced by 3-4% (~0.8% on an integrated present-value basis using a 4%/yr pure discount rate), primary energy use would be reduced by 20-25%, and nuclear energy would experience a ~100% increase (necessitating a deployment rate of ~80 GWe/yr in the out years around 2100). The ratio of present value of all carbon taxes to present value of lost GWP (again, using a 4%/yr pure discount rate) amounts to ~1.3 over most of the computational period. The PRI is increased by only 5-6% for the maximum nuclear-energy implementation (*e.g.*, strongest carbon tax rate) in ~2100. Specifically, the explicit relationship between these relative measures of (increased) proliferation risk and (decreased) global temperature rise (Fig. 80) indicates that for this 5-6% increase in PRI, ΔT in 2100 is reduced from 2.4 K for the no-carbon-tax case to 1.4-1.5 K, but again, global temperature continues to rise at a rate of 0.5 K/100yr in 2100 for the strong carbon tax rates. These correlative results between proliferation risk and GCC impacts, however, project only relative trends; the “real” implications of the base (*e.g.*, for no carbon tax) PRI growing to ~0.14, \pm 5-6% with or without carbon-tax-induced growths in nuclear energy, along with the assessment of “actual” impacts of decreasing the global temperature rise by ~ 1 K over ~100 years, needs resolution.

These interim conclusions derive from a highly aggregated model of global energy-economy interactions and both the nuclear-materials and costing algorithms used to feed input to the ERB market-share and the nuclear-proliferation models. Shortcomings related

both to model aggregation and simplification define the agenda for future work, key elements of which are listed below:

- *Nuclear Costing*: Attempts to fit a “bottom-up” feature in the costing of nuclear energy to the generically “top-down” ERB model need expansion to include more detail in both the fuel cycle (UC_{FC}) and the capital cost (UTC) inputs to the composite unit cost of energy (\$/GJ) used ultimately to determine nuclear energy market shares and related proliferation *versus* climate-change tradeoffs; central to improving fuel-cycle costing algorithms is the need to select regional and temporal plutonium recycle options base on economics rather than an (region-dependent) exogenous driver.
- *Nuclear Materials Flows/Inventories*: While resolution into ACC, REC, SEP = FF + RP, and REA forms with which proliferation risks can be assessed is adequate, a rule-based algorithm for inter-regional transport and accumulations of plutonium based both on costs and sanctions needs development to resolve and optimize local plutonium demand and supply;²⁰ as noted below, consideration of both commercial LMRs and LWR-supportive FSBs expand the scope of this problem and need.
- *Breeder Requirements*: Integration of plutonium requirements of an evolving breeder economy *vis à vis* a coupling of regional and temporal breeding ratios to other parts of the nuclear fuel cycle is needed for any study that seriously evaluates and optimizes the potential and need for breeder reactors.
- *Fast Spectrum Burners*: Comments made in connection to the last three items as related to improved understanding of the short- and long-term role of FSBs in closing the nuclear fuel cycle apply here also; the model described in Appendix A (Sec. III.C.) and evaluated in Sec. III.B.4.) is only a beginning.
- *Neutronics*: The neutronics model used to feed the nuclear materials flow and inventory model represents a highly approximate description of the time-averaged reactor core isotopics (Appendix A, Sec. III.A. and III.B.); the relationships between the parameters listed on Fig. 3B and in Table IV need a firmer connection with “real” neutronics computations, particularly with regard to the averaged relationships between x_{Pu}^{BOL} , x_{Pu}^{EOL} , BU, fMOX, and f_{49} (Figs. 58 and 59).
- *Greenhouse Warming*: Modeling both the dynamics and economics of GHG-driven climate change need further advancement in relating costs of both EI (demand-side) and NC (supply-side) approaches to CO₂ abatement to actual damage costs and/or benefit

dividends; approaches like those outlined in Ref. 12 need to be incorporated into the multi-regional ERB model; enlargement of the carbon-tax model, along with sectoral, temporal, and regional discounting procedures, need to be integrated and formulated into an assessment approach for global optimizations of GHG abatement/mitigation paths.

- *Non-Carbon Energy Sources*: The primary non-carbon (NC) energy source considered in this study is nuclear energy; nuclear energy must compete in the NC approach to dealing with greenhouse warming with other NC energy sources. Improved modeling of the competition, particularly biomass³⁸ is needed in the context of the present version of the ERB model.

ACKNOWLEDGMENTS

The invaluable, time-saving computational advice and code conversions of C. G. Bathke, and the scenario kabitzings with E. D. Arthur are most gratefully acknowledged.

APPENDIX A. Simple Models to Estimate Plutonium Accumulations, LWR-Recycle, and Fast-Spectrum Burner Impacts

I. INTRODUCTION

While the nuclear fuel-cycle and material-flow models¹⁵ used in conjunction with the ERB global E³ model^{3,4,15} are highly simplified compared to those used in the industry, key interactions tend to be obscured when operated “under” the ERB formalism. This appendix focuses on modeling single-region nuclear-material flows that are driven externally by growth and economic forcing functions to illustrate essential trends and tradeoffs. This appendix also gives the derivation of the relationships used in Sec. III.B.4. to estimate the materials and economic impacts of Fast-Spectrum Burners (FSBs) operated in conjunction with LWRs for plutonium control.

II. BACKGROUND

Plutonium bred into the cores discharged from LWRs accumulates. If recycled back to the LWRs as MOX, the plutonium accumulates at a diminished rate, depending): a) on the number of LWR recycles, N ; b) the rate of MOX core introduction, $\lambda_{\text{MOX}}(1/\text{yr})$; c) the level of (driver) plutonium burnup in the MOX; d) the rate of plutonium creation in the MOX core regions *versus* that in the remainder of the reactor core (UOX); and e) the rate that nuclear energy grows, $\epsilon(1/\text{yr})$. Figure A-1 depicts a simplified flow model that has been created to illustrate related “top-level” tradeoffs. In this model, plutonium being generated from thermal-spectrum reactors is accumulated as either LWR-recyclable material (ACC) or material that has been fully recycled (REC), with material in the REC category being destined either for repository or a fast-spectrum burner (FSB, *e.g.*, and LMR^{44,45} or an accelerator-based neutron source^{46,47})

A simplified material balance is described, wherein a relationship between the fraction of the LWR core that operates as MOX, f_{MOX} , and the rates of plutonium accumulation in each of the above-described categories, $R_{\text{ACC,REC}}(\text{kgPu}/\text{MWe}/\text{yr})$, are related to the number of MOX recycles, N . Figure 1 also includes a synergistic option wherein the respective inventories, $I_{\text{ACC}}(\text{kgPu})$ or $I_{\text{REC}}(\text{kgPu})$, might provide fissile material for either

LMR- or ATW-based FSBs. The degree to which LWRs would provide plutonium to FSBs is determined by the internal technical and economic characteristics of the LWR fuel cycle, as well as plutonium burning capabilities of the generally more expensive FSBs. Plutonium within the LWRs *per se* is modeled as residing in either the MOX or non-MOX (*i.e.*, UOX) parts of the core, with y_{Pu}^i ($i = \text{MOX, UOX}$) designating respective weight fractions of bred plutonium and x_{Pu} designating driver-fuel plutonium weight percent in the MOX region of the core; x_{Pu} must be specified at the beginning and at the end of the core fuel cycle. Key assumptions forming the basis of the material-flow models are listed below:

- a steady state is assumed that can be described in terms of average core properties and continuously (this assumption is later relaxed);
- a differentiation is made between plutonium bred into the non-MOX (UOX) part of the core at concentration y_{Pu}^{UOX} , plutonium bred into the MOX part of the core at concentration y_{Pu}^{MOX} , and “virgin” plutonium initially loaded into the MOX part of the core at concentration x_{Pu}^{BOL} (BOL = beginning-of-life) and discharged from that part of the core at concentration x_{Pu}^{EOL} (EOL = end-of-life); the final plutonium concentration in the MOX part of the core is $\sim x_{Pu}^{\text{EOL}} + y_{Pu}^{\text{MOX}}$;
- the artificial distinction described above is characterized by the fraction, f_{49} , of all fissions occurring in the MOX that take place in the “virgin” plutonium originally loaded therein;
- the fraction of all plutonium discharged from the MOX portion of the core that is no longer (efficiently) usable in a thermal neutron spectrum and, hence, joins the accumulated plutonium category REC, is given by $1/N$, where N is the number of recycles;
- highly aggregated economic parameters are used to assess the relative merits of using ATW- or LMR-based FSBs to burn plutonium arising in the REC category (or more).

The simplicity of the models used in this analysis allows simultaneous descriptions of both model and results. The following results section is divided into: a) steady-state analyses of plutonium generated in LWRs; b) time-dependent analyses of plutonium generated in LWRs; and c) the economics of LMR- *versus* ATW-based FSBs to deal with plutonium

arising in either REC or ACC forms. The FSB model described below has been incorporated into the ERB model to provide the preliminary results reported in Sec. III.B.4. When discretized to match the 15-year time step, the approach described herein is largely that used in the nuclear part of ERB.¹⁵

III. MODELS AND RESULTS

A. Steady-State Analysis

The following expression gives the steady-state plutonium balance, under the assumption that all plutonium that qualifies (*e.g.*, on average has experienced less than N cycles) is recycled back to the LWR:

$$(1 - f_{\text{MOX}})y_{\text{Pu}}^{\text{UOX}} + f_{\text{MOX}}(1 - 1/N) (y_{\text{Pu}}^{\text{MOX}} + x_{\text{Pu}}^{\text{EOL}}) = f_{\text{MOX}} x_{\text{Pu}}^{\text{BOL}} \quad (\text{A-1})$$

If BU(MWtd/kgHM) is the nominal core burnup [BU = FPD PD/< ρ >, where FPD(d) is full-power-day exposure, PD(MWt/m³) is the average core power density, and < ρ >(kg/m³) is the average core mass density], a simple energy balance gives the following relationship between $x_{\text{Pu}}^{\text{BOL}}$, $x_{\text{Pu}}^{\text{EOL}}$, and f_{Pu} :

$$\frac{f_{49} \text{ BU}}{x_{\text{Pu}}^{\text{BOL}} - x_{\text{Pu}}^{\text{EOL}}} = \frac{E_f e N_A \text{ spd}}{A_{39}/1000} = 938.5 \text{ (MWtd/kgPu)} , \quad (\text{A-2})$$

where $E_f = 200 \text{ MeV/fission}$, $e = 1.602 \times 10^{-19} \text{ J/eV}$, $N_A = 6.023 \times 10^{23} \text{ entities/mole}$, $\text{spd} = 24 \times 3600 \text{ s/d}$, and $A_{39} = 239$; for $x_{\text{Pu}}^{\text{BOL}} = 0.04$, $f_{49} = 0.5-0.7$, and BU = 40 MWtd/kgHM. Given that $\Delta y + y_{\text{Pu}}^{\text{UOX}} - y_{\text{Pu}}^{\text{MOX}} \sim 0$, the net rate of plutonium consumption, $\Delta x = x_{\text{Pu}}^{\text{BOL}} - x_{\text{Pu}}^{\text{EOL}}$ depends directly on BU and the direct fission factor, f_{49} .

Equation (A-1) is rearranged into the following expression for the value of f_{MOX} permitted by the steady-state mass balance described.

$$f_{\text{MOX}} = \frac{y_{\text{Pu}}^{\text{UOX}}}{\left(x_{\text{Pu}}^{\text{BOL}} - x_{\text{Pu}}^{\text{EOL}}\right) + \left(y_{\text{Pu}}^{\text{UOX}} - y_{\text{Pu}}^{\text{MOX}}\right) + \left(y_{\text{Pu}}^{\text{MOX}} + x_{\text{Pu}}^{\text{EOL}}\right)/N} \cdot \quad (\text{A-3})$$

The asymptotic (large N) value of f_{MOX} for these (sustainably) steady-state conditions is given by

$$f_{\text{MOX}}^f = \frac{y_{\text{Pu}}^{\text{UOX}}}{\left(x_{\text{Pu}}^{\text{BOL}} - x_{\text{Pu}}^{\text{EOL}}\right) + \left(y_{\text{Pu}}^{\text{UOX}} - y_{\text{Pu}}^{\text{MOX}}\right)} \cdot \quad (\text{A-4})$$

Equation (A-2) gives the relationship for $x_{\text{Pu}}^{\text{EOL}}$, provided that $x_{\text{Pu}}^{\text{BOL}}$, BU , and f_{Pu} are specified. Lastly, the rate at which fully cycled plutonium accumulates, R_{REC} (kgPu/MWe/yr), is given by

$$R_{\text{REC}}(\text{kgPu}/\text{yr}) = \frac{R_{\text{REC}_o}}{1 + \frac{\left(x_{\text{Pu}}^{\text{BOL}} - x_{\text{Pu}}^{\text{EOL}}\right) + \left(y_{\text{Pu}}^{\text{UOX}} - y_{\text{Pu}}^{\text{MOX}}\right)}{\left(y_{\text{Pu}}^{\text{MOX}} + x_{\text{Pu}}^{\text{EOL}}\right)} N} \cdot \quad (\text{A-5})$$

where $R_{\text{ACC}_o} = p_f y_{\text{Pu}}^{\text{UOX}} \text{ dpy}/\left(\eta_{\text{TH}}^{\text{LWR}} \text{ BU}\right)$, p_f is the plant capacity or availability factor, $\eta_{\text{TH}}^{\text{LWR}}$ is the thermal-conversion efficiency, and $\text{dpy} = 365 \text{ d/yr}$. With ξ defined as the ratio of concentrations given in the denominator of Eq. (A-5), R_{REC} can be expressed in terms of the time τ_{LMR} , needed to accumulate an amount of fully recycled plutonium that is sufficient to supply the start-up needs of one LMR having a specific inventory of SI_{LMR} (kgHM/MWt) and an average plutonium concentration $x_{\text{Pu}}^{\text{LMR}}$. With τ_{LWR} representing the core lifetime for the LWR, it follows that

$$\frac{\tau_{\text{LMR}}}{\tau_{\text{LWR}}} = \frac{\text{SI}_{\text{LMR}}}{\text{SI}_{\text{LWR}}} \frac{x_{\text{Pu}}^{\text{LMR}}}{y_{\text{Pu}}^{\text{UOX}}} \frac{\eta_{\text{TH}}^{\text{LWR}}}{\eta_{\text{TH}}^{\text{LMR}}} \frac{(1 + \xi N)}{P_E^{\text{LWR}}/P_E^{\text{LMR}}} \cdot \quad (\text{A-6})$$

Equations (A-3)-(A-6) have been evaluated in Fig. A-2 as a function of number of MOX recycles, N, for the parameters listed on Table A-I.

B. Time-Dependent Analysis

The stationary equilibrium calculation described above is extended to include the time dependent introduction of MOX and P_E^{LWR} , according to the following driver functions:

$$f_{MOX} = f_{MOX}^f (1 - e^{-\lambda_{MOX}t}) \quad (A-7)$$

$$P_E^{LWR} = P_{Eo}^{LWR} e^{\epsilon t} \cong P_{Eo}^{LWR} (1 + \epsilon t) \quad (A-8)$$

Using the relationship $\tau_{LWR} P_f PD / \langle \rho \rangle = BU/dpy$, the rate of accumulation of recyclable plutonium from LWRs, $R_{ACC} = dI_{ACC}/dt$, is given by

$$R_{ACC}(\text{kgPu}/\text{yr}) = \frac{P_f (P_E / \eta_{TH}^{LWR})}{BU/dpy} \left[y_{Pu}^{UOX} - f_{MOX} (\langle y \rangle + x_{Pu}^{BOL} \tau_{LWR} \epsilon) \right], \quad (A-9)$$

where $\langle y \rangle = (1 - f_{MOX}) y_{Pu}^{MOX} + f_{MOX}(1 - 1/N)(y_{Pu}^{MOX} + x_{Pu}^{EOL})$. Defining a critical MOX core fraction, $f_{MOX}^{CRT} = y_{Pu}^{UOX} / (\langle y \rangle + x_{Pu}^{BOL} \tau_{LWR} \epsilon)$, and the ratio $\rho = f_{MOX}^f / f_{MOX}^{CRT}$, Eq.(A-9) is integrated to the following expression for the inventory of accumulated recyclable plutonium using the Eq. (A-7)-(A-8) driver functions:

$$\frac{I_{ACC} - I_{ACC}^o}{R_{ACC}^o} (1/\text{yr}) = \frac{1 - \rho}{\epsilon} (e^{\epsilon t} - 1) + \frac{\rho}{\epsilon - \lambda_{MOX}} \left[e^{(\epsilon - \lambda_{MOX})t} - 1 \right]. \quad (A-10)$$

Figure A-3 plots Eq. (A-10) for a range of f_{MOX}^f values; an ACC deficit ($I_{ACC} < 0$) indicates that recyclable plutonium must be imported from external sources for the demands of the functions driving f_{MOX} and P_E^{LWR} to be met. The rates of accumulation of non-recyclable (to LWRs, ACC) and total (ACC + REC) plutonium, respectively, are given by

$$R_{\text{REC}}(\text{kgPu}/\text{yr}) = \frac{p_f (P_e / \eta_{\text{TH}}^{\text{LWR}})}{\text{BU}/\text{dpy}} f_{\text{MOX}} [y_{\text{Pu}}^{\text{MOX}} + x_{\text{Pu}}^{\text{EOL}}] / N , \quad (\text{A-11})$$

and

$$R_{\text{TOT}}(\text{kgPu}/\text{yr}) = \frac{p_f (P_E / \eta_{\text{TH}}^{\text{LWR}})}{\text{BU}/\text{dpy}} \left[y_{\text{Pu}}^{\text{UOX}} - f_{\text{MOX}} (x_{\text{Pu}}^{\text{BOL}} \tau_{\text{LWR}} \varepsilon + \Delta x_{\text{Pu}} + \Delta y_{\text{Pu}}) \right] , \quad (\text{A-12})$$

where, $\Delta x_{\text{Pu}} = x_{\text{Pu}}^{\text{BOL}} - x_{\text{Pu}}^{\text{EOL}}$, $\Delta y_{\text{Pu}} = y_{\text{Pu}}^{\text{UOX}} - y_{\text{Pu}}^{\text{MOX}}$, and $\text{TOT} = \text{ACC} + \text{REC}$.

C. Fast-Spectrum Burners

1. General Considerations

As is indicated on Fig. A-1, plutonium accumulated in the REC inventory builds according to Eq. (A-11). This plutonium can be fissioned efficiently only in devices that operate with epi-thermal or harder neutron spectra; the LMR^{44,45} and the ATW^{46,47} offer two candidates for these Fast-Spectrum Burners (FSBs). Given that either FSB generates a net-electric power P_E^i ($i = \text{LMR}, \text{ATW}$), with overall plant efficiency $\eta_p^j = \eta_{\text{TH}}^j (1 - 1/Q_E^j)$, where the engineering gain or ratio of gross electric to recirculating power is Q_E^j , the rate of plutonium consumption for either is given by

$$R_{\text{FSB}}(\text{kgPu}/\text{yr}) = \alpha p_f P_E / \eta_p , \quad (\text{A-13})$$

where $\alpha = (A_{49}/1000) \text{ spy}/(e E_f N_A) = 0.3901 \text{ kgPu}/\text{MWt}/\text{yr}$. The engineering gain, while generally high for LWRs and LMRs (≥ 25), is introduced to model more accurately the internal power requirements of the ATW-based FSB. Given that either burner operates with a specific inventory SI_j (kgHM/MWt) and an average plutonium weight fraction x_{Pu}^j , the

net rate of plutonium consumption is re-expressed in terms of key system parameters as follows:

$$R_{\text{REC}}(\text{kgPu}/\text{yr}) = R_{\text{BNR}} \left[(1 - \text{CR}) + \frac{(\text{SI})_j x_{\text{Pu}}^j}{\alpha p_f} \varepsilon_j \right], \quad (\text{A-14})$$

where CR is a (minimum) plutonium conversion ratio (CR ~ 0.6 for LMRs and 0.0 for ATWs), and $\varepsilon_j(1/\text{yr})$ is the rate at which the respective FSB is introduced into the LWR-FSB synergistic power system (Fig. A-1). The two terms in Eq. (A-14) represents two plutonium “consumption” modes: a) ACC inventory reduction by actual fissioning in the burner; and b) ACC inventory reduction by shifting of locale (*e.g.*, from ACC inventories to FSBs).

Table A-II lists typical parameters of the LMR and ATW fast-spectrum systems. A comparison of the ratio $R_{\text{REC}}/R_{\text{FSB}}$ indicates the CR = 0.0 advantage of the ATW is counteracted in part by the lower value of active specific inventory, $(\text{SI})_j x_{\text{Pu}}^j$. For the comparison parameters used on Table A-II, the ATW is capable of burning 1.5 time the plutonium on a thermal power basis, or 1.7 times on a net-electric basis, than that of the LMR. For the two systems to be comparable for the parameters used (Table A-II), CR for the LMR would have to be decreased to $\text{CR} \lesssim 0.1$. Ultimately, however, these kinds of comparisons should be made on a cost basis; the following section gives such an estimate.

2. Economic Considerations

Either the LMR or the ATW represent systems that can have higher capital and operating costs than the client LWRs being served. Important elements in the economic equation are: a) the revenues generated by the FSB through the sale of electrical energy; and b) the extent to which the higher costs of the FSBs can be spread over the client LWRs being served. Except for the accelerator (capital and operating) costs, the LMR and ATW power plants are assumed similar in added complexity and cost; they are both liquid-metal systems that would operate with integral, low-inventory chemical processing. The spreading of FSB costs over the client LWRs is best measured in terms of the support ratio $\text{SR}_{\text{FSB}} = P_{\text{E}}^{\text{LWR}} / P_{\text{E}}^{\text{FSB}}$, where again P_{E}^j is the net-electric power delivered for sale to the electrical

grid. The relative economics of this synergistic LWR-FSB system is discussed after giving a quantitative definition of the all-important support ratio, SR_{BNR} .

a. Support Ratio

The rate at which plutonium is generated by the LWRs is given by

$$R_{\text{Pu}}(\text{kgPu}/\text{yr}) = \frac{p_f (P_E^{\text{LWR}} / \eta_{\text{TH}}^{\text{LWR}})}{\text{BU}/\text{dpy}} \langle y_{\text{Pu}} \rangle, \quad (\text{A-15})$$

where the nominal weight fraction $\langle y_{\text{Pu}} \rangle$ varies from y^{UOX} for once-through LWR operations to any of the bracketed quantities in Eqs. (A-9), (A-11), or (A-12) for modes that involve some degree of plutonium recycle back to LWRs. Equating this last expression to Eq. (A-14) under the assumption of steady state gives the following expression for SR_{BNR} :

$$SR_{\text{FSB}} = \alpha \frac{p_f^{\text{FSB}} \eta_p^{\text{LWR}}}{p_f^{\text{LWR}} \eta_p^{\text{FSB}}} (\text{BU}/\text{dpy}) \frac{1 - \text{CR} + \frac{SI_{\text{FSB}} x_{\text{Pu}}^{\text{FSB}} \epsilon}{\alpha p_f^{\text{FSB}}}}{\langle y_{\text{Pu}} \rangle}. \quad (\text{A-16})$$

This expression has been evaluated in Table A-II for $\langle y_{\text{Pu}} \rangle = y_{\text{Pu}}^{\text{UOX}}$, which corresponds to a once-through LWR fuel cycle. While higher values of SR_{FSB} and better cost sharing would result if the lower values of $\langle y_{\text{Pu}} \rangle$ that result from the various recycle modes suggested by Eqs. (A-9), (A-11), or (A-12) were used, the relative costs of these variants must be examined. This level of costing is beyond the capabilities of a simple model, but estimates of the impact of SR_{FSB} and FSB type on cost sharing can be made.

b. Cost Impacts

The costs of constructing and operating the FSBs are expressed as a fractional increase in the cost of electricity, COE(mill/kWeh), of the ensemble of power producers comprised of the LWRs and the supporting FSBs. In general, if UTC(\$/We) is the capital cost per unit of total electric power generated, P_{ET} (MWe), the total cost of the system is $\text{TC}(\text{M\$}) = \text{UTC } P_{\text{ET}} (1 + \delta)$, where δ represents an incremental charge for the ATW

related explicitly to the accelerator. Expressing the annual charge associated with the capital cost in terms of a fixed charge rate, FCR(1/yr), and treating the annual operating and maintenance (O&M) charges (including chemical processing) as fraction $f_{OM}(1/yr)$ of the total capital charges, the annual charges incurred in operating any power station (LWR, ATW, or LMR) is given by

$$AC(\text{M}\$/\text{yr}) = (\text{FCR} + f_{OM}) \text{UTC} P_{ET} (1 + \delta) , \quad (\text{A-17})$$

where $\delta = 0$ for LWR and LMR systems. A given system generates annually $E(\text{kWeh}) = p_f P_E 10^3 \text{ hpy}$ units of net electric energy, where $P_E/P_{ET} = 1 - 1/Q_E$, and $\text{hpy} = 8760 \text{ hr/yr}$. Dividing AC by $E(\text{kWeh})$ gives the following expression for the cost of electricity:

$$\text{COE}(\text{mill}/\text{kWeh}) = \frac{10^6}{\text{hpy}} (\text{FCR} + f_{OM}) \frac{\text{UTC} (1 + \delta)}{p_f (1 - 1/Q_E)} . \quad (\text{A-18})$$

For example, using the typical financial and costing parameters listed in Table A-III, Eq. (A-18) yields $\text{COE} = 51.0 \text{ mill/kWeh}$ when $\delta = 0.0$ and $Q_E = 25$ (*i.e.*, 4% recirculating power fraction, assumed to be typical of LWRs and LMRs).

The parameter δ for the ATW represents the total cost associated with the accelerator relative to that associated with the rest of the power plant. This “rest” of the power plant is assumed to differ little in cost from that of an LMR, which in turn is assumed to be $\geq 50\%$ that of an LWR (*e.g.*, $\text{UTC}_{LMR}/\text{UTC}_{LWR} \sim 1.5$).

If $\text{UC}_{ACC}(\$/\text{Wb})$ is defined to represent the unit cost of the accelerator per unit of beam power, $P_B = E_B I_B$, where E_B and I_B are the beam energy and currents, respectively, and the power $P_A = P_B/\eta_B$ is the accelerator power used with efficiency η_B to generate the beam, then that part of the total cost associated with the accelerator *per se* is $\text{UC}_{ACC} (P_B/P_A) (P_A/P_{ET}) P_{ET} = \text{UC}_{ACC} \eta_B f_{ACC} P_{ET}$, where $f_{ACC} = (P_A/P_{ET})$ is the recirculating power fraction associated only with the accelerator. It is easily shown⁴⁶ that

$$f_{\text{ACC}} = \frac{1}{\eta_{\text{TH}} \eta_{\text{B}} (1 + \beta)} , \quad (\text{A-19})$$

where $\beta = (E_f/E_B) Y k_{\text{eff}}/(1 - k_{\text{eff}})$, $Y \sim (E_B - E_{\text{Bo}})/y$, and k_{eff} is the neutron multiplication of the accelerator-driven fission assembly; typically, the target-yield fitting parameters are $y \sim 35$ MeV/n and $E_{\text{Bo}} \sim 200$ MeV/p. For these parameters, $k_{\text{eff}} = 0.95$, and $\eta_{\text{B}} = 0.45$, a 2000 MeV proton beam would require a fraction $f_{\text{ACC}} = 0.072$ of the total electrical power, P_{ET} , to be diverted to the accelerator for $\eta_{\text{TH}} = 0.40$; in this case that part of the engineering gain taken up by the accelerator amounts to $1/f_{\text{ACC}} = 13.9$, and $\beta = 76$.

Using f_{ACC} as determined above, the contribution of the accelerator to the total cost is given by,

$$\delta = \frac{UC_{\text{ACC}}/UTC_{\text{ATW}}}{\eta_{\text{TH}}^{\text{ATW}} (1 + \beta)} . \quad (\text{A-20})$$

For the parameters listed in Table A-III, $\delta = 0.174$, and superposing the same engineering gain associated with the LMR on the non-accelerator part of the ATW power plant gives $1/Q_{\text{E}}^{\text{ATW}} = 1/Q_{\text{E}}^{\text{LMR}} + f_{\text{ACC}} = 1/25 + 0.072 = 1/8.93 = 0.11$.

Considering a power-generating system of total net capacity delivered by SR_{FSB} LWRs and the supporting FSBs, $P_{\text{E}}^{\text{LWR}} (1 + 1/SR_{\text{FSB}})$, the average cost of electricity for this system relative to that of the LWR system alone is given by

$$\frac{\langle \text{COE} \rangle}{\text{COE}_{\text{LWR}}} = \frac{SR_{\text{FSB}} + \frac{\text{FCR} + f_{\text{FSB}}^{\text{OM}} \text{UTC}_{\text{FSB}}}{\text{FCR} + f_{\text{OM}}^{\text{LWR}} \text{UTC}_{\text{LWR}}}}{SR_{\text{FSB}} + \frac{p_{\text{f}}^{\text{FSB}} (1 - 1/Q_{\text{E}}^{\text{FSB}})}{p_{\text{f}}^{\text{LWR}} (1 - 1/Q_{\text{E}}^{\text{LWR}})}} . \quad (\text{A-21})$$

With $UTC_{ATW} = UTC_{LMR} (1 + \delta)$, Eq. (A-21) has been evaluated under the assumptions that: $p_f^{LWR} = p_f^{FSB}$; $Q_E^{LMR} = Q_E^{LWR}$, and FCR is the same for all systems. As shown in Table A-II for SR_{BNR} evaluated under both growth and no-growth scenarios (*e.g.*, $\epsilon = 0.02$ or 0.0 1/yr), the internal plutonium requirement for the LMR (*e.g.*, $CR \geq 0.6$) is countered by the added economic requirements for the ATW [*e.g.*, $\delta = 0.17$ and $Q_E = 8.9$ versus 25. for the LMR (and LWR)] to suggest within the uncertainty bounds of this estimate that both FSB approaches to closing the LWR fuel cycle will add ~20% to the cost of energy delivered by the composite or symbiotic LWR/FSB system. The comparable economics and related tradeoffs of either approach to FSBs to plutonium inventory management also result when Eq. (A-21) is used in the ERB model (Sec. III.B.4.), with the temporal and regional dependence of SR_{FSB} being determined by local conditions and exogenously imposed (FBR) growth-rate restrictions.

IV. SUMMARY

Closing the nuclear fuel cycle in the broadest and long-term context means stemming the growing quantities of plutonium while stably isolating the hazardous waste products of fission for times require for them to achieve benignity. Significant reductions in the cost and hazards of dealing with the latter will follow from resolution of the former. The separation of plutonium from fission products followed by recycle can, under optimal conditions, extend resources, reduce proliferation risk, and conserve repository capacity.⁴⁵ As has been noted,⁴⁸ however, much of the reduction of ACC and REC inventories results from the second term in Eq. (A-14) - an inventory shift to active plutonium flows within the FSBs.

REFERENCES

1. P. Schwartz, *The Art of the Long View: Planning for the Future in an Uncertain World*, Doubleday Press, New York (1996)
2. H. McRae, *The World in 2020: Power, Culture, and Prosperity*, Harvard Business School Press, Boston, Massachusetts (1994).
3. J. Edmonds and J. M. Reilly, *Global Energy: Assessing the Future*, Oxford University Press, New York (1985).
4. R. A. Krakowski, "Global Nuclear Energy/Materials Modeling in Support of Los Alamos Nuclear Vision Project: Long-Term Tradeoffs Between Nuclear- and Fossil-Fuel Burning," Proc. Global Foundation Energy Conference, Miami Beach, Florida (November 8-10, 1996) [to be published, Plenum Press, New York (1997); also Los Alamos National Laboratory document LA-UR-96-4873(Rev.) (February 14, 1997)].
5. N. Nakicenovic (Study Director), "Global Energy Perspective to 2050 and Beyond," World Energy Council (WEC) and International Institute for Applied Systems Analysis (IIASA) report (1995).
6. World Energy Council (WEC) Commission, "Energy for Tomorrow's World: the Realities, the Real Options, and the Agenda for Achievement," Kogan Page, St. Martin's Press, Kogan Page Ltd., London (1993).
7. H. F. Wagner (Chairman), "Global Energy Outlook, "Symposium on Nuclear Fuel Cycle and Reactor Strategy: Adjusting to New Realities, Vienna (June 2-6, 1997).
8. E. D. Arthur and R. L. Wagner, Jr., "The Los Alamos National Laboratory Nuclear Vision Project," Proc. Global Foundation Energy Conference, Miami Beach, FL (November 8-10, 1996), Plenum Press, New York, NY (1997).
9. R. A. Krakowski, J. W. Davidson, C. G. Bathke, E. D. Arthur, and R. L. Wagner, Jr., "Nuclear Energy and Materials in the 21st Century," Intern. Symp. on Nuclear Fuel Cycle and Reactor Strategies: Adjusting to New Realities, IAEA, Vienna (June 3-6, 1997).
10. M. A. Wise, private communication, Battelle Pacific Northwest Laboratory, Washington D.C. (1995).
11. J. C. Hourcade, "Modelling Long-Run Scenarios: Methodological Lessons from a Perspective on a Low-CO₂ Intensive Country," *Energy Policy*, 21(3), 309 (1993).
12. R. A. Krakowski, "Mitigation of Atmospheric Carbon Emissions Through Increased Energy Efficiency *versus* Increased Non-Carbon Energy Sources: a Trade Study Using a Simplified "Market-Free Global Model," Los Alamos National Laboratory document LA-UR-97-3581 (September 5, 1997).

13. J. F. Clarke, "The Cost and Benefit of Energy Technology in the Global Context," Proc. Conf. Technology Responses to Global Environmental Challenges: Energy Collaboration for the 21st Century, p. 521, Kyoto Japan (November 6-8, 1991).
14. A. S. Manne and R. G. Richels, *Buying Greenhouse Insurance: The Economic Costs of Carbon Dioxide Emission Limits*, Massachusetts Institute of Technology Press, Cambridge, MA (1992).
15. R. A. Krakowski, "Global Energy Modeling in Support of Understanding Long-Term Nuclear (Materials) Futures," Los Alamos National Laboratory document LA-UR-96-1931 (June 5, 1996).
16. W. Leontief, *Input-Output Economics*, Oxford University Press (1966).
17. "Uranium: 1995 Resources, Production, and Demand," Nuclear Energy Agency of the Organization for Economic Co-operation and Development (NEA/OECD) and the International Atomic Energy Agency (IAEA) joint report, OECD, Paris (1996).
18. W. Burch, E. Rodwell, I. Taylor, and M. Thompson, "A Review of the Economic Potential of Plutonium in Spent Fuel," Electric Power Research Institute report TR-106072 (February 1996).
19. R. A. Krakowski, "A Multi-Attribute Utility Approach to Generating Proliferation-Risk Metrics," Los Alamos National Laboratory document LA-UR-96-3620 (October 11, 1996).
20. C. B. Russell, R. A. Krakowski, C. G. Bathke, and K. A. Werley, "Plutonium Inventory and Transport Algorithm (PITA) for Long-Term Global Assessment of Nuclear Energy," Los Alamos National Laboratory document (in preparation, 1997).
21. J. C. Fisher and R. H. Pry, "A Simple Substitution Model of Technology Change," *Technological Forecasting and Social Change*, 3, 75, (1971).
22. C. Marcetti and N. Nakicenovic, "The Dynamics of Energy Systems and the Logistic Substitution Model," International Institute of Applied Systems Analysis report RR-79-13 (December 1979).
23. W. Kwasnicki, *Knowledge, Innovation, and Economy: An Evolutionary Exploration*, Edward Elgar, Cheltenham, UK (1996).
24. M. Benedict, T. H. Pigford, and H. W. Levi, *Nuclear Chemical Engineering*, McGraw-Hill Book Company, New York, NY (1981).
25. P. Silvennoinen, *Nuclear Fuel Cycle Optimization: Methods and Modelling Techniques*, Pergamon Press, Oxford, UK (1982).
26. R. G. Cochran and N. Tsoulfanidis, *The Nuclear Fuel Cycle: Analysis and Management*, American Nuclear Society, La Grange Park, IL (1990).
27. R. A. Krakowski and C. G. Bathke, "Reduction of Worldwide Plutonium Inventories Using Conventional Reactors and Advanced Fuels: A Systems Study," Los Alamos National Laboratory document LA-UR-96-2808 (July 17, 1997).

28. R. A. Krakowski, C. G. Bathke, and P. Chodak, III, "Reduction of Worldwide Plutonium Inventories Using Conventional Reactors and Advanced Fuels: A Systems Study," Proc. Global97 Intern. Conf. on Future Nuclear Systems, Yokohama, Japan (October 5, 1997).
29. R. L. Keeney and H. Raiffa, *Decisions with Multiple Objectives: Preferences and Value Tradeoff*, Cambridge University Press, Cambridge UK (1993).
30. R. T. Clemen, *Making Hard Decisions: An Introduction to Decision Analysis*, 2nd Ed., Duxbury Press, New York, NY (1996).
31. C. W. Kirkwood, *Strategic Decision Making: Multiobjective Decision Analysis with Spreadsheets*, Duxbury Press, New York, NY (1997).
32. P. Silvennoinen and J. Vira, "An Approach to Quantitative Assessment of Relative Proliferation Risks from Nuclear Fuel Cycle," *J. Oper. Res.*, 32, 457 (1981).
33. P. Silvennoinen and J. Vira, "Quantifying Relative Proliferation Risks from Nuclear Fuel Cycles," *Prog. Nuclear Energy*, 17(3), 231 (1986).
34. I. A. Papazoglou, E. P. Gyftopoulos, M. M. Miller, N. C. Rasmussen, and H. A. Raiffa, "A Methodology for the Assessment of the Proliferation Resistance of Nuclear Power Systems," Massachusetts Institute of Technology report MIT-EL 78-021/022 (September 1978).
35. C. D. Heising, I. Saragossi, and P. Sharafi, "A Comparative Assessment of the Economics and Proliferation Resistance of Advanced Nuclear Fuel Cycles," *Energy*, 5, 1131 (1980).
36. T. L. Saaty, "A Scaling Method for Priorities in Hierarchical Structures," *J. Math. Psychol.* 15, 234 (1977).
37. J. Edmonds and D. W. Barns, "Factors Affecting the Long-Term Cost of Global Fossil Fuel CO₂ Emissions Reductions," *Intern. J. Global Energy Issues*, 4(3), 140 (1992).
38. J. Edmonds, M. A. Wise, and D. W. Barns, "The Cost and Effectiveness of Energy Agreements to Alter Trajectories of Atmospheric Carbon Dioxide Emissions," *Energy Policy*, 23(4/5), 309 (1995).
39. R. Richels and J. Edmonds, *The Economics of Stabilizing Atmospheric CO₂ Concentrations*, *ibid*, p. 373.
40. S. Messner and M. Strubegger, "User's Guide for MESSAGE III, International Institute of Applied Systems Analysis report WP-95-69 (1995).
41. S. Ghatak, *Introduction to Development Economics*, 3rd Ed., Routledge Press, London (1995).

42. K. Hasselmann, S. Hasselmann, R. Giering, and V. Ocana, "Optimization of CO₂ Emissions Using Coupled Integral Climate Response and Simplified Cost Models: A Sensitivity Study," *Climate Change: Integrating Science, Economics, and Policy*, (N. Nakicenovic, W. D. Nordhaus, R. Richels, and F. L. Toth, Eds.) International Institute of Applied Systems Analysis report CP-96-1 (1995).
43. E. D. Mansfield, *Power, Trade, and War*, Princeton University Press, Princeton, NJ (1994).
44. T. Wakabayashi, K. Takahashi, and T. Yanagisawa, "Feasibility Studies on Plutonium and Minor Actinide Burning in Fast Reactors," *Nucl. Technol.* 118(4), 14 (1997).
45. C. E. Boardman, D. C. Wadekamper, C. S. Ehrman, C. Hess, M. Ocker, and M. Thompson, "Integrated ALWR and ALMR Fuel Cycles," personal communication, Nuclear Energy Division, General Electric Company (1996)
46. R. A. Krakowski, "Accelerator Transmutation of Waste Economics," *Nucl. Technol.*, 110(6), 295 (1995).
47. J. C. Browne, F. Venneri, N. Li, and M. A. Williamson, "Accelerator-Driven Transmutation of Waste, Los Alamos National Laboratory document LA-UR-97-958 (1997).
48. T. H. Pigford and C. Choi, "Inventory Reduction Factors for Actinide-Burning Liquid-Metal Reactors," *Trans. Am. Nucl. Soc.*, 64, 123 (November 1991) [also, T. H. Pigford and J. S. Choi, "Reduction in Transuranic Inventory by Actinide-Burning Liquid-Metal Reactors," University of California at Berkeley report UCB-NE-4183 (June 1991)].
49. U. Cubasch, K. Hasselmann, H. Maier-Riemer, E. Mikolajewicz, B.D. Santer, and R. Sauser, "Time-Dependent Greenhouse Warming Computations with a Coupled Ocean-Atmosphere Model," *Climate Dynamics* 8, 55 (1992).
50. R. A. Krakowski, "The Role of Nuclear Power in Mitigating Greenhouse Warming," Los Alamos National Laboratory document (in preparation, 1997).
51. P. Bagnoli, W. J. McKibbin, and P. J. Wilcoxon, "Global Economics Prospects: Medium Term Projections and Structural Change," *Brookings Discussion Paper No. 121 in International Economics* (January 1996).
52. C. Azar, "The Marginal Cost of CO₂ Emissions," *Energy*, 19(12), 1255 (1994).

NOMENCLATURE

A_j	scenario identifier (Ref. 5,6; Table I)
A_{ij}	atomic mass (i = last digit of atomic number, j = last digit of atomic number)
AC_j (M\$/yr)	annual charge for j^{th} item or account
ACC	recyclable (to LWRs) accumulated plutonium; also, accelerator
AEEI	autonomous energy efficiency improvement ¹⁴
ATW	accelerator transmutation of waste
B	scenario identifier (Ref. 5,6; Table I)
BAS	basis scenario or case
BAU	business as usual
BOL	beginning of (core) life
BU(MWtd/kgHM)	fuel exposure or burnup
C_j	scenario identifier (Ref. 5,6; Table I)
CAN	Canada
CE	uranium conversion (to UF_6) and enrichment
CHINA ⁺	China
CIS	Commonwealth of Independent States (FSU)
COE(mill/kWeh)	cost of electricity
CON_j	global concentration of j^{th} parameter/item (Ref. 43, Fig. 15)
CSF	spent-fuel cooling storage
CST	cost (of proliferation activity)
CR	conventional (uranium) resources; conversion ratio.
CV	(uranium) conversion (to UF_6)
D&D	Decommission and Decontamination
DEV	developing countries (ME + NAFR + SAFR + LA + IND + SEA)
DR(1/yr)	discount rate (for proliferation risk discounting ^{19,25,32} , or for estimating present worths of GWP or carbon taxes)
DT	development time (for proliferation), doubling time (for LMR)
DU	depleted uranium (tailings)
dpy	day per year, 365
E(kWeh)	annual electrical generation
E^3	economics/energy/environmental
E_B (MeV)	proton beam energy
E_{Bo} (MeV)	target-yield fitting parameter
E_f (MeV)	energy per fission, 200
EAR-I,II	estimated additional (uranium) resources
EEU	Eastern Europe
EI(MJ/\$)	energy intensity, ratio of primary or final energy to GNP
ENV	(political) environmental parameter for proliferation risk.
EOL	end of (core) life
EPA	Environmental Protection Agency
EPRI	Electric Power Research Institute

ERB	Edmonds, Reilly, Barns model ³
ES	energy services (residential/commercial, transportation, industrial)
e(J/eV)	electronic charge, 1.6021×10^{-19}
FC	nuclear fuel cycle
FCR(1/yr)	fixed charge rate
FF	fuel fabrication
FP	fission product
FPD(d)	full power day
FSB	fast spectrum burner (LMR/IFR, ATW)
FSU	Former Soviet Union
f_{ACC}	accelerator recirculating power fraction, P_A/P_{ET}
f_{BNR}	fraction P_E generated by FSBs
f_{COE}	FSB-induced COE increase [Eq. (A-21)]
f_j	fraction of fissions from j^{th} fuel ($j = 25$ for ^{235}U , 49 for ^{239}Pu)
f_{LMR}	fraction of nuclear power that is generated by LMRs
f_{LWR}	fraction of nuclear power that is generated by LWRs
f_{MOX}	volume fraction of LWR core that is MOX
$f_{OM}(1/\text{yr})$ O&M	charge rate as fraction of total plant cost
f_{Pu}	fraction of MOX fissions occurring in driver (plutonium) fuel
f_{UTC}	ratio of UTCs for LMR relative to LWR
G(B\$)	gross world product, also GWP
GCC	global climate change
GDP(B\$/yr)	gross domestic product
GHG	greenhouse gas
GNP(B\$/yr)	gross national product
GRI	Gas Research Institute
GWP(B\$/yr)	gross world product
HEU	highly enriched uranium
HM	heavy metal
HV	high (nuclear energy growth) variant
HT	high carbon tax rate (50 \$/tonneC/15yr)
HYDRO	hydroelectric
hpy	hours per year, 8760
$I_B(A)$	accelerator beam current
$I_j(\text{kgPu})$	plutonium inventory ($j = \text{ACC, REC, REA, SEP, etc.}$)
IAEA	International Atomic Energy Agency
IEA	Institute of Energy Analysis (ORNL)
IFR	Integral Fast Reactor
IIASA	International Institute for Applied Systems Analysis
IND	India
IRV	industrial revolution ($t_{IRV} = 1800$)
ITD _j	inherent technical difficult for proliferation activity ($j = \text{MP or NW}$)
i	indices for PE or nuclear materials stream
j	indices for SE, FC process, or PRI attribute
KR	known uranium resources
k	indices for FC or ES (in ERB model)
k_{eff}	blanket neutron multiplication

LA	Latin America
LMR	liquid metal (breeder) reactor
LP	linear programming
LV	low (nuclear energy growth) variant
LWR	light water reactor
l	region index (in ERB model)
M_{CO_2} (GtonneC)	accumulated CO_2 emissions from start of computation (1975)
\dot{M}_{CO_2} (GtonneC/yr)	rate of CO_2 emissions
M_{Pu}^j (kgPu)	plutonium inventory (j = ACC, REC, REA, SEP, REP)
M_U (Mtonne)	culmative uranium use
MA	minor actinides (neptunium, americium, curium)
MAU	multi-attribute utility (analysis)
ME	Middle East
MM	(uranium) mining and milling
MIT	Massachusetts Institute of Technology
MOX	mixed (uranium, plutonium) oxide fuel
MP	material processing
MV	medium (nuclear energy growth) variant
m	time index in ERB model
N	number of MOX recycles in LWR
N_A (entities/mole)	Avagadro's number, 6.0249×10^{23}
NAFR	Northern Africa
NC	non-carbon energy sources
NE	nuclear energy
NM	nuclear materials
NT	no carbon taxes
NUCL	nuclear
NW	nuclear weapon (fabrication)
NWA	nuclear weapons aspiration parameter
nl	number of regions modeled in ERB (nl = 13)
O&M	operation and maintenance
OECD	Organization for Economic Cooperation and Development (USA + CAN + OECD-E + OECD-P)
OECD-E	OECD-Europe
OECD-P	OECD-Pacific
OKR	other known (uranium) resources
ORAU	Oak Ridge Associated Universities
ORNL	Oak Ridge National Laboratory
P_A (MW)	accelerator power
P_B (MW)	accelerator beam power
P_E (MWe)	net electric generation capacity
P_{ET} (MWe)	total electric generation capacity
PD (MWt/m ³)	average reactor core power density
PE	primary energy [oil, gas, solids (coal + biomass), nuclear solar, hydroelectric]
POP	population
PRI	proliferation risk index
PRI_o	proliferation risk index without carbon taxes
PV	present value computed using discount rate DR
P_f	plant capacity factor

Q_E^j	engineering Q-value of gain (ratio total-to-net electric power; $j = \text{ATW, LWR, LMR}$)
R	reactor
$R_{\text{CO}_2, l}$ (GtonneC/yr)	carbon emission rate from l^{th} region; for world total, ($l = n_l + 1$), same as \dot{M}_{CO_2}
R_j (kgPu/yr)	rate of plutonium accumulation in j^{th} category
RAR	reasonably assured (uranium) resources
RP	reprocessing
RS	repository
REA	reactor plutonium
REC	fully recycle (N recycles to LWRs) plutonium
REF	(economically) reforming countries (EEU + FSU); reference case
REP	reprocessing
RPU	reactor plutonium
RU	recycled uranium (from LWR)
SAFR	Southern Africa
SANC	(international) sanction parameter
SE	secondary energy (liquids, gases, solids, electricity)
SE/PE	PE \rightarrow SE conversion
SEA	South and East Asia
SEP	separated plutonium (RP + FF)
SF	spent fuel
SFT	total spent fuel
SI(kgHM/MWt)	specific inventory
SPU	separated plutonium (RP + FF)
SR	speculative resources
SR_{FSB}	FSB support ratio, $P_E^{\text{LWR}} / P_E^{\text{FSB}}$
SW	separative work
SWU	separative work unit
spd	seconds per day, $8.64(10)^4$
spy	seconds per year, 3.1536×10^7
T_j (yr)	half-time for j^{th} process/item
TH	thermal \rightarrow electric conversion
TOT, TOTAL	total, world
TR	transportation; total (uranium) resources
TX	present worth of carbon taxes over period to 2095
t_{IRV}	time industrial revolution commences, 1800
t_{REF}	reference time or base year for ERB, 1975
t(yr)	time
UC_j	unit cost for j^{th} process/item
UCS	unconventional uranium sources
UOX	non-MOX part of LWR core
USA	United States of America
UTC_j (\$/We)	unit total cost of j^{th} nuclear energy system
<u>	grand utility function ¹⁹
vppm	volume parts per million

W (Gtonne)	atmospheric carbon-dioxide (carbon) accumulation
W_e	electrical watt
W_o (Gtonne)	integrated atmospheric carbon-dioxide (carbon) emissions from time t_{IRV} (1800)
W_{IRV} (Gtonne)	atmospheric carbon-dioxide (carbon) inventory at time $t_{IRV} = 1800$ (594 Gtonne, or 289 vppm, given 2.13 GtonneC/vppm)
W_t	thermal watt
WEC	World Energy Council
WP(yr)	warning period (to detect proliferation activity)
x_{Pu}	fuel plutonium weight fraction
x_j	^{235}U weight fraction in j^{th} material stream (p = product, t = tailings, f = feed)
y (Mev/n)	target-yield fitting parameter
y_{Pu}^j	bred plutonium weight fraction in region j (UOX, MOX)
Y (n/p)	accelerator target yield
Z_{lm}	population in region l at time interval m
α (kgPu/MWt/yr)	constant, $\text{spy}(A_{49}/1000)/(E_f e N_A) = 0.39 \text{ kgPu/MWt/yr}$
α_{klij}	transfer function relating ratio of process outputs to input for material j being transformed to material i in the l^{th} stream/process/operation of fuel cycle k
β	accelerator/target parameter, $(E_f/E_B) Y k_{\text{eff}}/(1 - k_{\text{eff}})$
ΔT (K)	average global temperature rise, referenced to time t_{IRV}
Δx	MOX driver fuel burnup fraction, $x_{Pu}^{\text{BOL}} - x_{Pu}^{\text{EOL}}$
Δy	MOX/UOX conversion deficit, $y_{Pu}^{\text{UOX}} - y_{Pu}^{\text{MOX}}$
δ	accelerator cost increment for ATW
ϵ (1/yr)	generalized annual growth rate, or recirculating power fraction, $1/Q_E$
ϵ_i (1/yr)	annual growth rate of entity i ($i = \text{POP, EI, PE, NE, etc.}$)
ϵ_k (1/yr)	annual growth rate of $\text{SE}(j) \rightarrow \text{ES}(k)$ transformation technologies, abbreviation for ϵ_{jk}
η_j	conversion efficiency [$j = \text{TH}$ (thermal-electric); p (overall plant); B (accelerator beam)]
λ_{MOX} (1/yr)	rate of MOX introduction, $\ln(2)/T_{\text{MOX}}$
$\langle \rho \rangle$ (tonne/m ³)	average reactor core density
τ_j (yr)	holdup time form j^{th} stream, or core life for j^{th} reactor
ξ	concentration ratio [Eq. (A-5)]

TABLES

Table I. Summary of Cases and Scenarios Used in the WEC/IIASA Long-Term Global Energy Study,⁵ as Elaborated from the Earlier WEC Study⁶

- Case A: “High Growth” future with no technological, geopolitical, or market limitations, and with high growths towards achieving global (energy-use, economic) equity:
 - Scenario A₁: “Gas and Oil” - No remarkable developments favoring either nuclear or coal occur, with the vast (global) potential of conventional and unconventional oil and gas being tapped, and with no need to resort to the coal “backstop”;
 - Scenario A₂: “Coal” - The greenhouse-warming debate (*e.g.*, consequences of increased atmospheric CO₂ *versus* cost of using reduced- or non-carbon energy sources) is resolved in favor of coal; deeper mines, *in-situ* gasification, synliquids, *etc.* are pursued to tap the vast global coal resource;
 - Scenario A₃: “Bio-Nuclear” - Large-scale exploitation of renewables and a new generation (*e.g.*, safer, smaller unit sizes, *etc.*) of nuclear power stations, with natural gas serving as a transition fuel.
- Case B: “Middle Course” - this case assumes modest economic growth, technological development, and reduced trade barriers, with the North-South economic “gap” being closed more slowly than under the “High-Growth” Case-A conditions; more reliance on fossil fuels results.
- Case C: “Ecology Driven” - this case is characterized by significant (global) transfer of advanced technologies and, therefore, is based on highly optimistic geopolitic and technology advances; a broad array of environmental controls (including carbon taxes) is invoked to meet CO₂ emission limits by 2100:
 - Scenario C₁: “Nuclear Phaseout” by 2100, with a strong move towards renewable energy sources presumed;
 - Scenario C₂: “Nuclear Renaissance” leading to small, safe and “sociable” nuclear systems.

Table II. Hierarchy of Scenario (Defining) Attributes

- Level I: “The Inevitable” - generally implemented on a fixed and relatively independent trajectory that describes a given scenario evolution, depending on time frame/horizon;
 - regional (and global) population growth;
 - global energy resource base, according to grade *versus* cost.
- Level II: “The Less-Inevitable” - less inevitable than Level I, but presented and used in a less-aggregated form:
 - local resource base, and fluctuations/uncertainties in amounts available for exploitation under a given grade *versus* cost relationship that includes extraction and related environmental costs;
 - regional and global GNP(GDP) growth; specification of Level-I and Level-II “rules” dictated regional evolution of *per-capita* GNP(GDP), and rules implemented at a lower level of the hierarchy (*e.g.*, attempts to impact *per-capita* GNP through policy changes) must be consistent with rules implemented at these higher levels:
 - workforce makeup and productivity, closely related to GNP (GDP) growth.
- Level III: “Policy Determined” - generally, scenario rules/characteristics at this level of classification are regionally dependent and have technological and economic implications, primarily through institutional channels; often rules in this class are closely related to elements at lower hierarchal levels:
 - local taxes, tariffs, and sanctions;
 - regional GNP(GDP) growth feedback, as related to dependencies on balance-of-payment and energy-security concerns, which are related in turn to energy (resources, technologies) imports to the region in question;
 - resource utilization is distorted by/through government policy and/or support (fossil *versus* nuclear *versus* biomass *versus* solar energy exploitation);
 - technology advances (or inhibitions thereof) driven primarily through government policy [*e.g.*, efficiencies relating the primary-energy → energy-service transformation (PE → ES), related non-market PE choices, sensitivities of (local) ES demand to prices (subsidies) and living standards (local GNP/*capita*), *etc.*];

Table II. Hierarchy of Scenario (Defining) Attributes (Cont.-1)

- levels of environmental and extraction economic charges;
 - translation of (nuclear) proliferation risks into regional costs and sanctions;
 - translation of safety and (energy) security levels into costs/charges used to determine energy share/use fractions.
- Level IV: “Market Determined” - general economic/costing rules and algorithms used to project energy share fractions, technology penetration rates, price/(energy-service) demand relationships, *etc.* and related responses to forces/drivers having origins in Level-III rules/definitions:
 - dependence (*e.g.*, elasticity) of energy-service (ES) demand on key economic indicators [*e.g.*, primary- (PE) and secondary-energy (SE) prices, GNP(GDP), population, *etc.*]
 - dependencies of PE and SE share weights on prices, GNP(GDP), *etc.* required to fulfill a given ES demand;
 - economics of technology dynamics (*e.g.*, technology development → evolution → penetration → full-scale implementation → displacement/phaseout) and connectivity with (assumed) improvements (*e.g.*, decreases) in regional and sectoral energy intensities (*e.g.*, high economic growth rates imply rapid turnover of capital stocks and an enhance opportunity to improve efficiency of the PS → SE → ES transformation process through more rapid replacement; stagnated inefficient systems deliver their inefficiencies for longer periods of time to generally poorer populations).
 - Level V: “Technology Driven” - actual scientific and engineering progress and discovery that enhance the PS → SE → ES transformation process, open new energy sources (*e.g.*, clean-coal technologies, advanced conversion, advanced fission, new transportable fuels, methane clathrates, nuclear fusion, non-electric nuclear energy), reduced or shifted environmental burdens, *etc.*:
 - clean-coal technologies; advanced thermal-conversion systems;
 - advanced nuclear fission systems (reduced plutonium inventories, smaller/cheaper/safer, reduced/eliminated long-term waste streams, acceptably low proliferation risks and/or anti-proliferations enticements);
 - improved energy networks (distribution and transmission), leading to markets for smaller units, changes in competitive generation mixes, *etc.*;
 - alternative liquid fuels and/or electrification of the transportation ES sector.

Table III: Upper-Level (Externally Driven) Scenario Attributes Leading to Low-to-High Nuclear Energy Growth Rates

Attribute Identifier ^(e)	Impact on NE Growth	Population (billions)	GNP Productivity Multiplier	Energy Intensity (%/yr) ^c	Carbon Tax (\$/tonne/15 yr)	LWR Unit Capital Cost UTC (\$/We) ^(b)	LWR Pu Recycle $f_{\text{MOX}}^{(f)}$	LMR Unit Capital Cost UTC _{LMR} /UTC _{LWR}	Uranium Resource ^(a)
BAS	Medium	11.7	1.0	1.0	0.0	2.0 → 2.4	0.0	1.5(d)	KR
POP									
• POPL	Medium	10.0	1.0	1.0	0.0	2.0 → 2.4	0.0	1.5(d)	KR
• POPH	Medium	13.8	1.0	1.0	0.0	2.0 → 2.4	0.0	1.5(d)	KR
GNP									
• GNPL	Low	11.7	0.8	1.0	0.0	2.0 → 2.4	0.0	1.5(d)	KR
• GNPH	High	11.7	1.2	1.0	0.0	2.0 → 2.4	0.0	1.5(d)	KR
EI									
• EIL	High	11.7	1.0	0.0→1.0	0.0	2.0 → 2.4	0.0	1.5	KR
• EIH	Low	11.7	1.0	1.0→2.0	0.0	2.0 → 2.4	0.0	1.5	KR
TAX	High	11.7	1.0	1.0	20. → 40.	2.0 → 2.4	0.0	1.5	KR
UTC ^(g)									
• UTCL	High	11.7	1.0	1.0	0.0	2.0 → (1.5,2.0)	0.0	1.5	KR
• UTCH	Low	11.7	1.0	1.0	0.0	2.0 → (3.0,4.0)	0.0	1.5	KR
RES ^(g)	Medium	11.7	1.0	1.0	0.0	2.0 → 2.4	0.0	1.5	CR → TR

(a) CR = Conventional Resources; KR = Known Resources; TR = Total Resource¹⁷.

(b) range indicates time evolution, with final (higher or lower) values achieved by ~ 2020.

(c) values given indicate annual reduction in secondary energy required to satisfy a given end-use requirement.

(d) high values chosen for some cases to artificially prevent LMR from competing economically.

(e) variations: BAS = base case; POP = population; L,H = low, high; GNP = Gross National (World) Product; EI = energy intensity; NE = nuclear energy; UTC = unit total cost; RES = uranium resources.

(f) varied only as a lower-level (internal driven) scenario attribute.

(g) “baseline” upper-level scenario attribute in this study.

Table IV Key Input Parameters to Nuclear Energy Module Used in ERB Model

LWR PARAMETERS	
UOX fuel burnup, BU_{UOX} (MWtd/kgHM)	40.
MOX core burnup, BU_{MOX} (MWtd/kgHM)	40.
fuel replacement or life time, τ_{LWR} (yr)	3.0
number of MOX recycles, N	4
specific inventory, SI_{LWR} (kgHM/MWt)	26.7
bred plutonium concentration in UOX spent fuel, y_{Pu}^{UOX}	0.0090
bred plutonium concentration in MOX spent fuel, y_{Pu}^{MOX}	0.0090
fraction of all actinides that are minor, f_{MA}	0.0
BOL weight fraction plutonium in MOX, x_{Pu}^{BOL}	0.0500
EOL weight fraction plutonium in MOX, x_{Pu}^{EOL}	0.0288
fraction of all plutonium fissionable, f_{Puf}	0.60
thermal-to-electric conversion, η_{TH}^{LWR}	0.325
plant availability for LWR, p_f^{LWR}	0.70(a)
engineering gain for LWR, Q_E^{LWR}	25.
fraction of fissions from ^{235}U , f_{25}	0.70
fraction of MOX fissions from 'virgin' Pu, f_{49}	0.60
LMR PARAMETERS	
burnup for LMR, BU_{LMR} (MWtd/kgHM)	80.
specific inventory for LMR, SI_{LMR} (kgHM/MWt)	67.5
thermal-conversion efficiency for LMR, η_{TH}^{LMR}	0.40
plant availability for LMR, p_f^{LMR}	0.70(a)
engineering gain for LMR, Q_E^{LMR}	25.
breeding ratio for LMR, BR	1.00
fuel concentration in LMR, x_{Pu}^{LMR}	0.10
total burnup fraction for LMR, x_{BU}	0.086
simple doubling time for LMR, DT(yr)	∞
market penetration time constant, λ_{LMR} (1/yr)	0.164

Table IV Key Input Parameters to Nuclear Energy Module Used in ERB Model (Cont.-1)

URANIUM ENRICHMENT AND LWR CONCENTRATIONS	
weight fraction ^{235}U in ER product stream, x_p	0.0300
weight fraction ^{235}U in ER feed stream, x_f	0.0071
status of uranium tailings optimizer ^{17,18}	on
initial weight fraction ^{235}U in ER tails stream, x_{t0}	0.0023
weight fraction ^{235}U in RU stream, x_{RU}	0.0006
total burnup fraction for LWR, x_{BU}	0.0421
^{235}U burnup fraction, x_{BU25}	0.0294
uranium ore grade (weight fraction), x_{ORE}	5.0×10^{-6}
accumulated uranium mined by 1990, $U_o(\text{kg})$	2.0×10^8
RECYCLE PARAMETERS	
initial fraction of load supplied by MOX, f_{MOX}^o	0.0
final fraction of load supplied by MOX, f_{MOX}^f	0.0 \rightarrow 0.3 ^(b)
half-time for $f_{MOX}^o \rightarrow f_{MOX}^f$, $T_{MOX}(\text{yr})$	10.
time when $f_{MOX}^o \rightarrow f_{MOX}^f$ rampup starts, $\tau_{MOX}(\text{yr})$	15.
hold-up time for LWR reprocessing, $\tau_{RP}^{LWR}(\text{yr})$	1.0
hold-up time for LWR fuel fabrication, $\tau_{FF}^{LWR}(\text{yr})$	0.5
hold-up time for LMR reprocessing, $\tau_{RP}^{LMR}(\text{yr})$	0.3
hold-up time for LMR fuel fabrication, $\tau_{FF}^{LMR}(\text{yr})$	0.3

Table IV Key Input Parameters to Nuclear Energy Module Used in ERB Model (Cont.-2)

COSTING PARAMETERS		
Uranium Resource Base: Redbook Know Resources ¹⁷	KR	
fitting constant for uranium ore cost, U_1	3.13×10^{-11}	
fitting constant for uranium ore cost, v	1.26	
unit cost of uranium ore in 1990, UC_{MM}^0 (\$/kgU)	100.0	
unit cost of uranium conversion, UC_{CV} (\$/kgU)	5.0	
unit cost of uranium separative work, UC_{SW} (\$/kg SW)	100.0	
unit cost of uranium fuel fabrication, UC_{FF}^{UOX} (\$/kgU)	200.0	
unit cost of MOX fuel fabrication, UC_{FF}^{MOX} (\$/kgHM)	400.0	
unit cost of spent fuel storage, UC_{SF} (\$/kg/yr)	10.0	
unit cost of fission prod. storage, UC_{FP} (\$/kg/yr)	10.0	
unit cost of SF/FP transport, UC_{TR} (\$/kgU)	0.0	
unit cost of reprocessing LWR, UC_{RP}^{LWR} (\$/kgHM)	1000.0	
unit cost of reprocessing LMR, UC_{RP}^{LMR} (\$/kgHM)	1500.0	
unit total cost (asymptote) for LWR, UTC_{LWR} (\$/We)	2.40	
unit total cost for LMR, UTC_{LMR} (\$/We)	$f_{UTC} \times UTC_{LWR}$	
unit total cost factor, f_{UTC}	varied	
fixed charge rate for LWR, FCR^{LWR} (1/yr)	0.0900	
fixed charge rate for LMR, FCR^{LMR} (1/yr)	0.0900	
O&M charge rate for LWR, f_{OM}^{LWR} (1/yr)	0.0200	
O&M charge rate for LMR, f_{OM}^{LMR} (1/yr)	0.0200	
FSB PARAMETERS ^(c)		
period when FSB implemented, T_{FSB}	LMR 2005-2020	ATW
engineering q-value, Q_E^{FSB}	25.0	8.0
thermal conversion efficiency, η_{TH}^{FSB}	0.40	0.40
conversion ratio, CR	0.60	0.0
specific inventory for fsb, SI_{FSB} (kgHM/MWt)	67.6	67.6
plutonium concentration, x_{Pu}^{FSB}	0.10	0.05
FSB capital cost factor, $f_{UTC}^{FSP} = UTC_{FSB} / UTC_{LWR}$	1.50	1.75
fixed charge rate, FCR_{FSB} (1/yr)	0.10	0.10
O&M charge rate for FSB, f_{OM} (1/yr)	0.04	0.04
availability factor for FSB, p_f^{FSB}	0.70	0.70
maximum linear deployment rate for FSB, ϵ_{FSB} (1/yr)	0.04	0.04
FSB time constant, τ_{BNR} (yr) ^(d)	123.7	24.7
capacity reduction for first period	0.50	0.50
power constraint as fraction of P_E	0.33	0.33

Table IV Key Input Parameters to Nuclear Energy Module Used in ERB Model (Cont.-3)

-
- (a) in actuality, beginning value with increase to 0.85 over course of ~100 year computation, following Ref. 7.
 - (b) parametically varied (Fig. 50).
 - (c) refer to Sec. III.C.2.b. for derivation and details of approach.
 - (d) $\tau_{\text{FSB}} = 2 \cdot \text{SI}_{\text{FSB}} \cdot x_{\text{Pu}}^{\text{FSB}} / [(1 - \text{CR}) p_f \alpha]$, where $\alpha = \text{spy}(A_{49}/1000) / (E_f e N_A) = 0.39$ kgPu/MWt/yr.

Table A-I. Parameters Used to Evaluate Steady-State Equations (A-3)-(A-6)

Specific inventories, SI_j (kgHM/MWt)	
• LWR	27.7
• LMR	67.6
Thermal conversion efficiencies, η_{TH}^j	
• LWR	0.325
• LMR	0.40
LWR burnup, BU_{LWR} (MWtd/kgHM)	40.
Bred plutonium LWR concentrations, y_{Pu}^j	
• UOX region	0.009
• MOX region	0.009
Fuel plutonium concentrations, x_{Pu}^j	
• LWR MOX region at BOL	0.04
• LWR MOX region at EOL	0.01 ^(a)
• LMR driver region	0.10
Plutonium (MOX) fission fraction, f_{49}	0.70
LWR capacity/availability factor, p_f	0.70
Power ratio, P_E^{LWR} / P_E^{LMR}	30. ^(b)
Reference Pu accumulation rate, R_{REC_0} / P_{E_0} (kgPu/yr/MWe)	0.177 ^(c)
Number of MOX recycles, N	4
Equilibrium MOX core volume fraction, f_{MOX}	Eq. (A-3)
Rate of MOX introduction, λ_{MOX} (1/yr)	0.0347 ^(d)
Asymptotic MOX core fraction, f_{MOX}^f	0 \rightarrow 0.3
LWR core recycle time, τ_{MOX} (yr)	3.0
Normalization parameter, $R_{ACC_0} y_{Pu}^{UOX} / P_{E_0}$ (kgPu/yr/MWe)	0.1769

(a) from Eq. (A-2)

(b) chosen only to evaluate the ratio τ_{LMR}/τ_{LWR} .

(c) $R_{REC_0} = dp y p_f y_{Pu}^{UOX} / (\eta_{TH}^{LWR} BU)$, using above-listed values.

(d) corresponds to a “half-time”, $T_{MOX} = \ln(2)/\lambda_{MOX} = 20$ yr.

Table A-II. Comparison of LMR and ATW Fast-Spectrum Burners (FSBs) of Plutonium

	LMR ^(a)	ATW ^(b)
Nominal thermal power, P_E/η_p	3000.	3000.
Thermal conversion efficiency	0.40	0.40
Engineering gain, ^(c) Q_E	25.	7.
Plant efficiency, η_p ^(d)	0.384	0.343
Minimum conversion ratio, CR	0.6	0.0
Average (core) power density, PD(MWt/m ³)	200.	300.
Average core (HM) density, $\langle\rho\rangle$ (kgHM/m ³)	4000.	2000.
Fuel weight fraction, x_{Pu}	0.10	0.10
Specific power, SI(kgHM/MWt)	50.	20.
Plutonium specific power, x_{Pu} SI(kgHM/MWt)	5.0	2.0
Plant availability, p_f	0.70	0.70
Time to fission active inventory, $SI x_{Pu}/\alpha/p_f$	18.3	7.3
FSB introduction rate, ϵ (1/yr)	0.02	0.02
Inventory buildup parameter, $\epsilon SI x_{Pu}/\alpha/p_f$	0.37	0.15
Burn capability, R_{ACC}/R_{BNR}	0.77	1.15
Specific burn rates:		
• per net-electric power, R_{ACC}/P_E (kgPu/MWe/yr)	0.55	0.92
• per gross thermal power, R_{ACC}/P_{TH} (kgPu/MWt/yr)	0.21	0.31
Net-electric support ratio, $SR_{FSB}^{(e)}$	3.1(1.6)	5.2(4.5)

(a) nominal values.

(b) Ref. 46,47.

(c) ratio of gross electric power to recirculated power; inverse of recirculating power fraction.

(d) $\eta_p = \eta_{TH} (1 - 1/Q_E)$.

(e) Eq. (A-16) for $\langle y_{Pu} \rangle = y_{Pu}^{UOX}$ and the values listed in this table; values in parentheses set $\epsilon = 0.0$ 1/yr (e.g., only actual plutonium burning).

Table A-III. Typical Financial and Costing Parameters

Fixed charge rate for capital, FCR(1/yr)		0.10
O&M costs as a function of		
total capital cost, $f_{OM}(1/yr)^{(a)}$		0.03
Unit total cost, UTC(\$/We) ^(b)		2.0
Plant availability, p_f		0.70
Unit cost of accelerator, $UC_{ACC}(\$/Wb)^{(c)}$		10.6
Relative cost penalty, $\langle COE \rangle / COE_{LWR}$	LMR	ATW
• no growth ($\epsilon = 0.0$) ^(d)	1.24	1.17
• growth ($\epsilon = 0.02$ 1/yr) ^(d)	1.15	1.15

(a) typically values of ~ 0.02 1/yr are found, but a higher rate was used here for both ATW and LMR systems because of the chemical processing associated with each system, and the assumption of the ultimate waste disposal placed on the FSBs.

(b) UTC is expressed per unit of total power and includes all indirect charges, which typically amounts to $\sim 70\%$ of direct costs.

(c) per unit of proton beam power delivered to the neutron spallation target.

(d) refer to last entry into Table A-II.

FIGURES

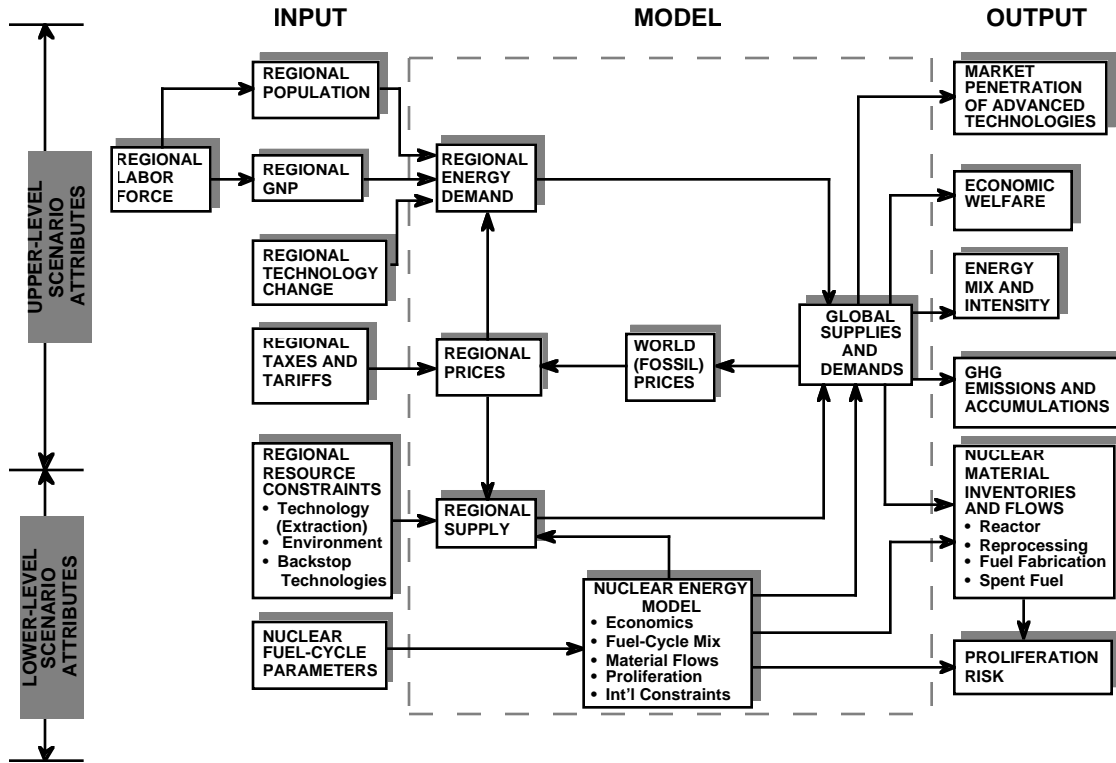


Figure 1. Structural layout of ERB global E³ model³ as adapted and modified for the present study: four main components comprise the ERB economic-equilibrium model: energy demand; energy supply; energy balance; and greenhouse-gas (GHG) emissions. The relationships between inputs and interated outputs, as well as the addition of a (higher fidelity) nuclear energy model (resources, costs, nuclear-materials flows and inventories, and proliferation risk) are also shown.

AREAL REGIONAL MAP

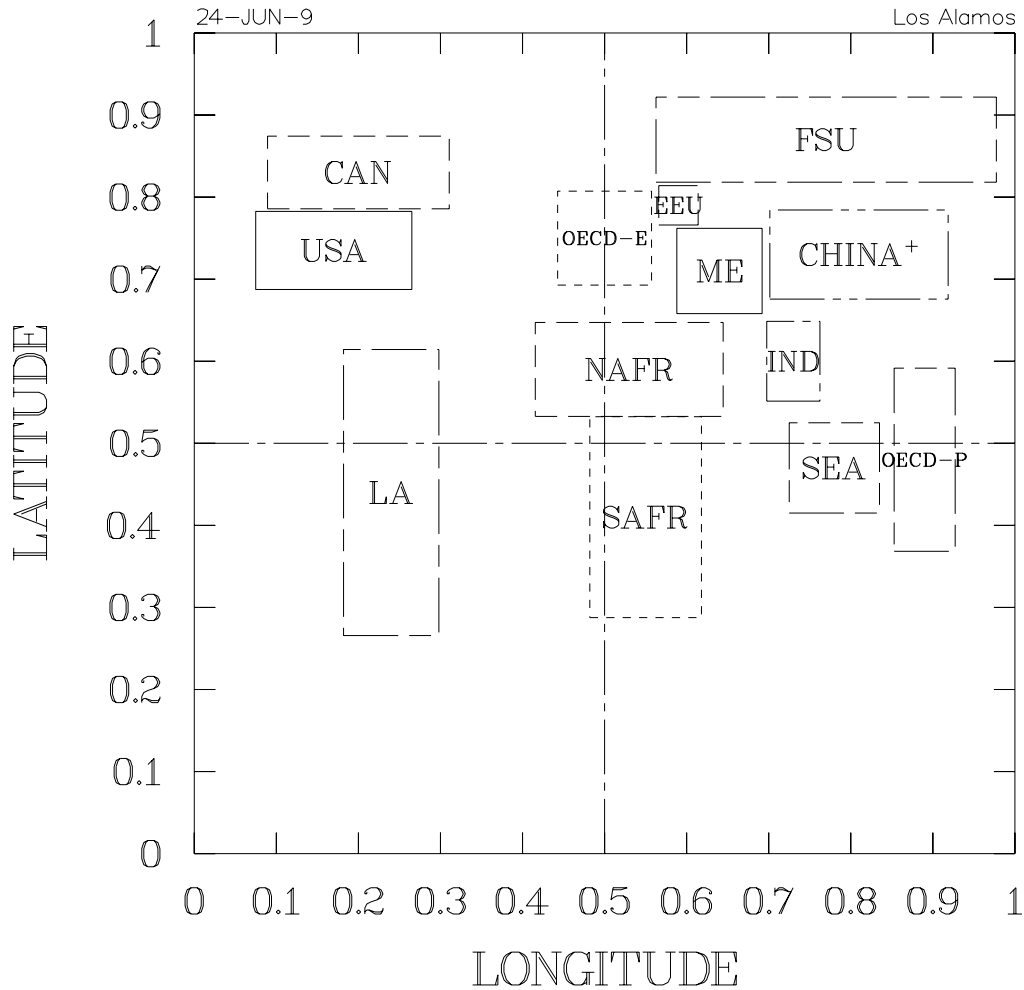


Figure 2. Schematic map of thirteen-region ERB model, with the area of each stylized rectangular region reflected the respective land masses. The following regional identifiers are used: 1) USA = United States; 2) CAN = Canada; 3) OECD-E = OECD-Europe; 4) OECD-P = Pacific; 5) EEU = Eastern Europe; 6) FSU = Former Soviet Union; 7) CHINA⁺ = China; 8) ME = Middle East; 9) NAFR = North Africa; 10) SAFR = Southern Africa; 11) LA = Latin America; 12) IND = India; and 13) SEA = South and East Asia.

Maro-regions aggregated as follows:

$OECD = USA + CAN + OECD-E + OECD-P$
 $REF = FSU + EEU$
 $DEV = LA + NAFR + SAFR + CHINA^+ + SEA + ME$

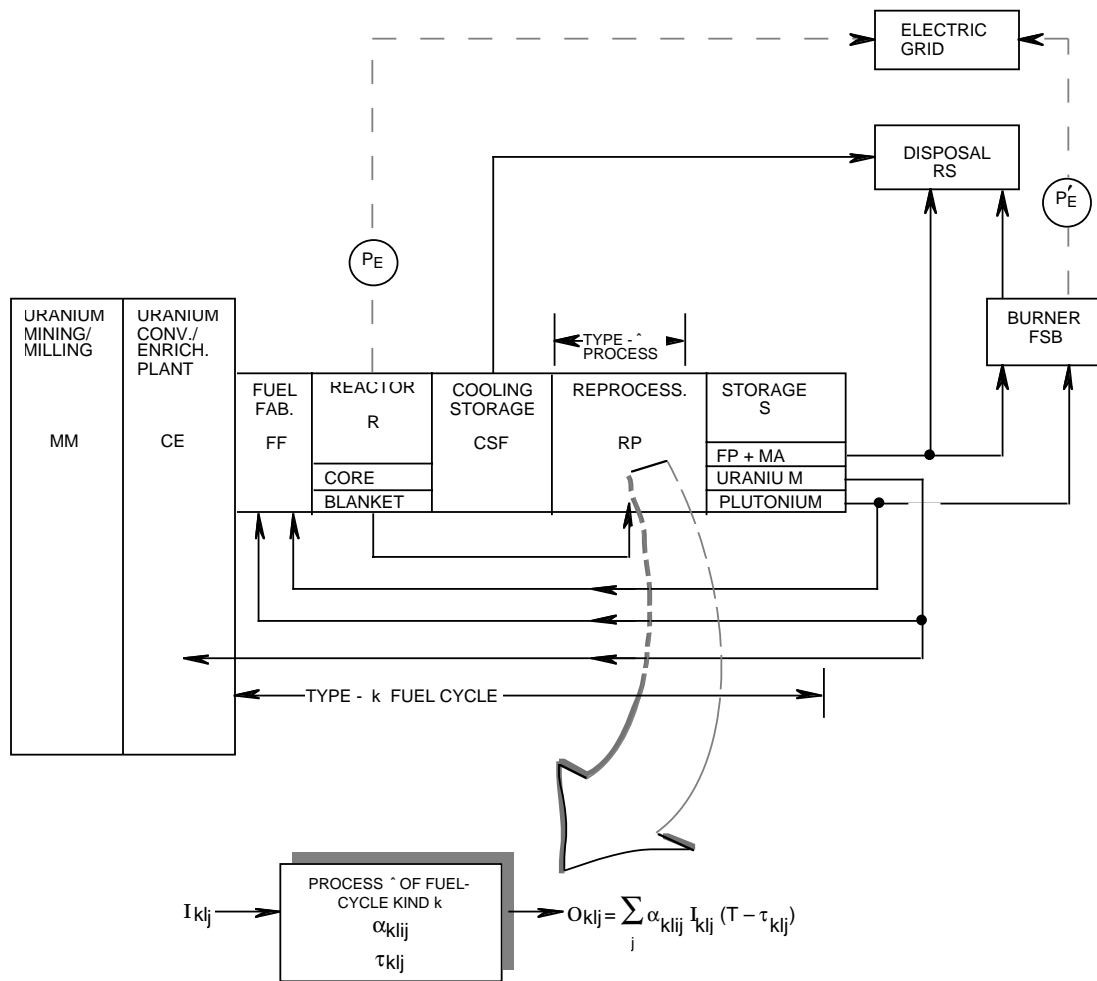


Figure 3A. Schematic diagram of nuclear materials model used in ERB: Condensation of nuclear fuel cycle into a series of generic fuel-cycle “building blocks” for use in estimating resource-constrained, multivariable optimizations²⁵ of nuclear-energy mixes and nuclear-materials flows and inventories; also shown is a generalized process-flow diagram illustrating input-output formulations²⁵ adopted for the fuel-cycle analyses performed “under” the ERB model.¹⁵

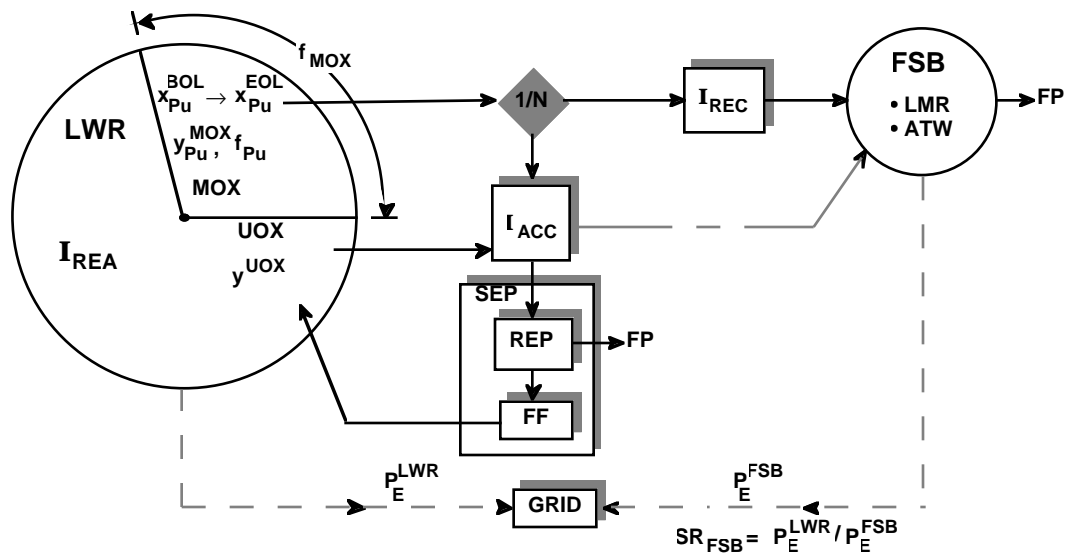


Figure 3B. Schematic diagram of nuclear materials model used in ERB: Nuclear material flows between reactor (REA), spent fuel (ACC = LWR-recyclable, REC = LWR-nonrecyclable), reprocessing (REP), and fuel fabrication (FF), with all separated plutonium identified as SEP = REP + FF; the integration with a Fast-Spectrum Burner (FSB = LMR or ATW) is indicated.

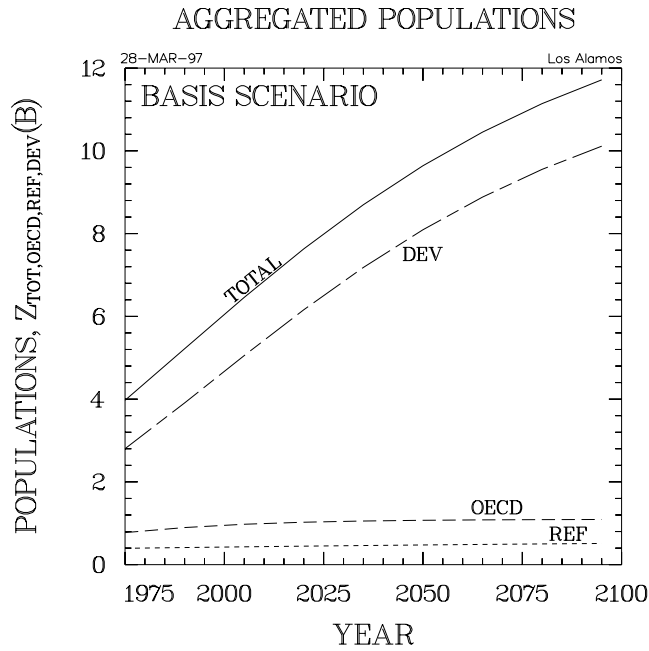


Figure 4A. Aggregated exogenous population growth used for basis scenario.

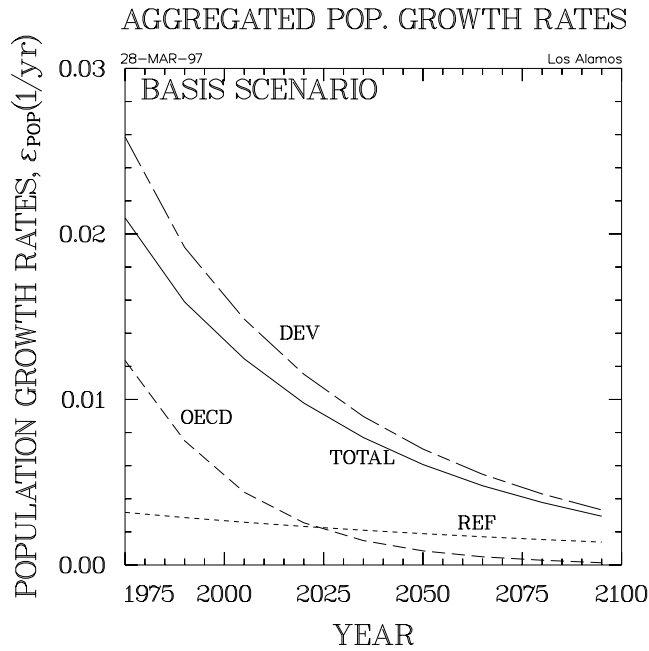


Figure 4B. Aggregated exogenous population growth rates used for basis scenario.

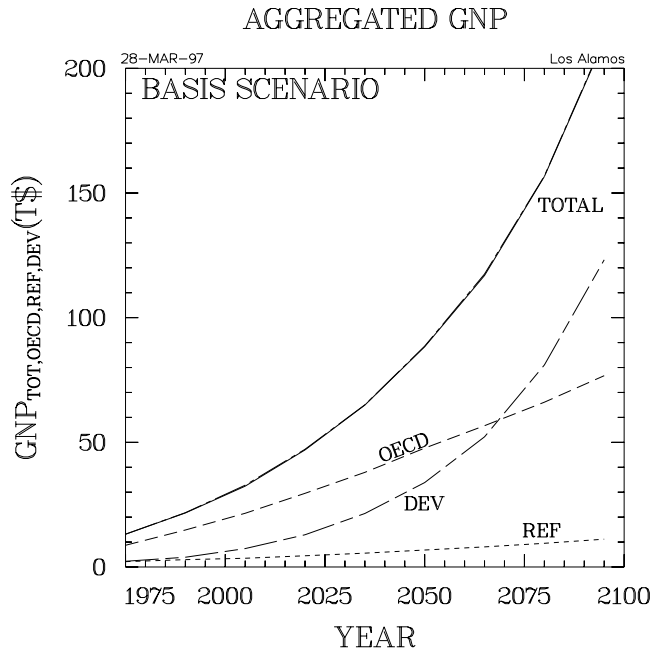


Figure 5A. Aggregated GNP that result from the basis scenario computation.

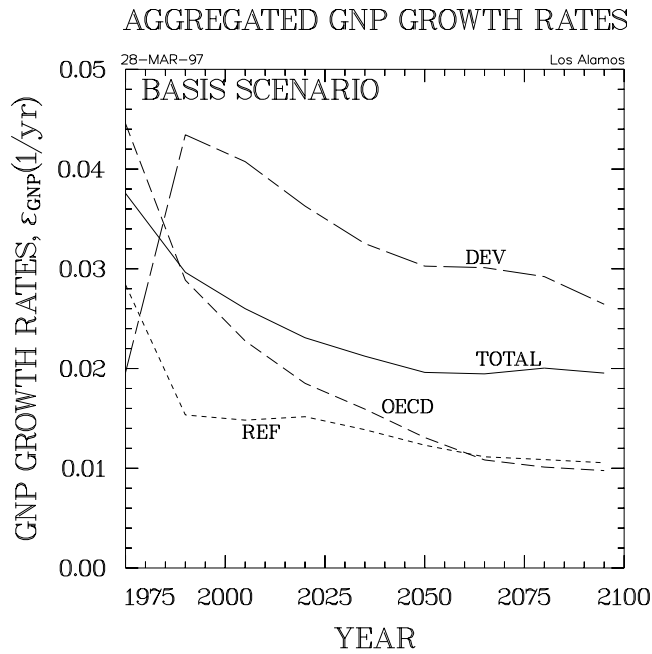


Figure 5B. Aggregated GNP growth rates that result from the basis scenario computation.

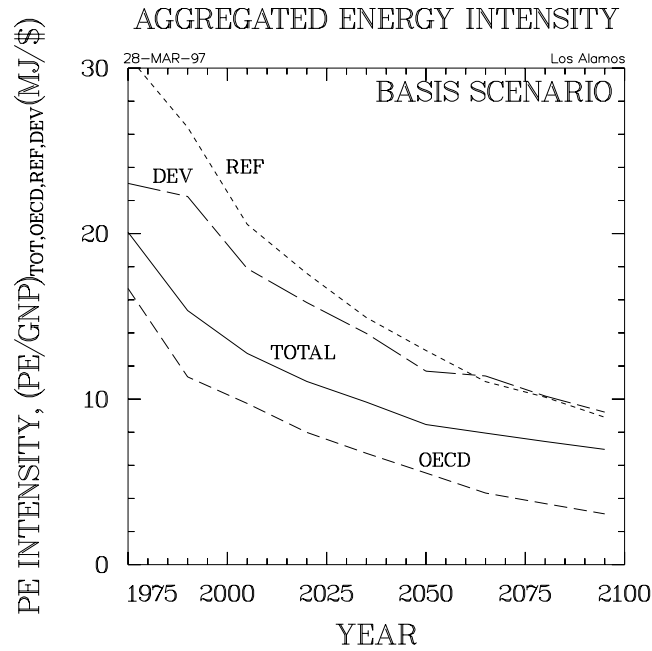


Figure 6A. Aggregated energy intensities that result from the basis scenario computation.

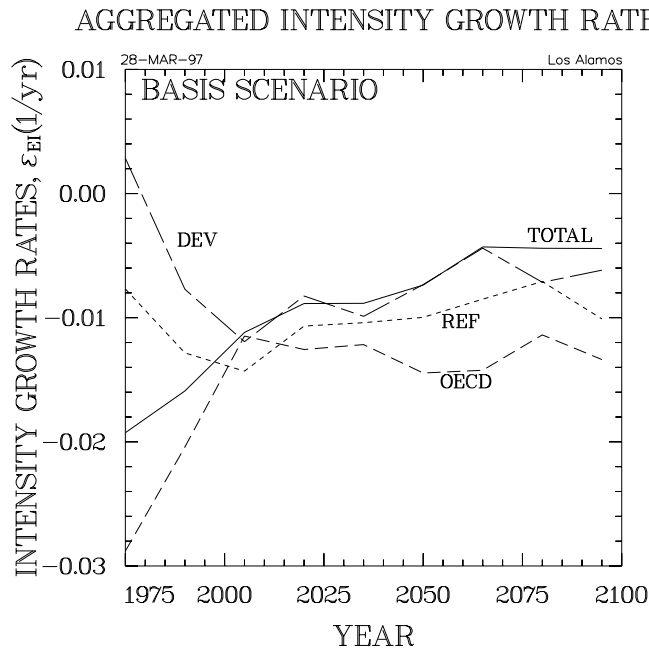


Figure 6B. Aggregated energy intensities rates of decrease that result from the basis scenario computation.

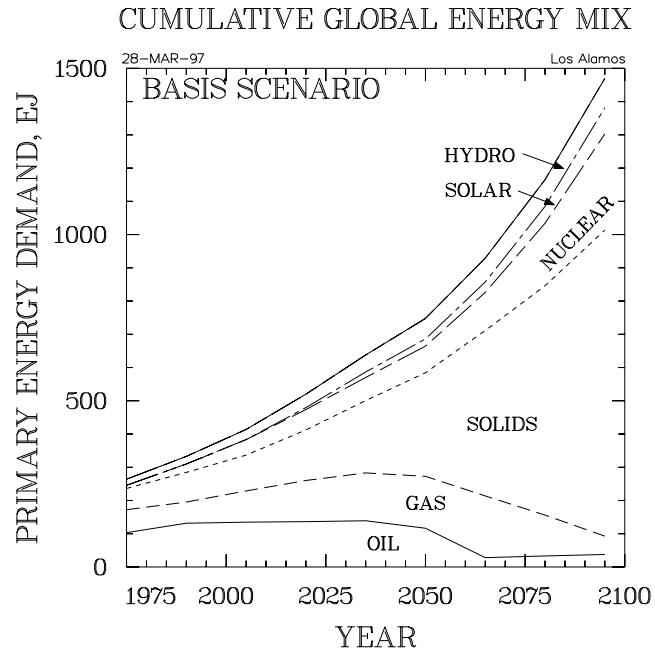


Figure 7. Cumulative evolution of global primary energy mix for the basis scenario (solids = coal + biomass).

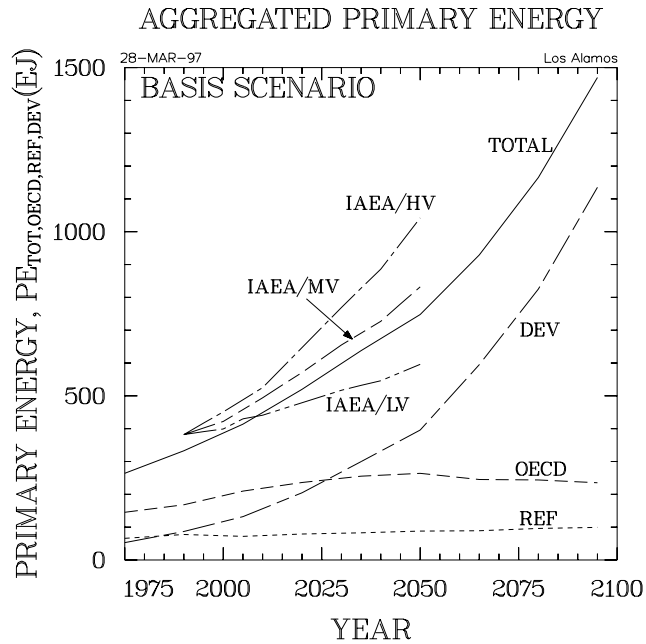


Figure 8A. Evolution of aggregated total primary energy for the basis scenario; a comparison is made with the Ref. 7. high (HV), medium (MV), and low (MV) variants, as adopted from the WEC/IIASA⁵ study.

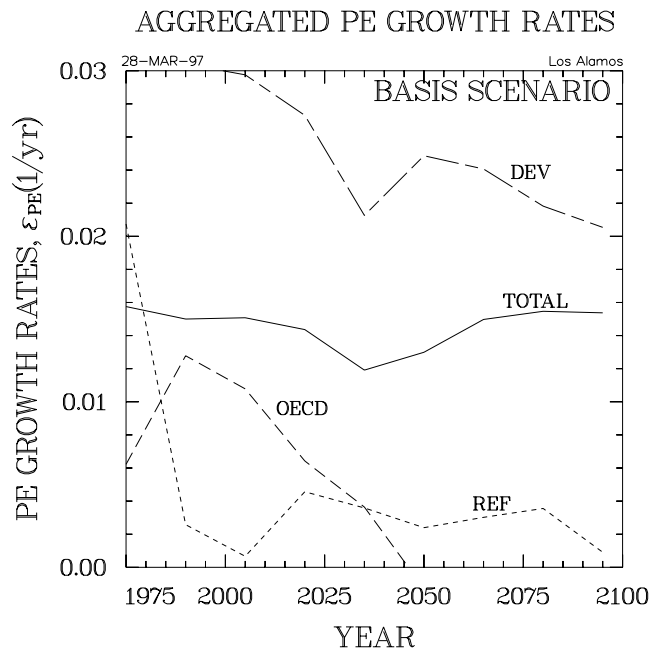


Figure 8B. Evolution of aggregated total primary energy growth rates for the basis scenario; a comparison is made with the Ref. 7. high (HV), medium (MV), and low (MV) variants, as adopted from the WEC/IIASA⁵ study.

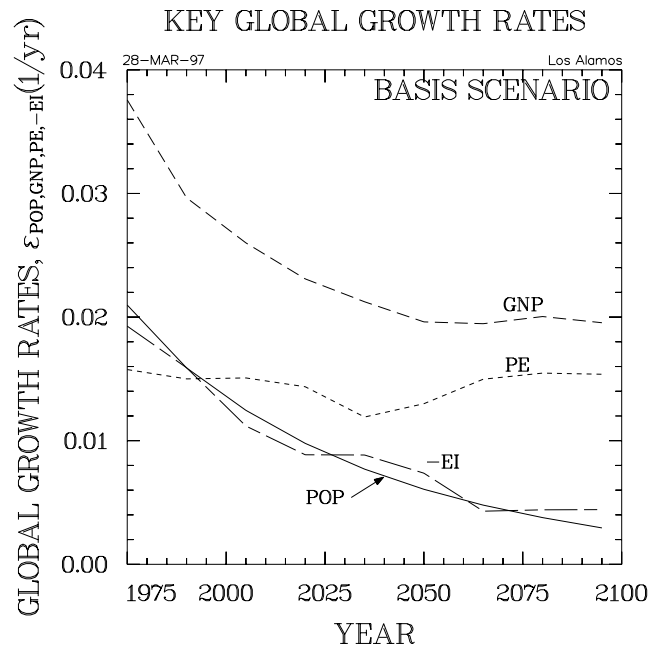


Figure 9. Summary of global growth rates for population, GNP, total primary energy, and energy intensity (decrease) for the basis scenario.

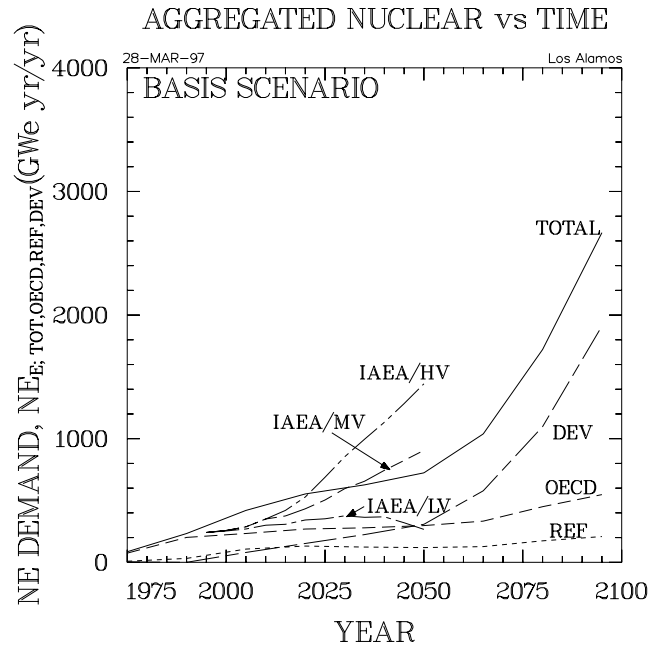


Figure 10A. Aggregated nuclear energy growth for the basis scenario; a comparison is made with the Ref. 7. high (HV), medium (MV), and low (MV) variants, as adopted from the WEC/IIASA⁵ study).

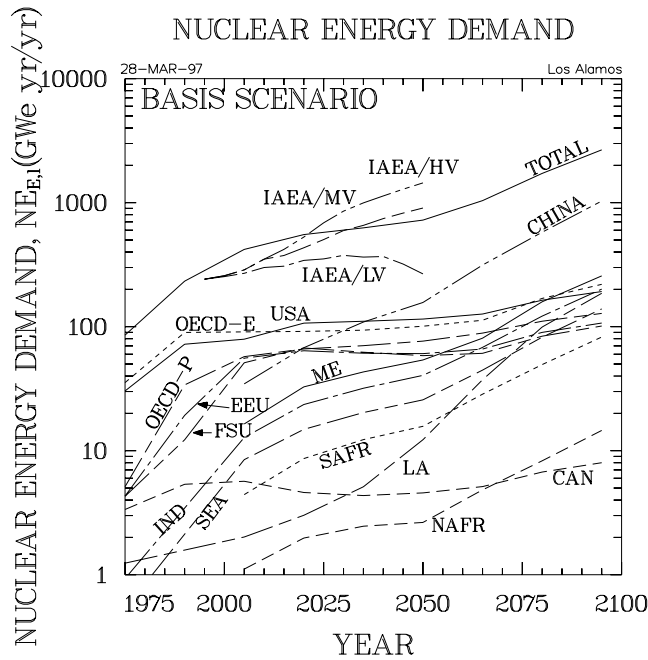


Figure 10B. Regional (13) nuclear energy growth for the basis scenario; a comparison is made with the Ref. 7. high (HV), medium (MV), and low (MV) variants, as adopted from the WEC/IIASA⁵ study (refer to Fig. 2 for regional notation).

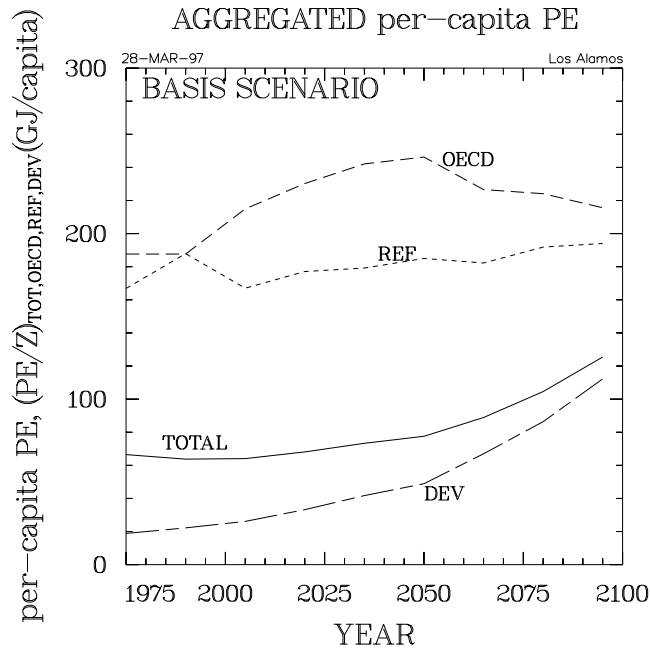


Figure 11. Aggregated evolution of *per-capita* (total) primary energy use for the basis scenario.

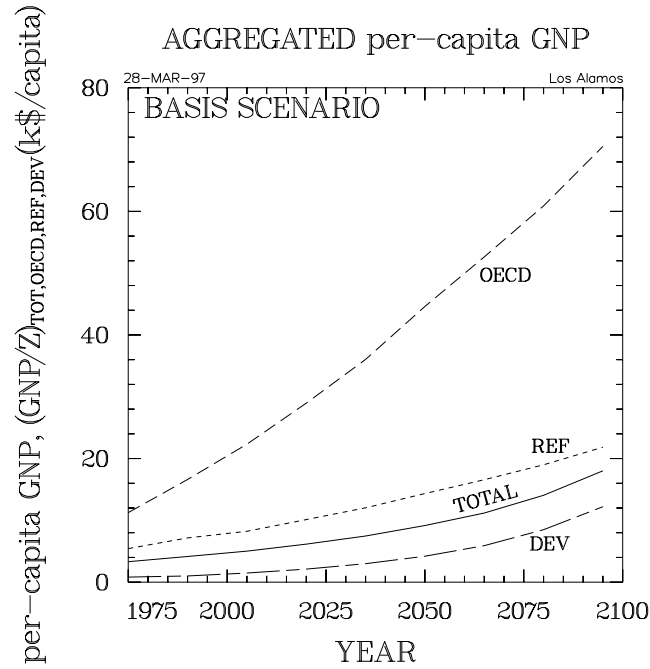


Figure 12. Aggregated evolution of *per-capita* GNP for the basis scenario.

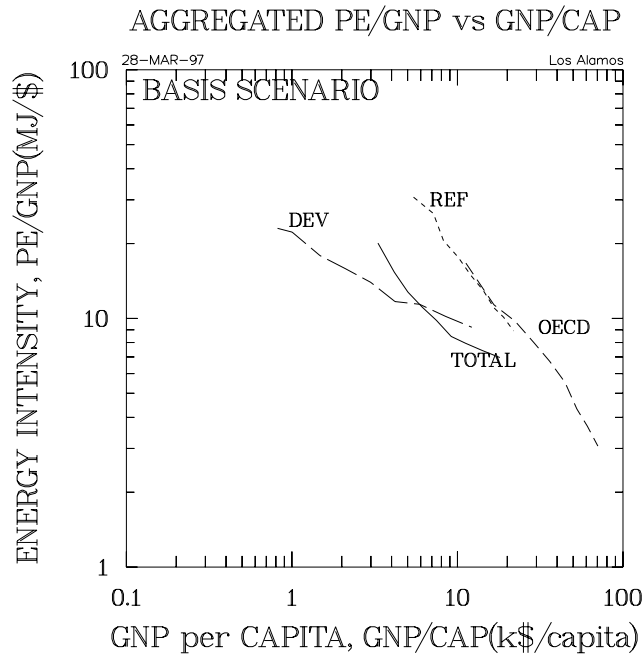


Figure 13A. Evolution of aggregated energy intensity and *per-capita* GNP for the basis scenario: Aggregated macro-regions.

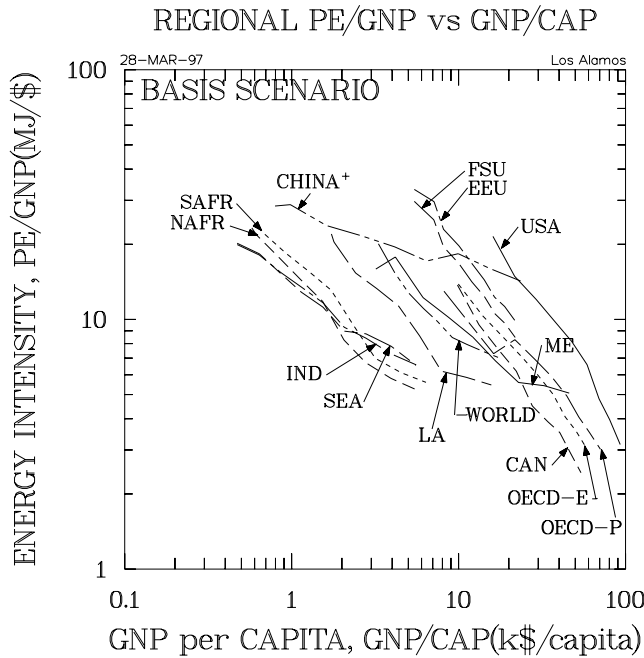


Figure 13B. Evolution of regional (13) energy intensity and *per-capita* GNP for the basis scenario: Thirteen model regions (refer to Fig. 2 for regional notation).

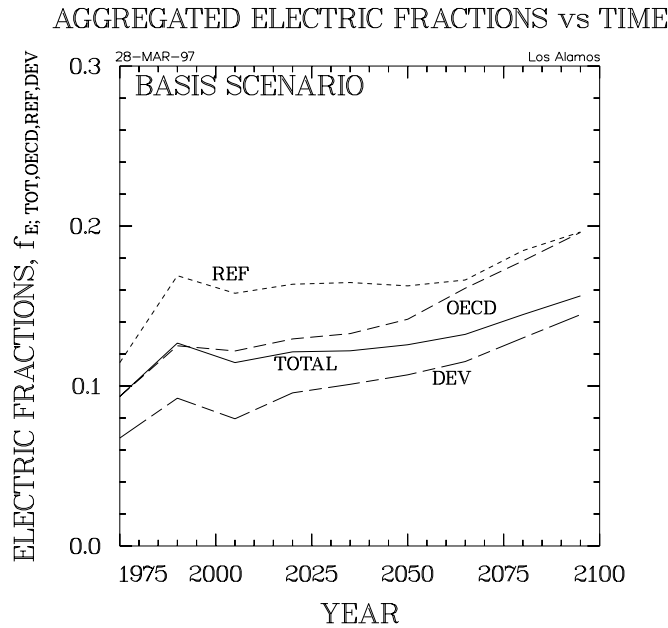


Figure 14. Aggregated evolution of electricity fractions for the basis scenario.

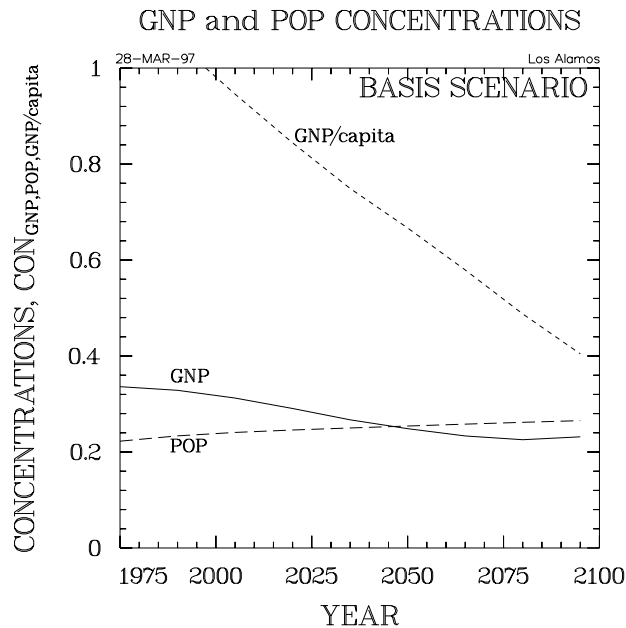


Figure 15. Evolution of global concentration⁴³ for population, GNP, and *per-capita* GNP for the basis scenario. The measure of concentration of a given global “capability” (to enforce change), CON_j is defined as

$$\sqrt{\left(\sum_i S_{ij}^2 - 1\right) / \left(1 - 1/N\right)},$$

where S_{ij} is the fraction of capability j (defense, economic, trade, *etc.*) shared by a given region i , N is the number of such regions (or actors), and $1/N$ would be the average value of capability S_{ij} were it uniformly distributed; $CON_j = 1$ infers a hegemonic world, and $CON_j = 0$ infers a fully equipartitioned world.

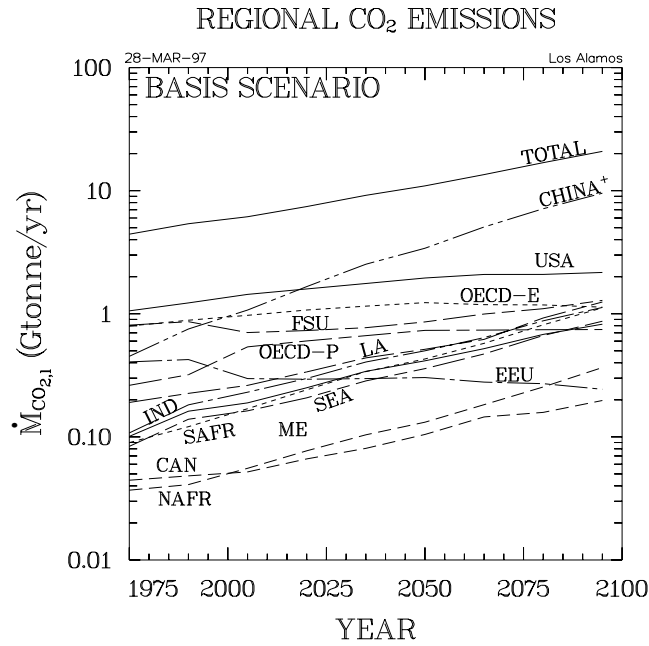


Figure 16. Carbon dioxide emissions as function of region for the basis scenario (refer to Fig. 2 for regional notation).

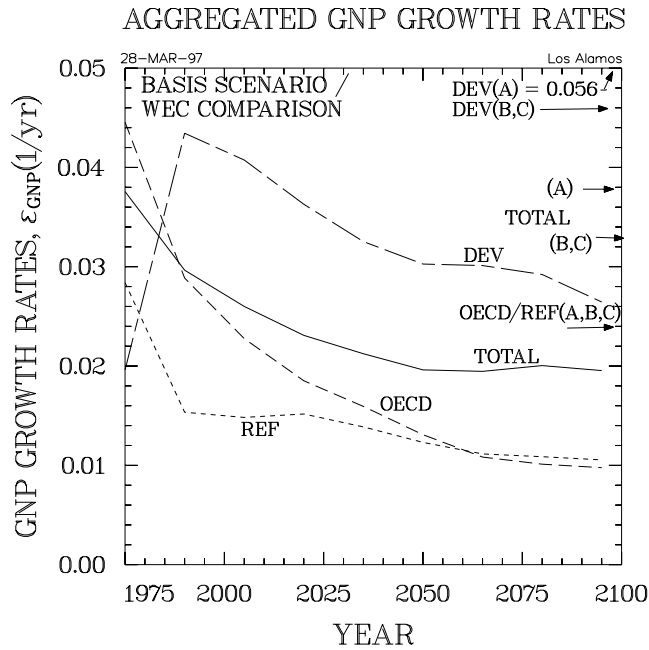


Figure 17. Comparison of growth in world GNP for the basis scenario with three WEC cases:^{5,6} Case A = High Growth; Case B = Base Case; Case C = Ecologically Driven.

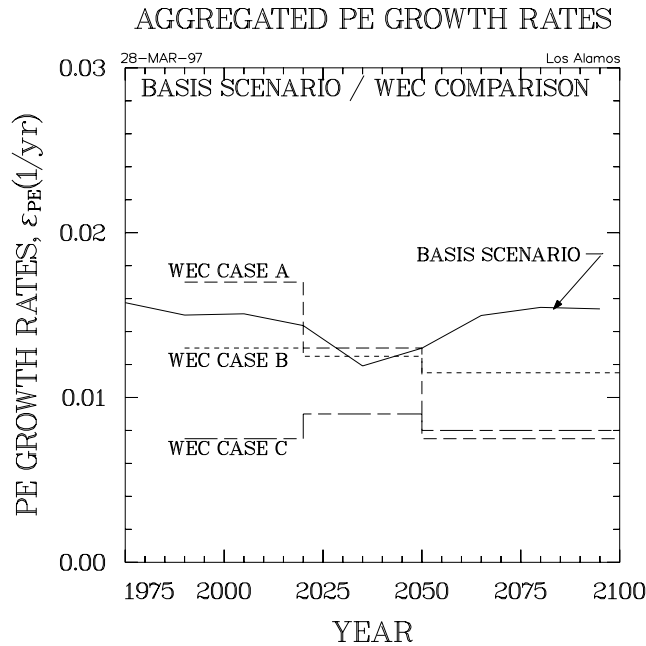


Figure 18. Comparison of growth in total primary energy demand for the basis scenario with three WEC cases:^{5,6} Case A = High Growth; Case B = Base Case; Case C = Ecologically Driven.

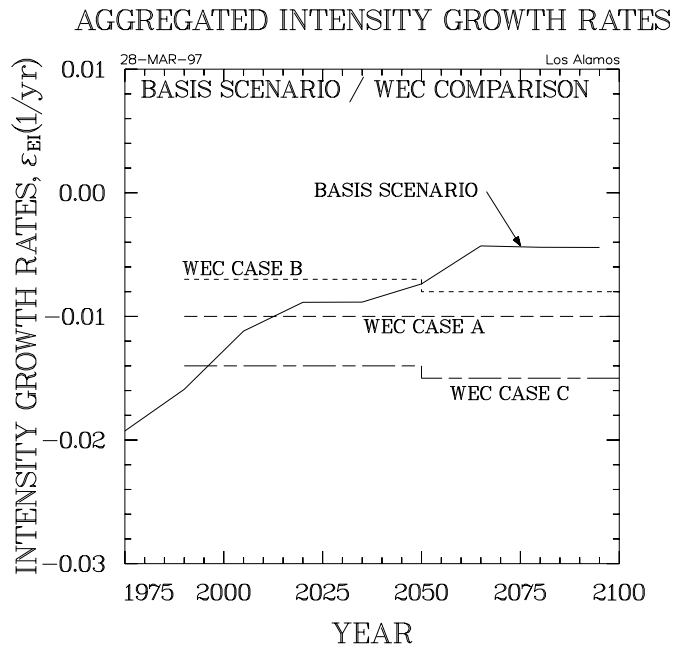


Figure 19. Comparison of rate of primary energy intensity decrease for the basis scenario with three WEC cases:^{5,6} Case A = High Growth; Case B = Base Case; Case C = Ecologically Driven.

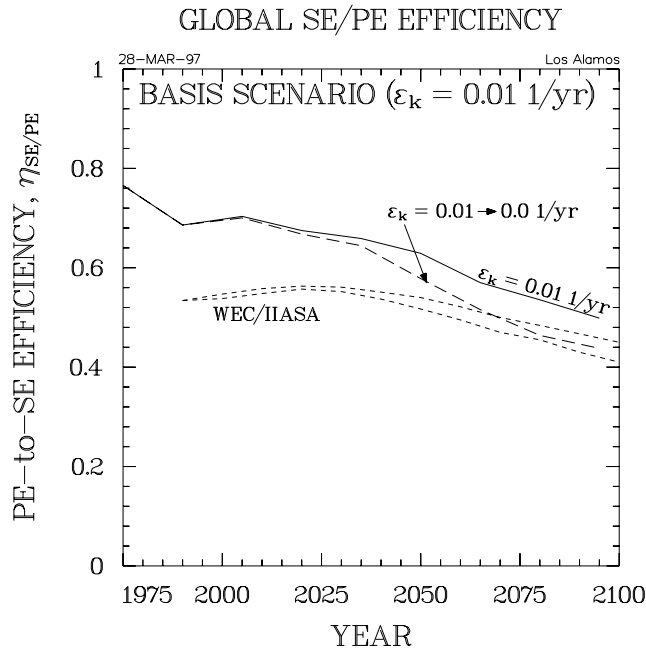


Figure 20. Comparison of primary-to-secondary energy efficiencies; ϵ_k is related to an autonomous energy efficiency improvement, AEEI,¹⁴ and reflects a non-price inducement to improve the conversion of secondary energy to energy services.

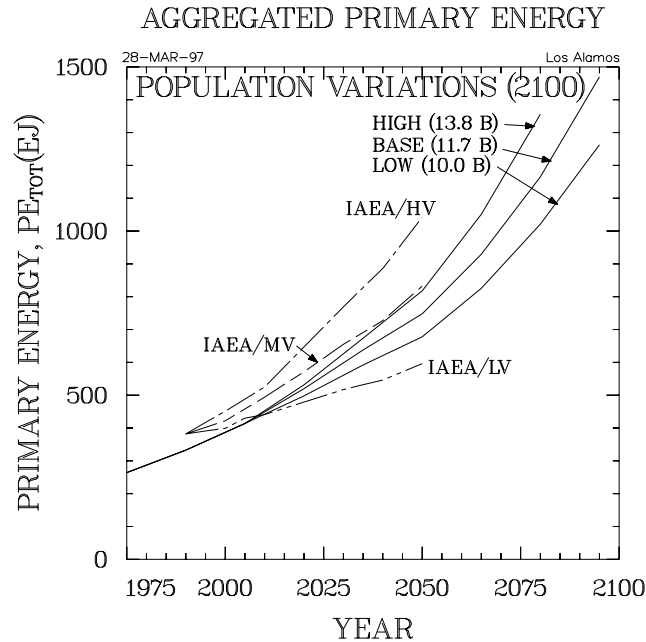


Figure 21. Impact of population variations on primary energy demand, and comparison with the Ref.-7 scenarios.

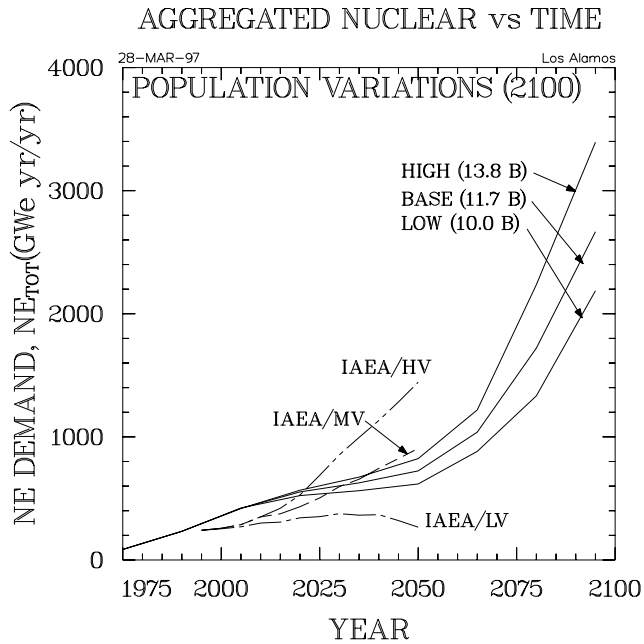


Figure 22. Impact of population variations on nuclear energy demand, and comparison with the Ref.-7 scenarios.

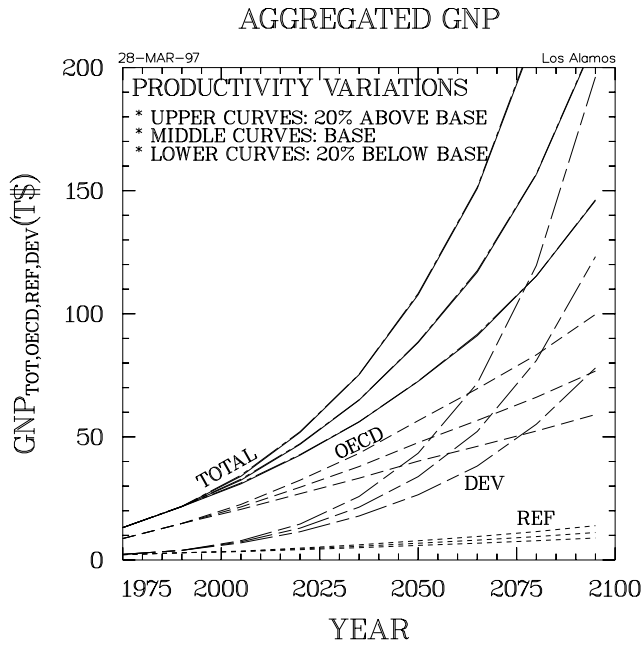


Figure 23. Impact of workforce productivity on GNP for three global aggregates: OECD, REF, and DEV.

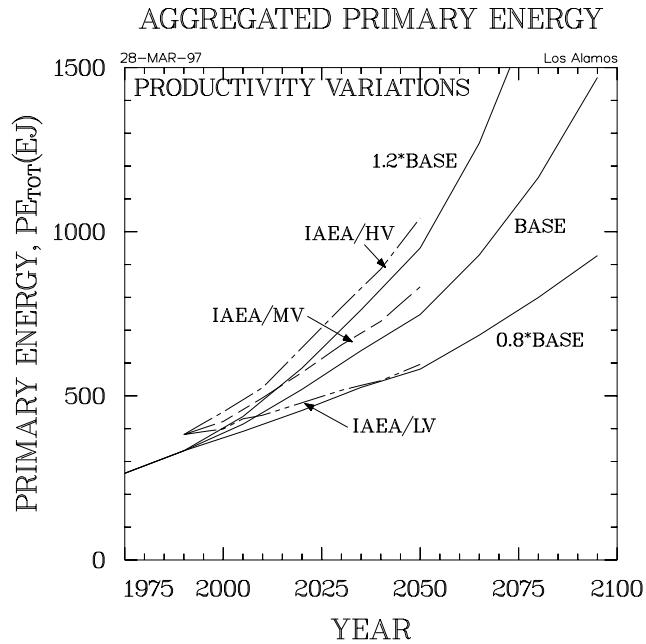


Figure 24. Impact of workforce productivity (GNP) on primary energy demand for three global aggregates: OECD, REF, and DEV, along with comparisons with the Ref.-7 scenarios.

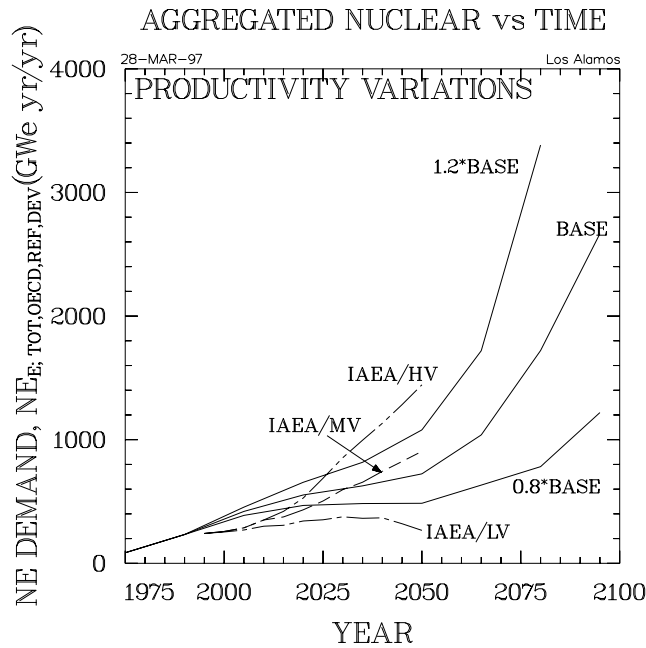


Figure 25. Impact of workforce productivity (GNP) on nuclear energy demand for three global aggregates: OECD, REF, and DEV, along with comparison with the Ref.-7 scenarios.

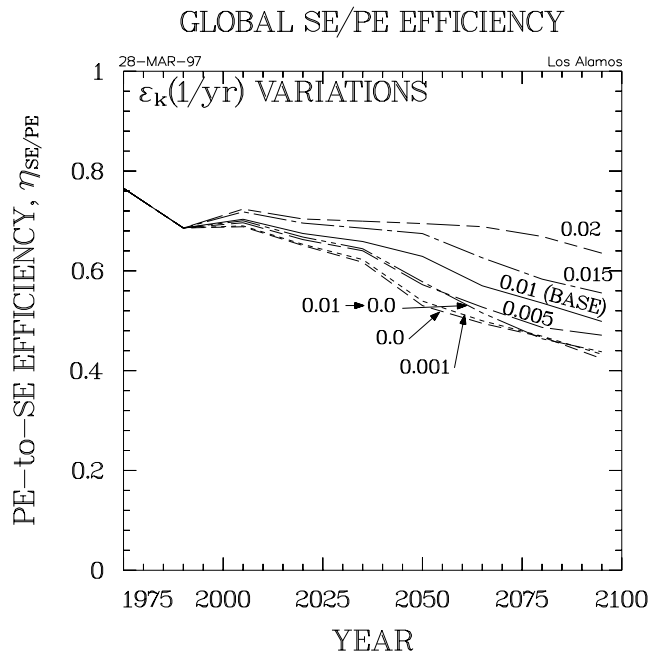


Figure 26. Impact of rate of technology improvement, $\epsilon_k(1/\text{yr})$, that relates j^{th} secondary energy required to meet k^{th} energy service on the primary-to-secondary energy conversion efficiency.

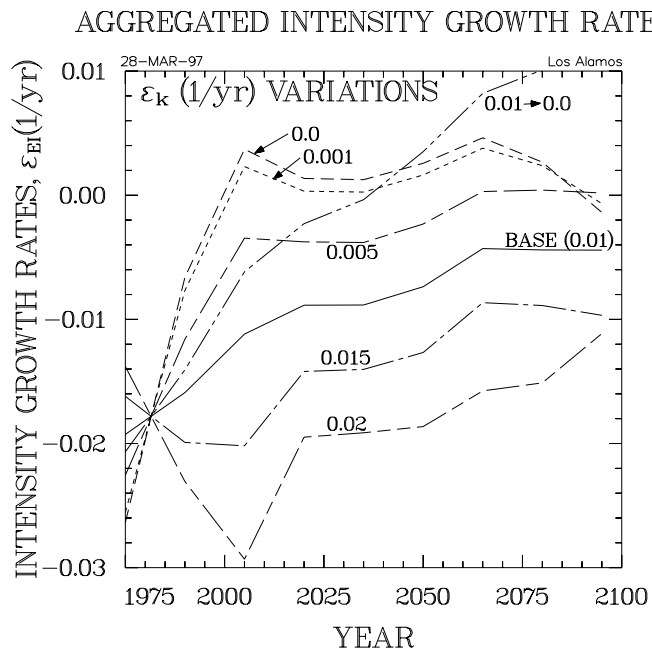


Figure 27. Relationship between primary energy intensity growth rate to rate at which the conversion secondary energy to energy service is improved.

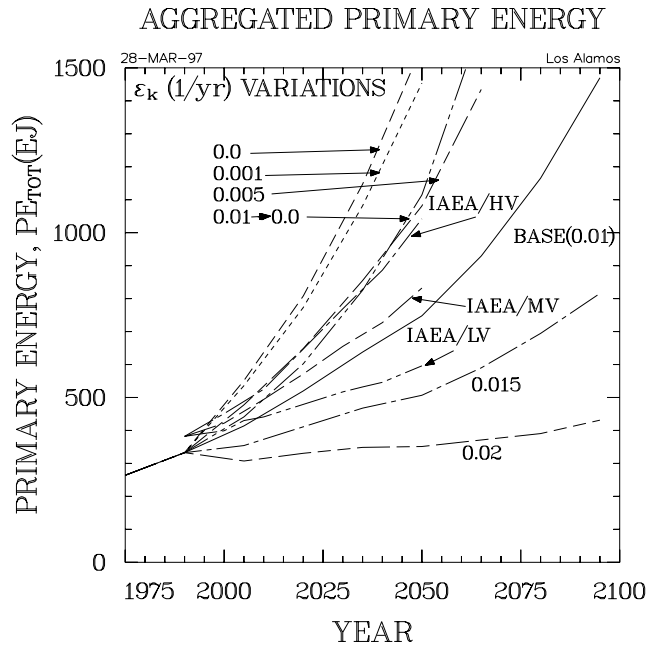


Figure 28. Impact of energy-service technology improvement on total primary energy demand, and comparison with the Ref.-7 scenarios.

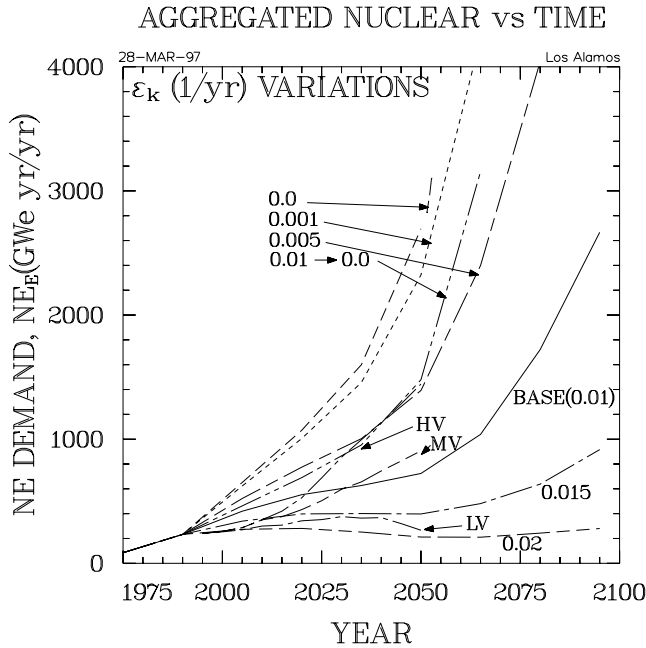


Figure 29. Impact of energy-service technology improvement on total nuclear energy demand, and comparison with the Ref.-7 scenarios.

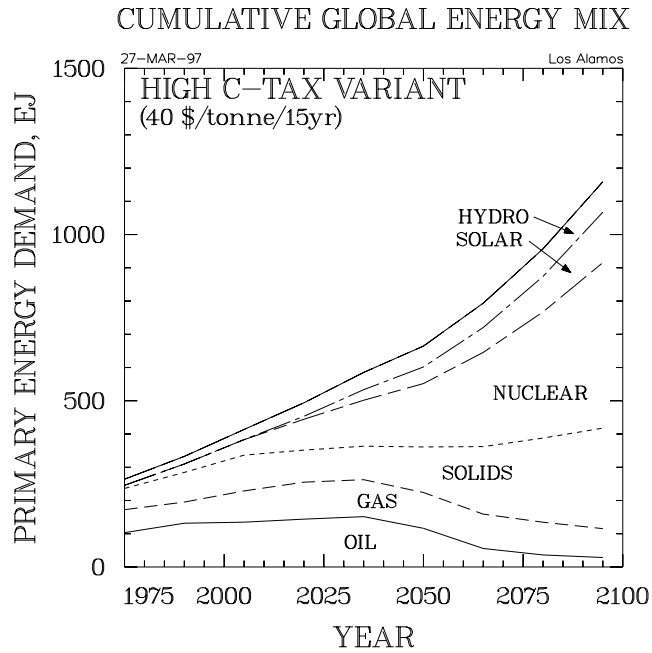


Figure 30. Impact of high carbon tax on total primary energy mix; Fig. 7 gives the comparable information for the basis scenario, when no carbon tax is imposed.

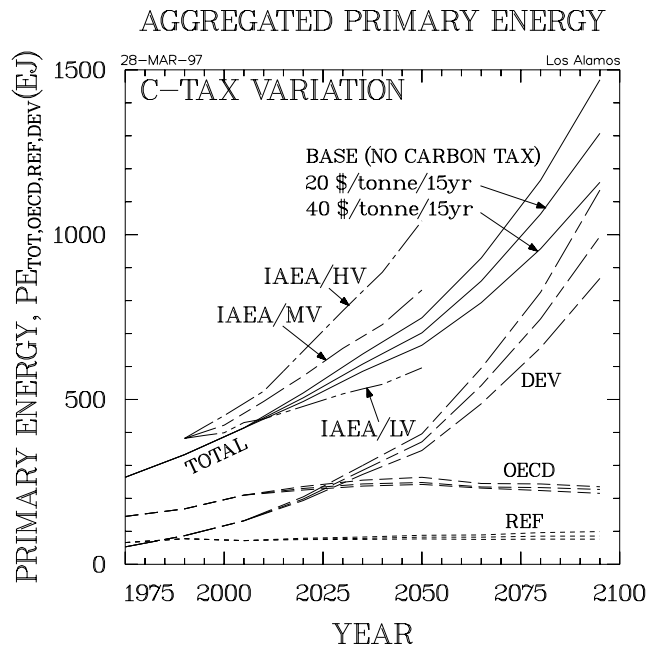


Figure 31. Impact of carbon taxes on primary energy demand for three global aggregates: OECD, REF, and DEV, along with comparison with Ref.-7 scenarios.

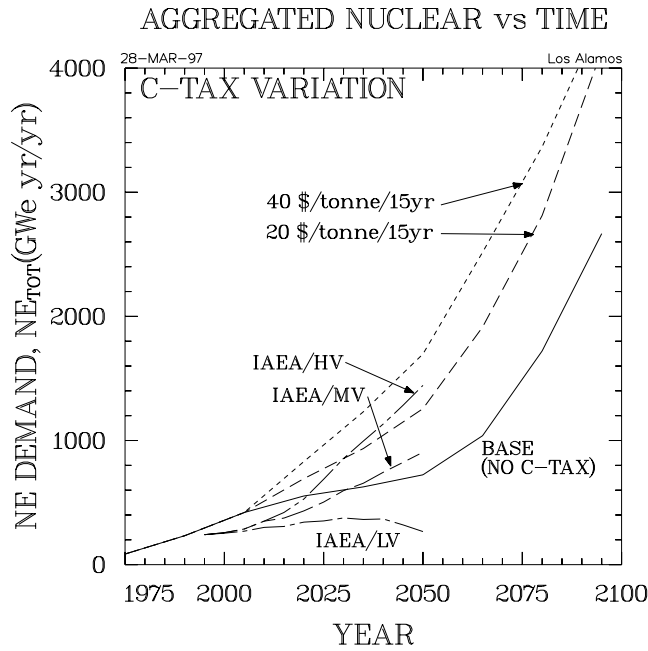


Figure 32. Impact of carbon taxes on nuclear energy demand, and comparison with the Ref.-7 scenarios.

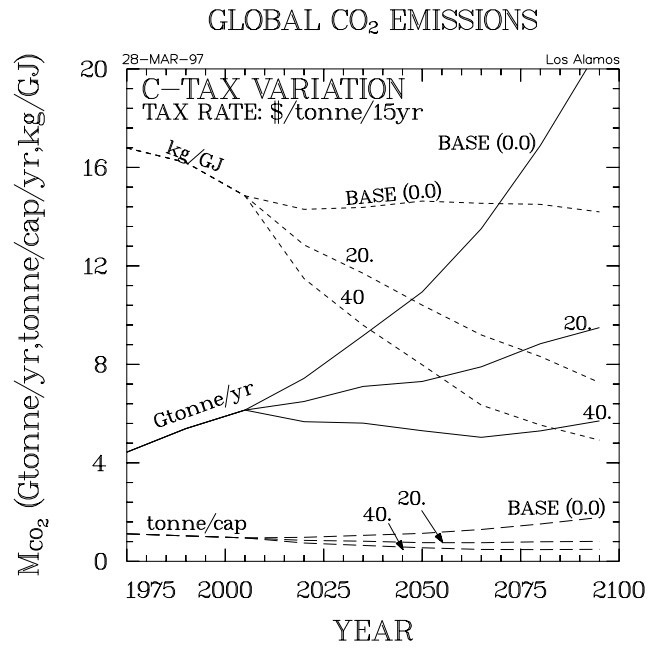


Figure 33. Impact of carbon taxes on total atmospheric carbon emission from carbon dioxide; total carbon *per capita* and per unit of primary energy are shown.

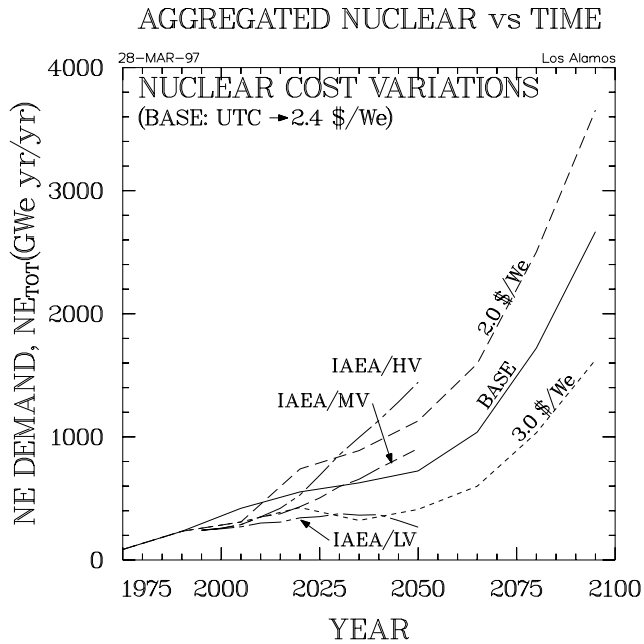


Figure 34. Impact of capital costs on total demand for nuclear energy, and comparison with the Ref.-7 scenarios.

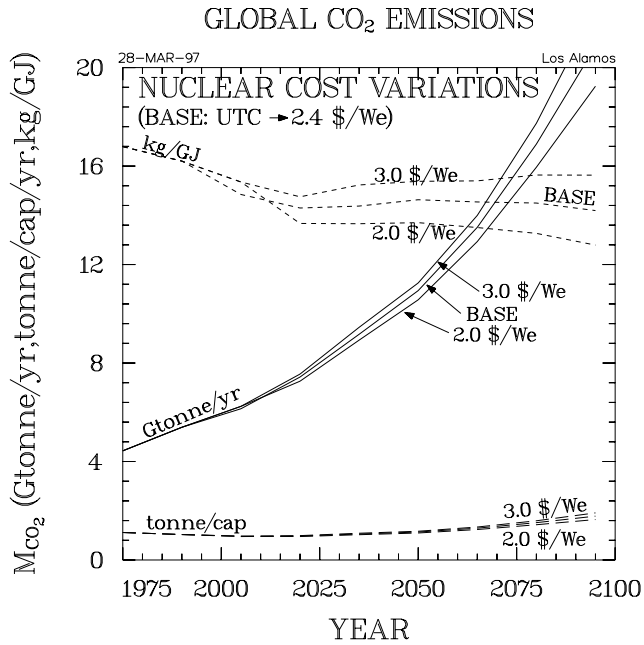


Figure 35. Impact of increased and decrease cost of nuclear energy on the rate of atmospheric carbon emission from carbon dioxide.

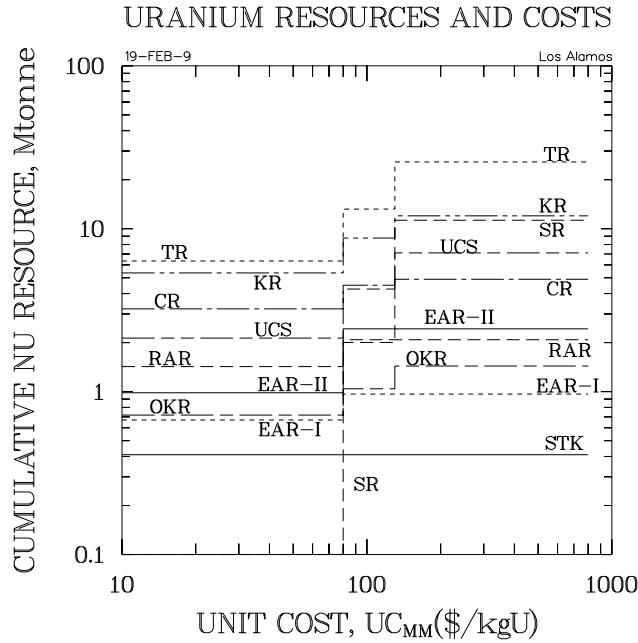


Figure 36A. Uranium resources:^{17,18} STK = reported stocks plus material from arms reductions RAR = reasonably assured resources EAR-I = estimated additional resources OKR = other known resources CR = conventional resources, sum of above (STK + RAR + EAR-I + OKR) UCS = unconventional sources KR = known resources, sum of above (CR + UCS) EAR-II = estimated additional resources SR = speculative resources TR = total resources, sum of above (KR + EAR-II + SR)

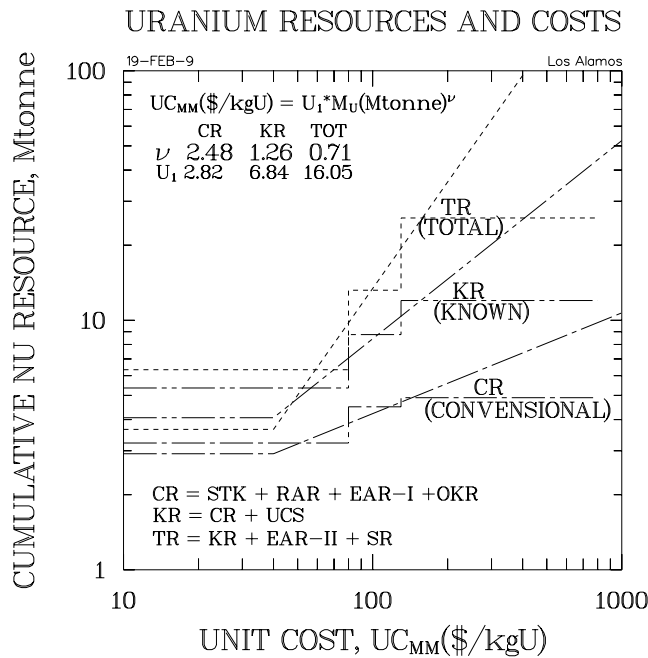


Figure 36B. Uranium resources *versus* cost^{17,18} Uranium resource cost models for Conventional Resources (CR), Known Resource (KR), and Total Resource (TR) assumptions.

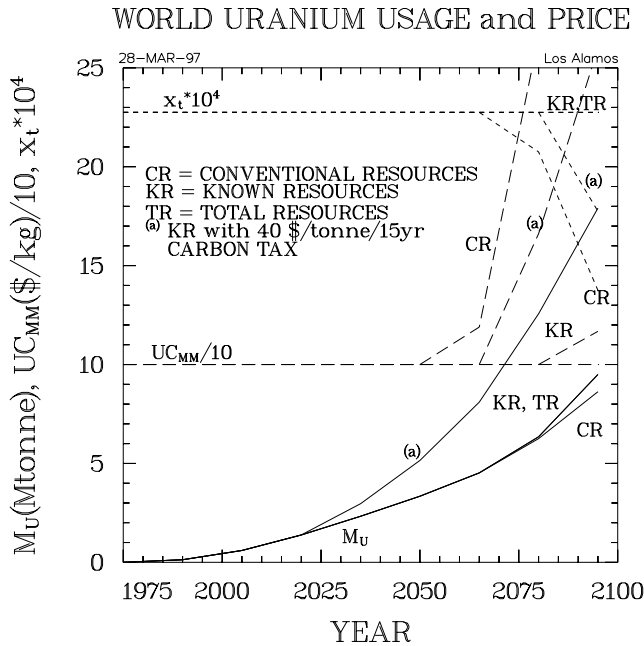


Figure 37. Uranium resource utilization, cost, and cost-optimum tailings concentrations^{24,25} for the basis scenario under three assumptions of resource availability.

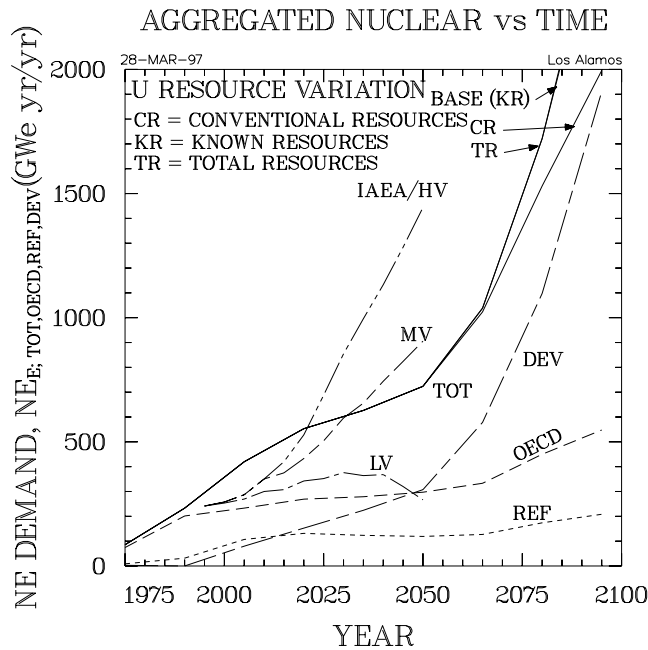


Figure 38. Impact of uranium resource assumption on nuclear energy demand, and comparison with the Ref.-7 scenarios; nuclear energy demand is shown for three global aggregates: OECD, REF, and DEV.

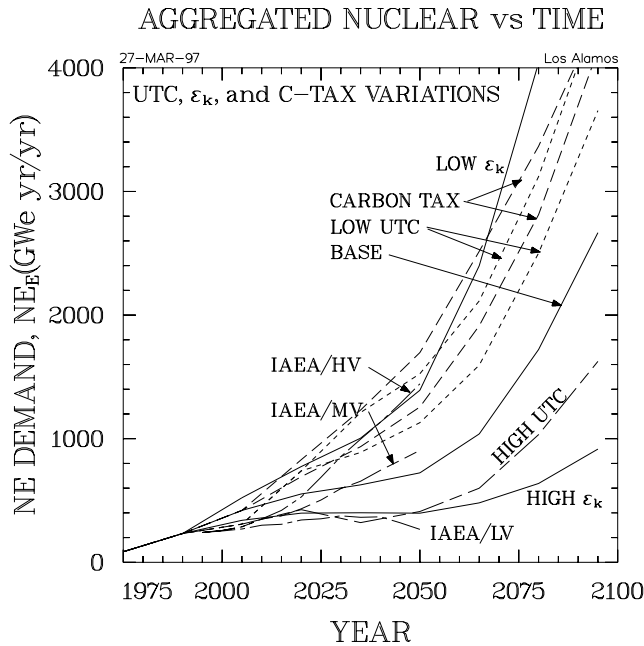


Figure 39. Summary of impacts on nuclear energy demand of energy intensity (SE \rightarrow ES technology improvements), nuclear energy capital costs, and globally uniform carbon taxes, along with comparison to the Ref.-7 scenarios.

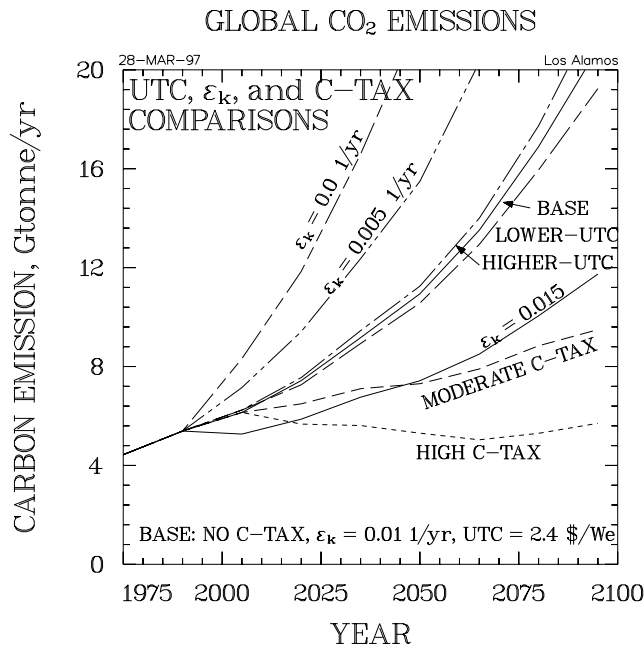


Figure 40. Summary of impacts on atmospheric carbon emissions of carbon taxes, nuclear energy capital costs, and energy-service (SE \rightarrow ES) technology improvement rates.

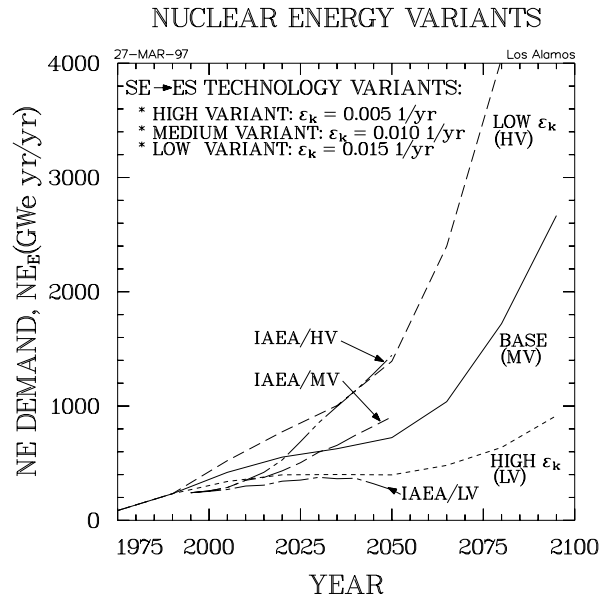


Figure 41. Summary of high-, medium-, and low-demand scenarios based on variations in the rate of technology improvement for conversion of secondary energy (SE) to energy services, ES. The $\epsilon_k = 0.01$ 1/yr corresponds to the basis scenario (Tables III and IV). Comparisons with the Ref.-7 IAEA scenarios are given.

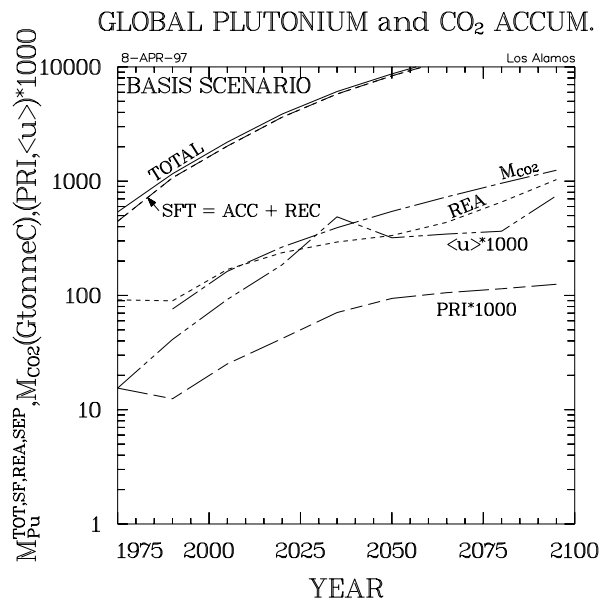


Figure 42. Plutonium and atmospheric carbon accumulations for the basis scenario. Spent-fuel plutonium is accumulated in two forms: recyclable (ACC) and fully recycled (REC); for the once-through LWR basis case, M_{Pu}^{REC} is negligible; average plutonium contained in LWRs is M_{Pu}^{REA} ; measures of proliferation risk are expressed in terms of a relative proliferation utility, $\langle u \rangle$, and a discounted sum of proliferation utilities or a proliferation risk index, PRI.^{4,19}

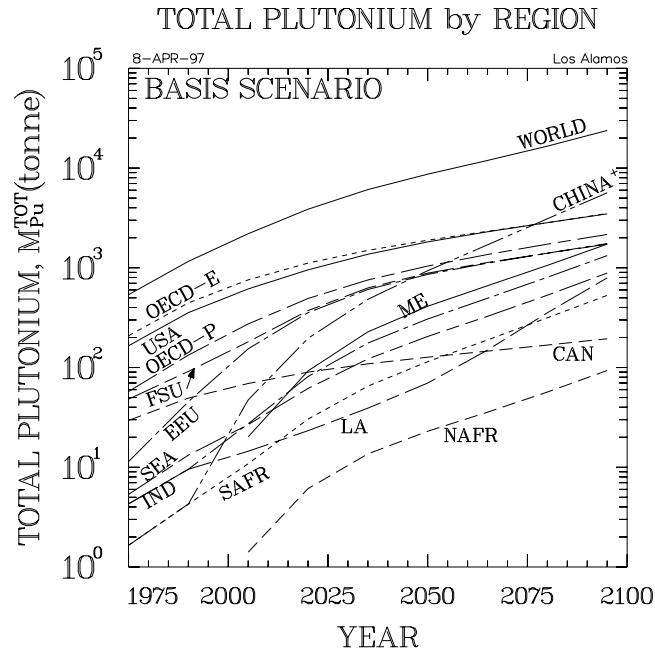


Figure 43A. Regional breakout of total accumulated plutonium for the basis scenario (refer to Fig. 2 for regional notation).

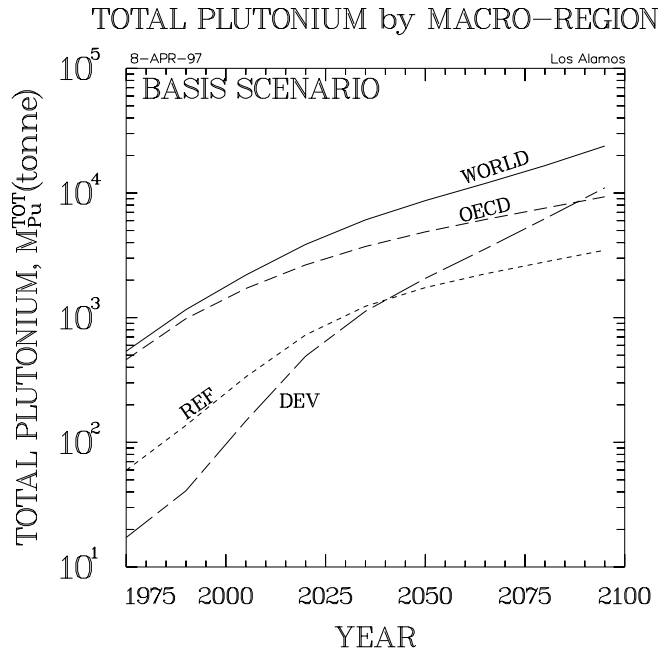


Figure 43B. Macro-regional breakout of total accumulated plutonium for the basis scenario.

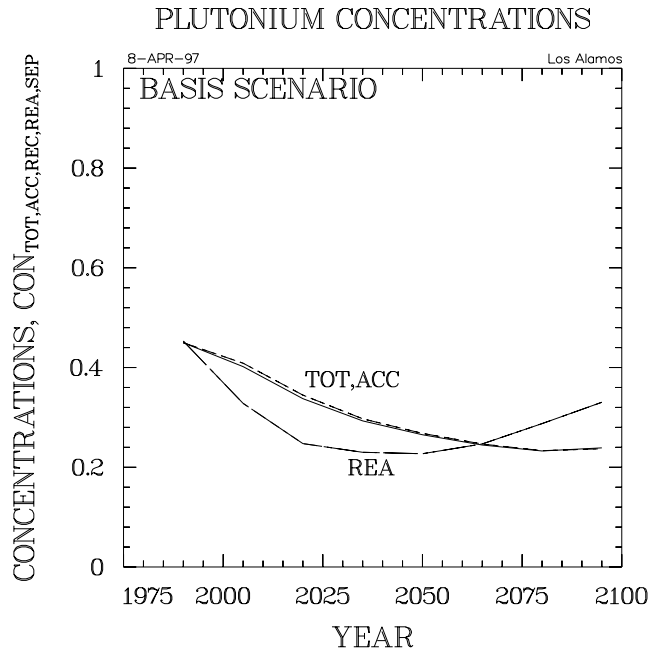


Figure 44. Global plutonium “concentrations” as a function of form and time (refer to Fig. 15 for explanation of global concentrations).

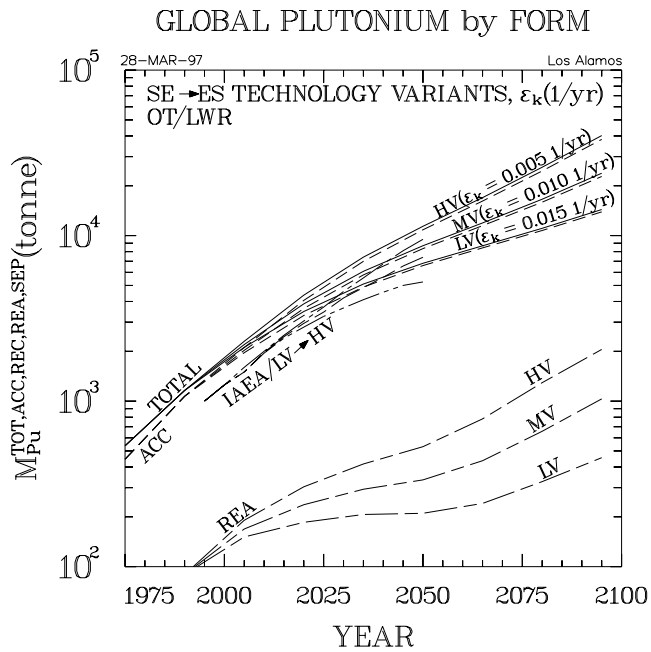


Figure 45. Impact of top-level nuclear energy demand scenarios (Fig. 41) on accumulated plutonium inventories and comparison with the Ref.-7 scenarios; all cases are based on a once-through LWR fuel cycle.

WORLD URANIUM USAGE and PRICE

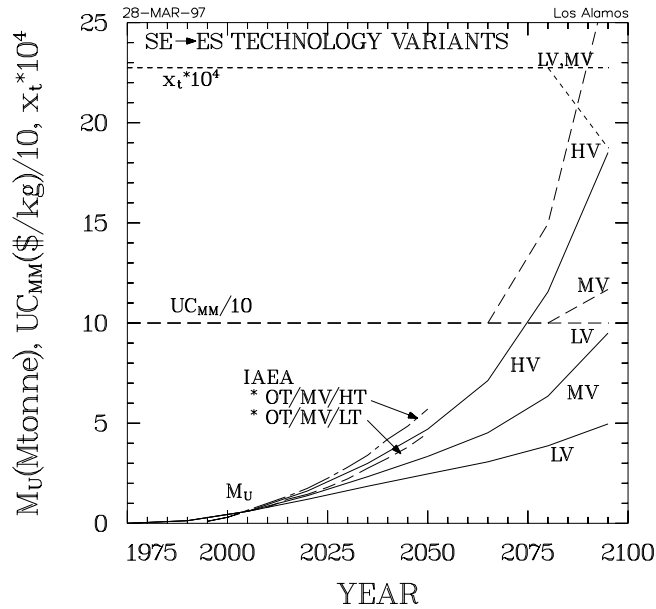


Figure 46. Impact of top-level nuclear energy demand scenarios (Fig. 41) on uranium resource requirements, showing comparison with the Ref.-7 results for the medium-variant (MV) nuclear energy demand scenarios under a once-through (OT) LWR fuel-cycle scenario. The Ref.-7 results fix the uranium tails assay, x_t , at a high value (HT) and a low value (LT), whereas the present study uses an optimized value^{24,25} for x_t .

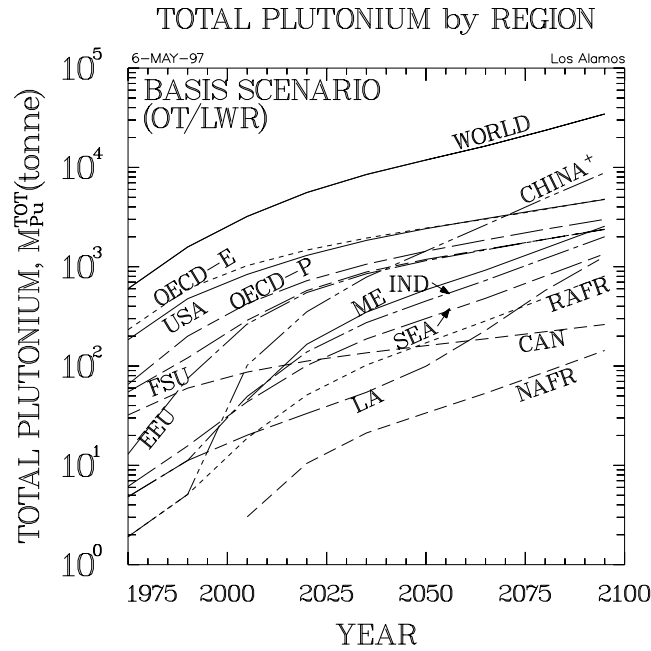


Figure 47A. Regional breakout of total accumulated plutonium for the modified basis scenario (relative to Fig. 43, refer to Fig. 2 for regional notation).

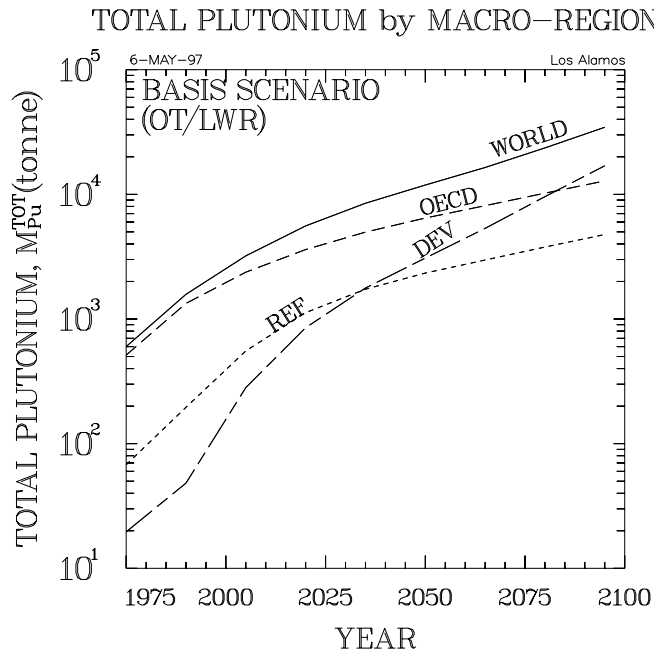


Figure 47B. Macro-regional breakout of total accumulated plutonium for the modified basis scenario (relative to Fig. 43).

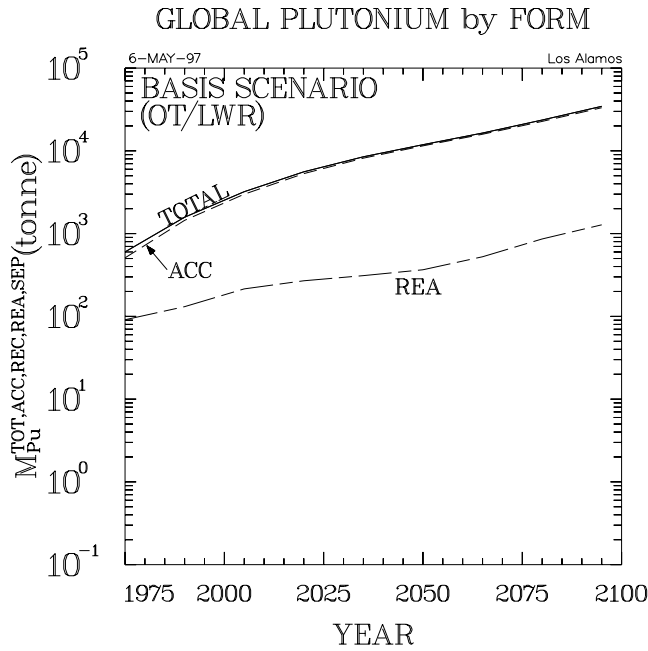


Figure 48A. Global plutonium inventory by form for modified basis scenario ($f_{\text{MOX}}^f = 0.0$, hence, fully recycled inventory, REC, and separated inventories, SEP, are nearly zero): total, accumulated as spent fuel (ACC), and reactor (REA).

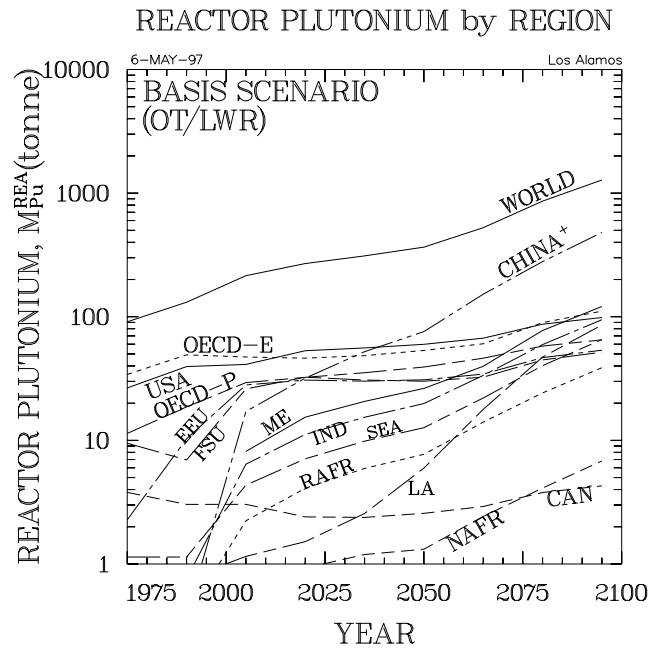


Figure 48B. Regional breakout of reactor plutonium inventory (refer to Fig. 2 for regional notation).

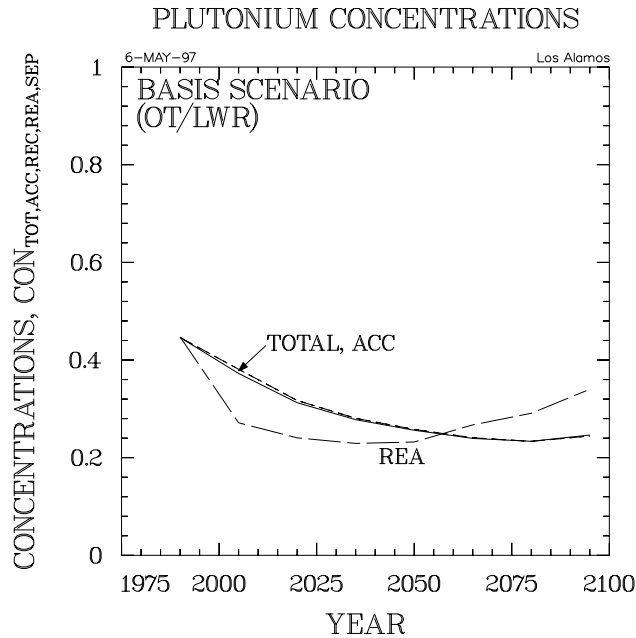


Figure 49. Global plutonium “concentrations” as a function of form and time for the modified basis scenario (relative to Fig. 44; refer to Fig. 15 for explanation of global concentrations).

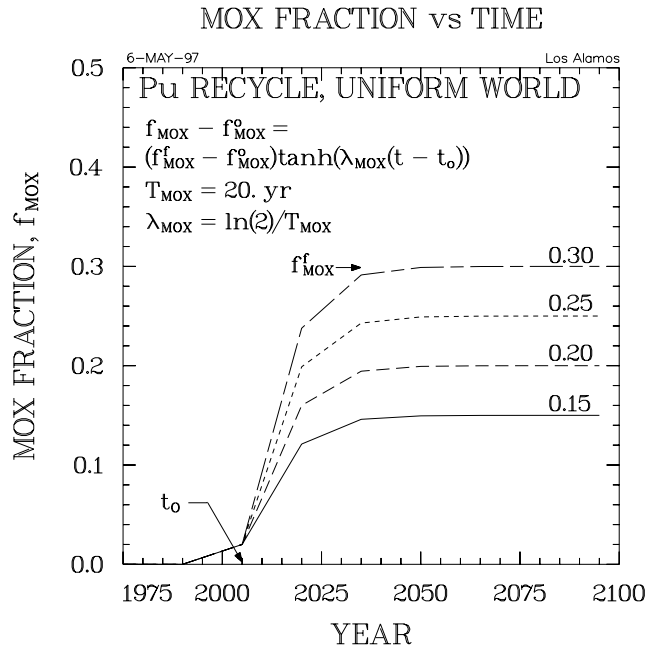


Figure 50. Forcing function used to determine fraction of LWR core operated on MOX. The key parameters f_{MOX}^o , f_{MOX}^f , t_o , and T_{MOX} are region dependent, but for the present studies, all regions are described by the same parameters.

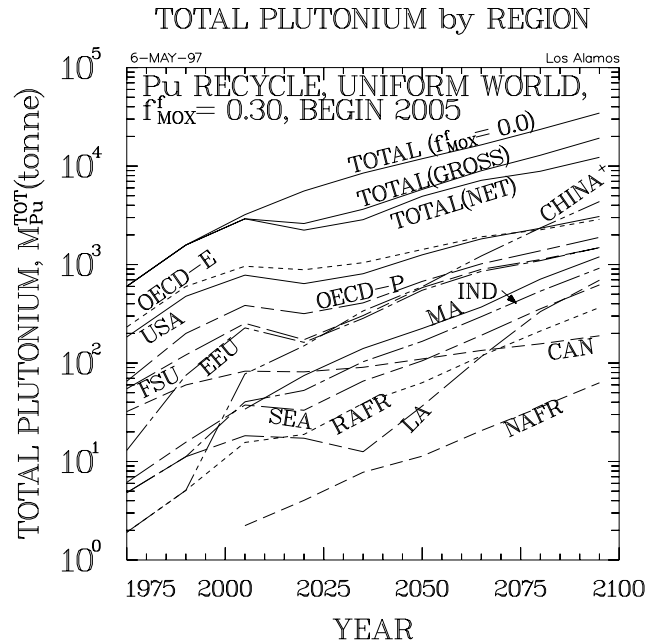


Figure 51A. Region breakout of total accumulated plutonium for for $T_{MOX} = 10$ yr, $f_{MOX}^f = 0.30$, and $t_0 = 2005$. A comparison with the once-through modified basis case is shown (refer to Fig. 2 for regional notation).

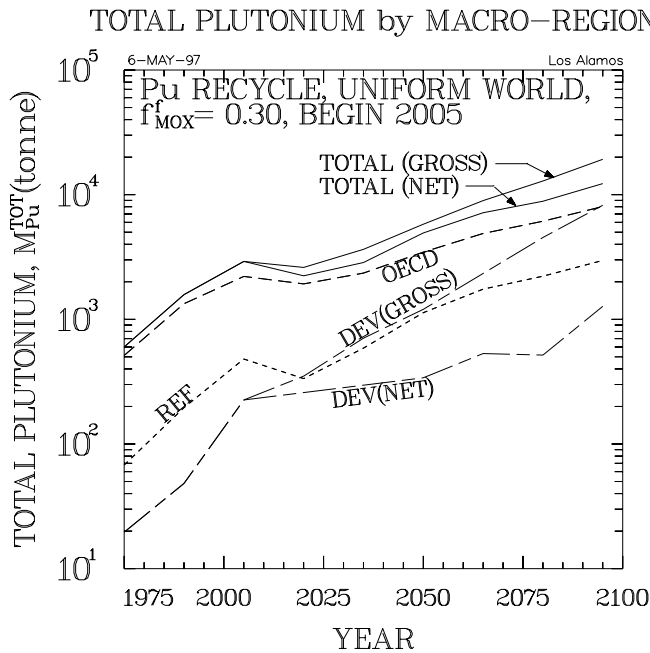


Figure 51B. Macro-regional breakout of total accumulated plutonium for for $T_{MOX} = 10$ yr, $f_{MOX}^f = 0.30$, and $t_0 = 2005$. A comparison with the once-through modified basis case is shown.

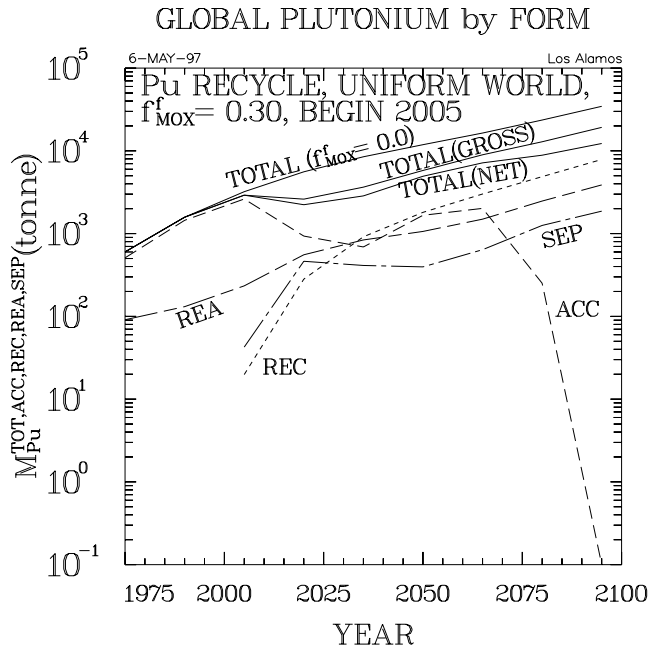


Figure 52A. Breakout of total plutonium inventory by form (ACC + REC + REA + SPU) for $T_{MOX} = 10$ yr, $f_{MOX}^f = 0.30$, and $t_0 = 2005$.

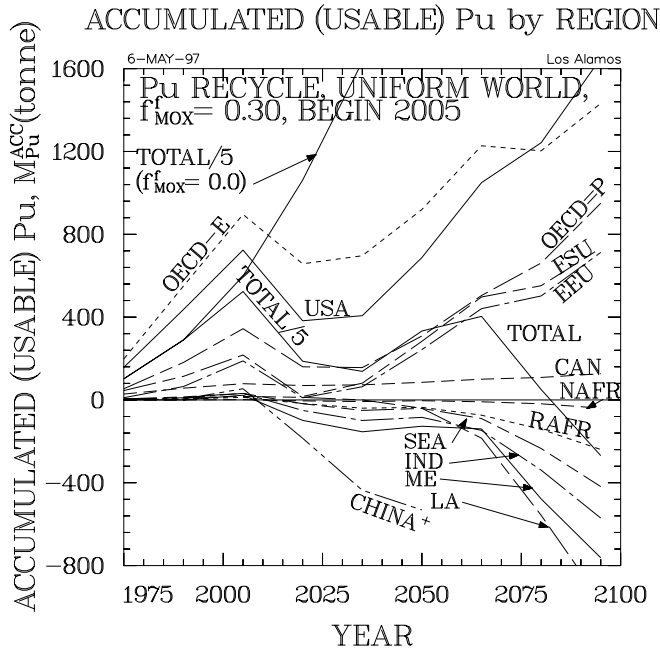


Figure 52B. Regional breakout of usable (recyclable) (ACC) plutonium inventory for $T_{MOX} = 10$ yr, $f_{MOX}^f = 0.30$, and $t_0 = 2005$ (refer to Fig. 2 for regional notation).

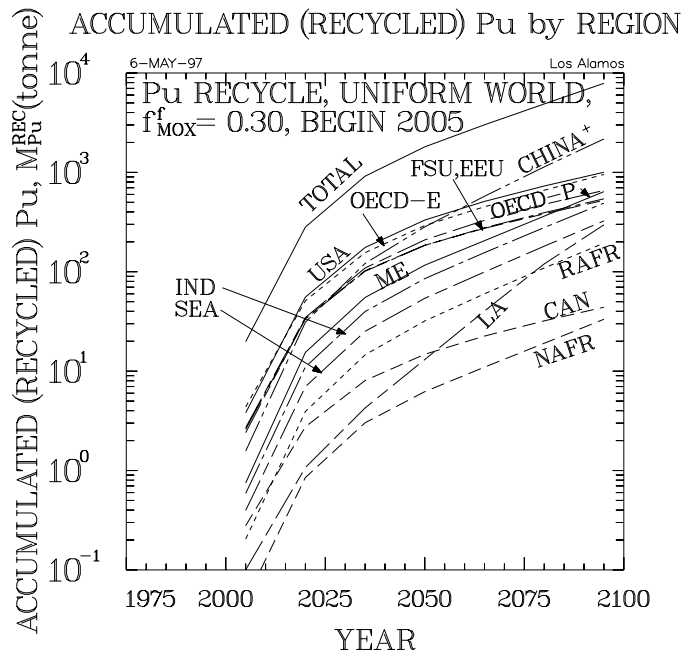


Figure 52C. Regional breakout of fully recycled (REC) plutonium inventory for $T_{MOX} = 10$ yr, $f_{MOX}^f = 0.30$, and $t_0 = 2005$ (refer to Fig. 2 for regional notation).

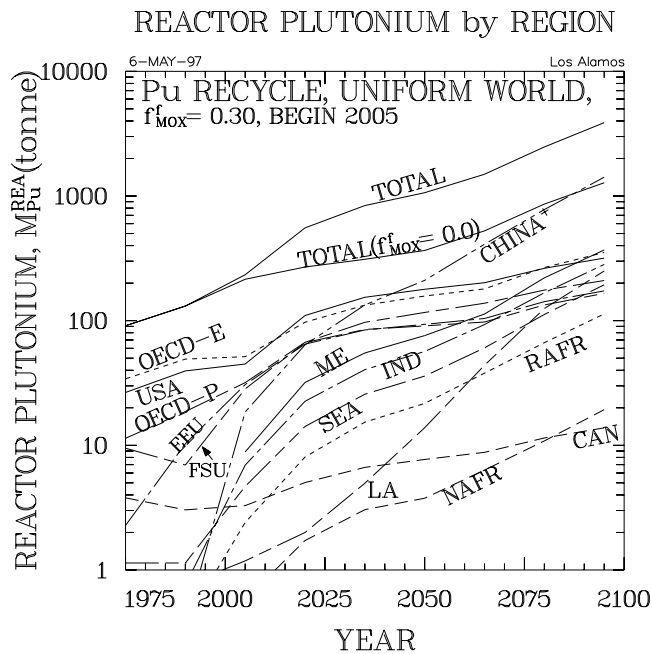


Figure 52D. Regional breakout of reactor (REA) plutonium inventory for $T_{MOX} = 10$ yr, $f_{MOX}^f = 0.30$, and $t_0 = 2005$ (refer to Fig. 2 for regional notation).

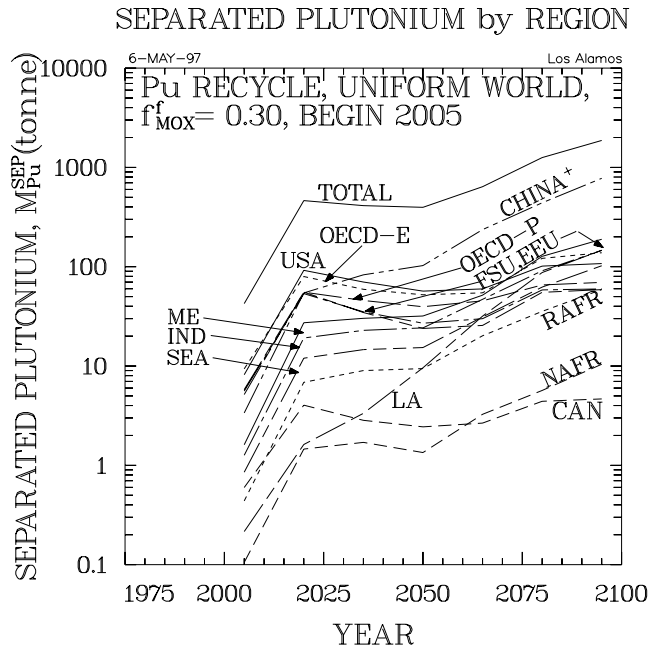


Figure 52E. Regional breakout of separated (SEP = REP + FF) plutonium inventory for $T_{MOX} = 10$ yr, $f_{MOX}^f = 0.30$, and $t_0 = 2005$ (refer to Fig. 2 for regional notation).

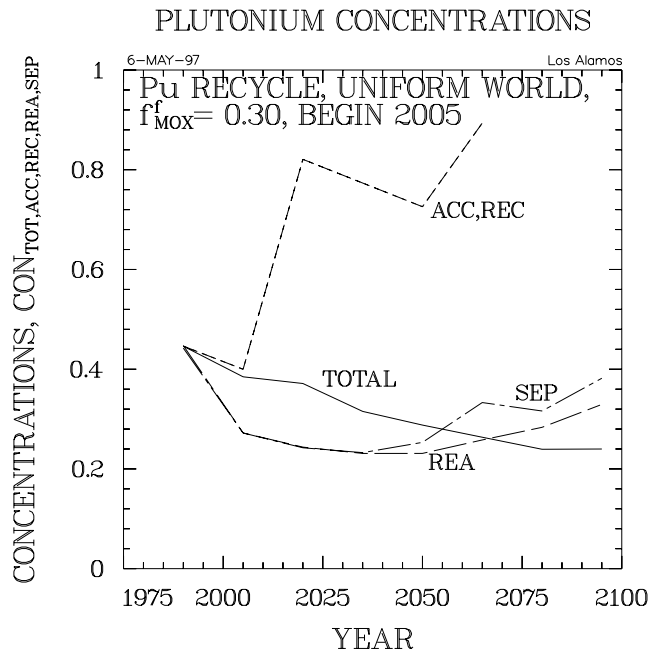


Figure 53. Global plutonium “concentrations” as a function of form and time for $T_{MOX} = 10$ yr, $f_{MOX}^f = 0.30$, and $t_0 = 2005$; refer to Fig. 15 for explanation of global concentrations.

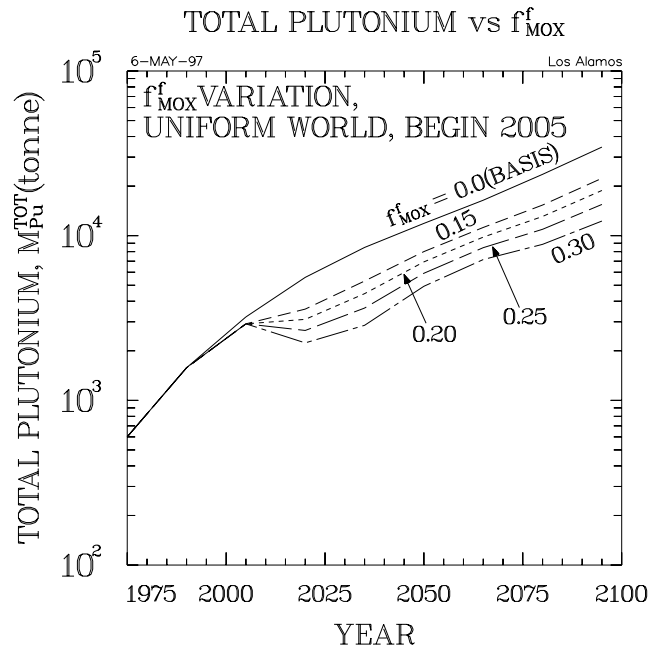


Figure 54. Impact of level of plutonium recycle on total global plutonium inventory.

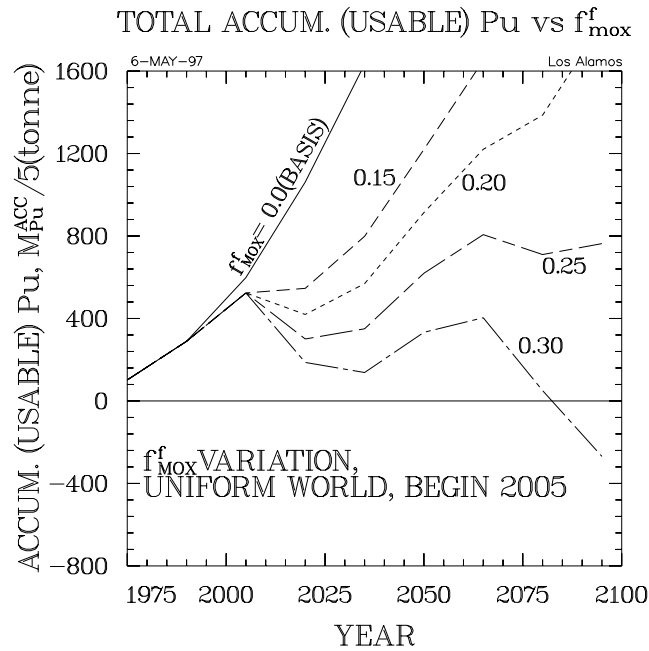


Figure 55. Impact of level of plutonium recycle on global inventory of LWR-recyclable plutonium (ACC).

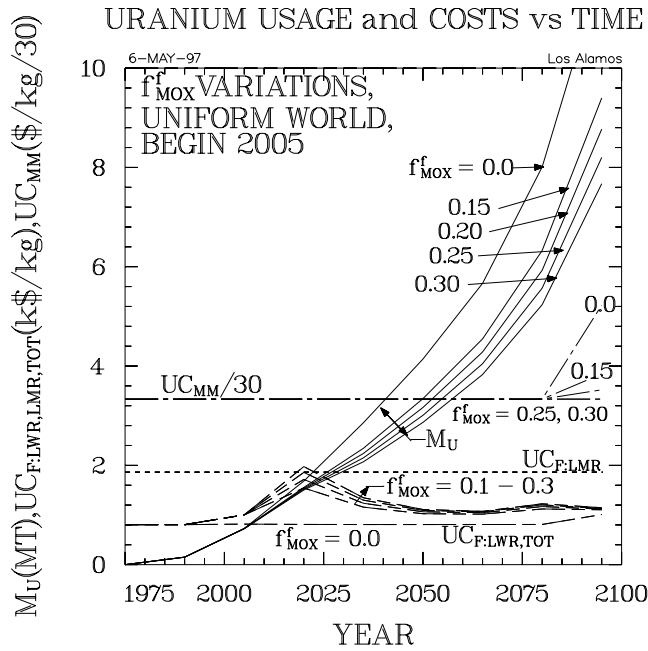


Figure 56. Impact of level of plutonium recycle on uranium resource requirements for a range of recycle scenarios, showing accumulated uranium usage, M_U , unit cost of mined/milled uranium, UC_{MM} , and unit cost of fuel cycle, UC_F .

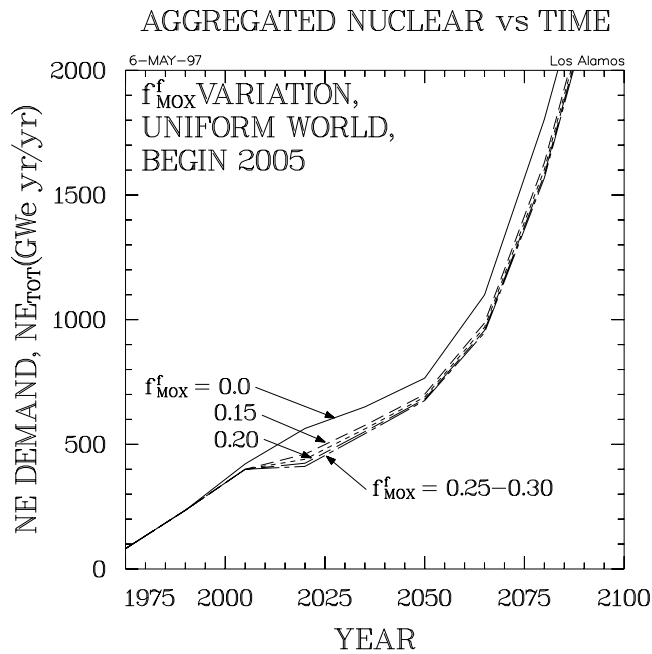


Figure 57. Impact of level of plutonium recycle on global nuclear-energy demand; increased fuel-cycle cost (for the KR uranium-resource category) decrease nuclear-energy share fraction somewhat.

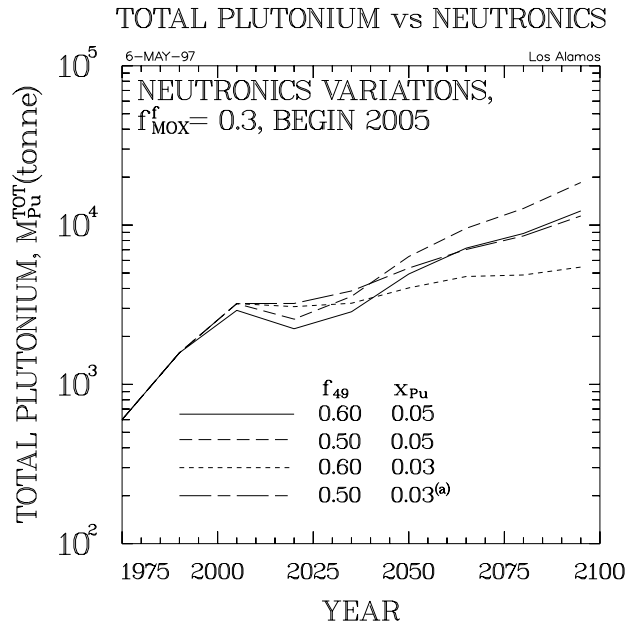


Figure 58. Sensitivity of total plutonium global inventory on MOX loading parameter, x_{Pu} , and fission factor, f_{49} , for $T_{MOX} = 10$ yr, $f_{MOX}^f = 0.30$, and $t_0 = 2005$.

(a) conditions used to generate LWR plutonium recycle results reported in Ref. 9.

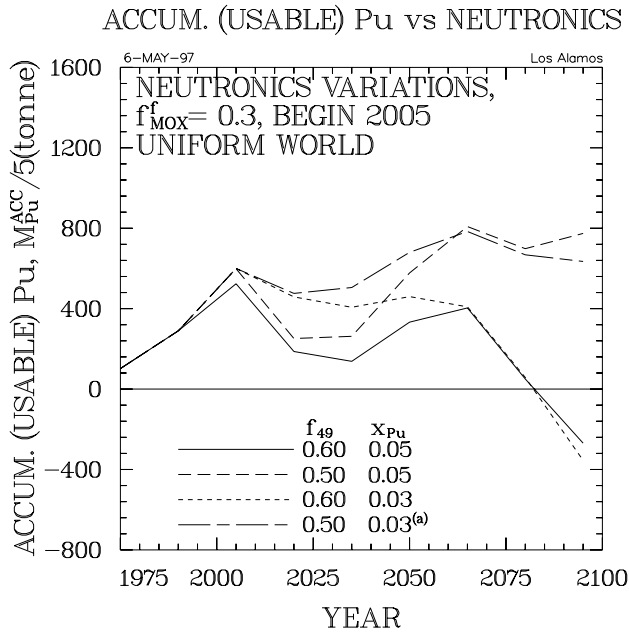


Figure 59. Sensitivity of global recyclable plutonium inventory (ACC) on MOX loading parameter, x_{Pu} , and fission factor, f_{49} , for $T_{MOX} = 10$ yr, $f_{MOX}^f = 0.30$, and $t_0 = 2005$.

(a) conditions used to generate LWR plutonium recycle results reported in Ref. 9.

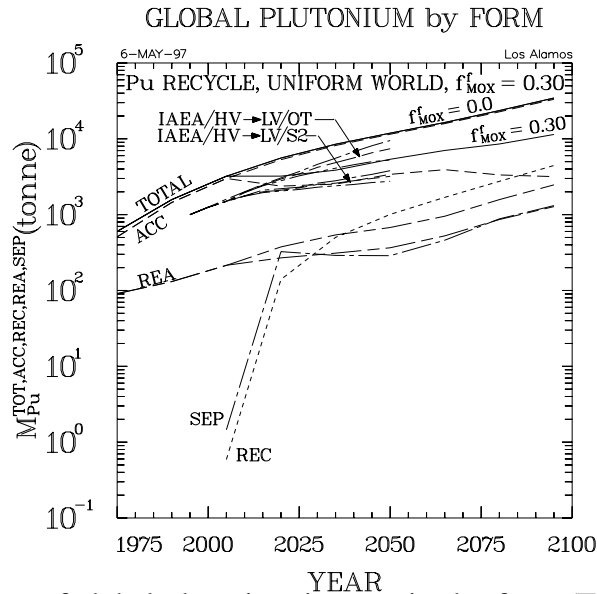


Figure 60. Summary of global plutonium inventories by form (TOTAL = ACC + REC + REA + SEP) for $T_{MOX} = 20$ yr, $f_{MOX}^f = 0.30$, $t_0 = 2005$, $f_{49} = 0.50$, and $x_{Pu} = 0.03$; Comparison is made with once-through ($f_{MOX}^f = 0.0$) case, as well as equivalent Ref.-7 cases (OT = once through; S2 = two full recycles, HV = high variant, and LV = low variant).⁷

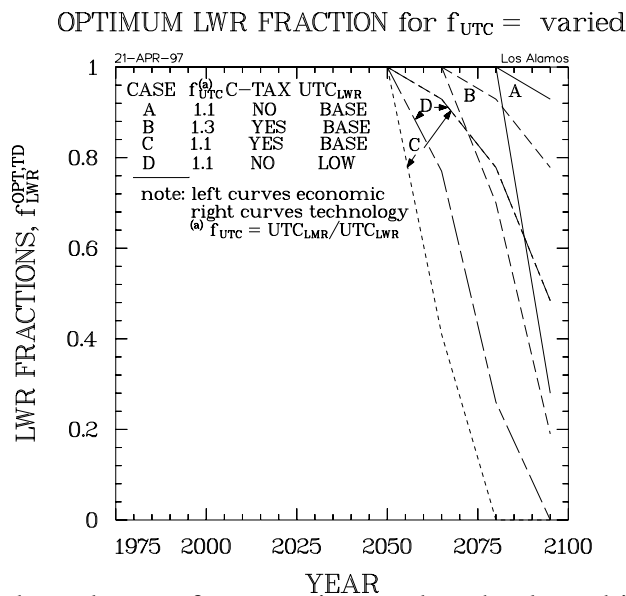


Figure 61. Time dependence of economics- and technology-driven introduction of LMRs on a range of favorable scenario attributes, where $f_{LWR} = 1 - f_{LMR}$ is the fraction of all nuclear energy generated from LWRs under the assumption of a homogeneous world (*i.e.*, all factors determining the time-dependence of f_{LWR} are independent of region); for all four cases indicated to enhance LMR introduction, the conservative CR uranium resource scaling (Fig. 36B) and the once-through LWR ($f_{MOX}^f = 0.0$) basis scenario were used.

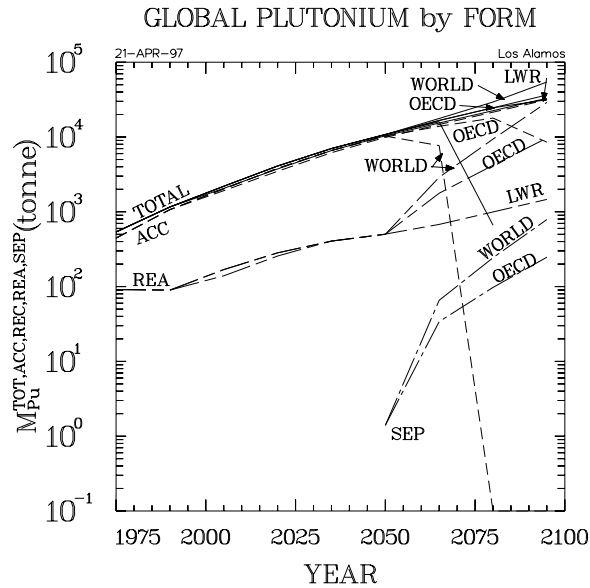


Figure 62. Time dependence of global plutonium inventories for a range of forms: ACC = accumulated (REC = plutonium that has been fully recycled in LWRs is zero for the basis scenario once-through fuel-cycle option); REA = actively fissioning reactor inventories; and SEP = non-LMR reprocessing and LMR fuel fabrication associate with plutonium having LWR origins, for the Case D scenario indicated on Fig. 61. In addition to showing the basis scenario (once-through LWR, but at reduced cost to facilitate comparison), a case where LMRs are implemented globally (WORLD) and only in OECD countries is shown.

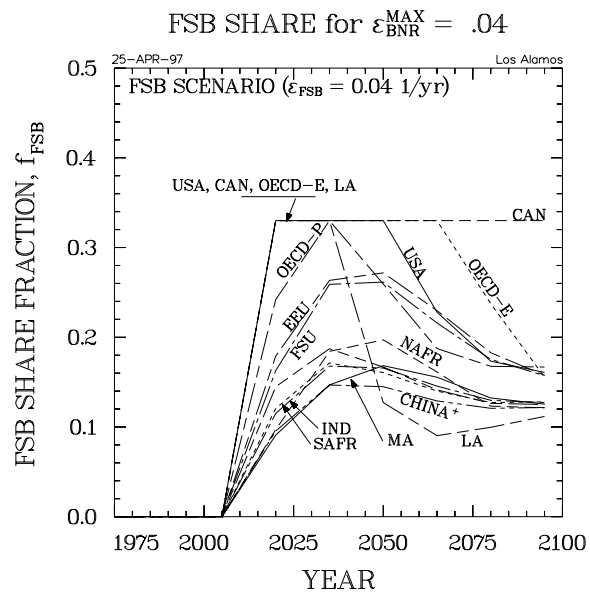


Figure 63. Regional and temporal dependence of FSB share fraction [support ratio, $SR_{FSB} = (1 - f_{FSB})/f_{FSB}$] for implementation rate limited to $\epsilon_{FSB} = 0.04$ 1/yr and 0.33 maximum FSB share fraction (refer to Fig. 2 for regional notation).

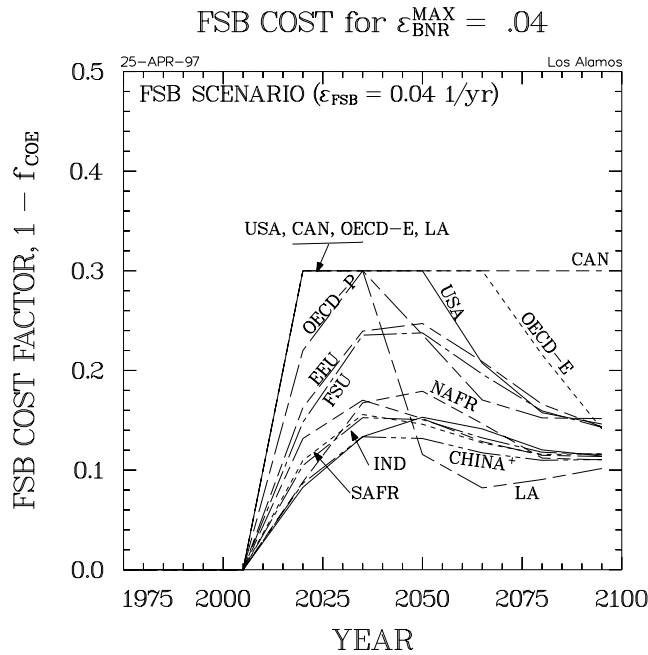


Figure 64. Regional and temporal dependence of COE increment that accompanies the respective f_{FSB} or SR_{FSB} [Eq. (A-21)] values reported in Fig. 63 (refer to Fig. 2 for regional notation).

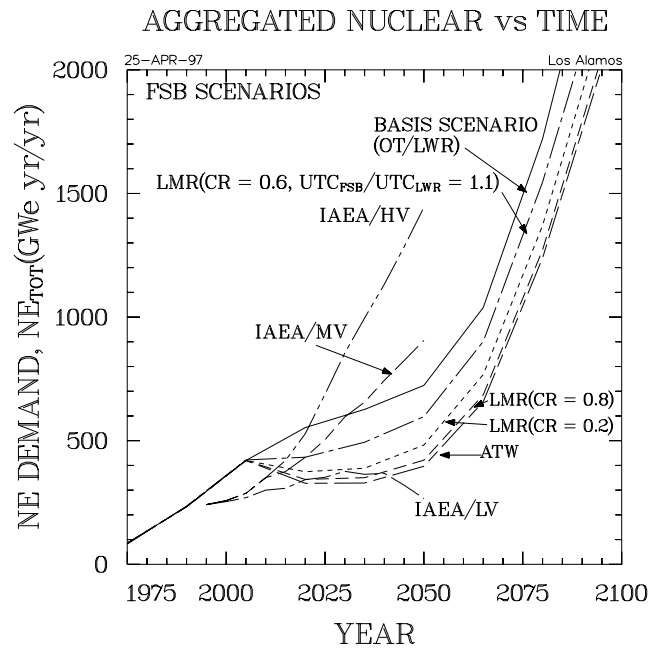


Figure 65. Impact of FSB implementation on nuclear energy demand for three FSB scenarios [Table A-III: LMR(CR = 0.6); LMR(CR = 0.2); and ATW] as determined by the COE increases reflected in Fig. 61; comparisons with the basis scenario (Fig. 10, Table IV), as well as the three IAEA variants,⁷ are given.

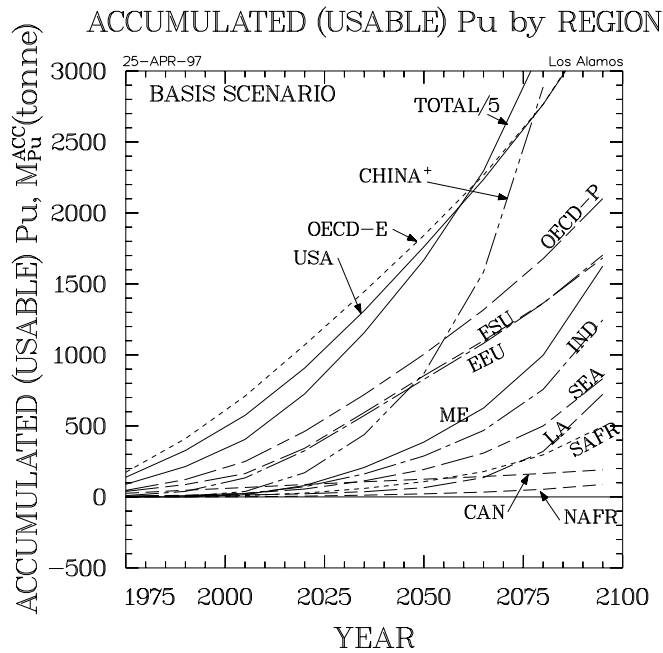


Figure 66A. Impact of LMR(CR = 0.6) FSB scenario on accumulated plutonium inventories for each of 13 global regions and world totals: basis scenario (once-through LWR, refer to Fig. 2 for regional notation).

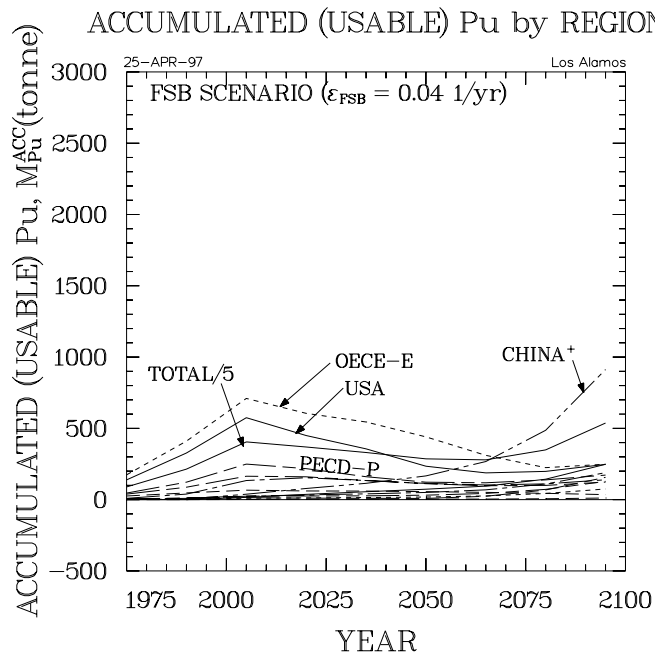


Figure 66B. Impact of LMR(CR = 0.6) FSB scenario on accumulated plutonium inventories for each of 13 global regions and world totals: LMR(CR = 0.6) FSB.

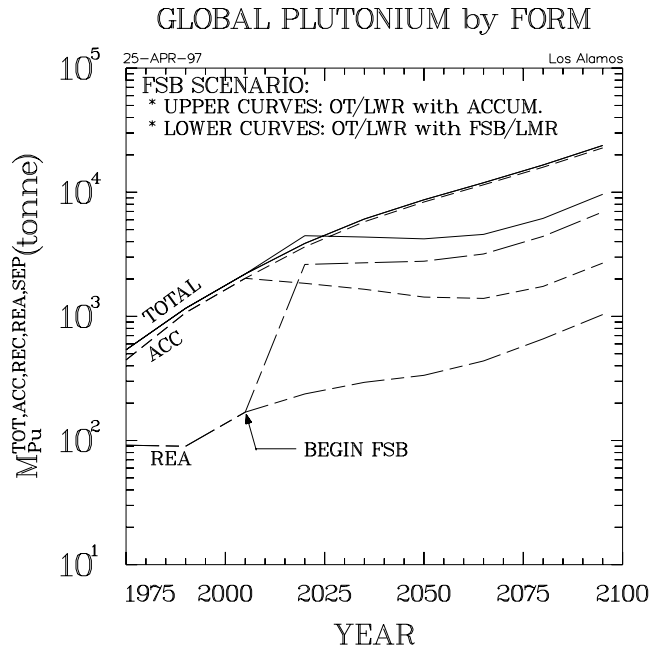


Figure 67. Impact of LMR(CR = 0.6) FSB scenario on accumulated, reactor, and total plutonium for the LMR(CR = 0.6) FSB scenario showing a factor of ~ 3 decrease in total plutonium, but a strong increase in reactor plutonium.

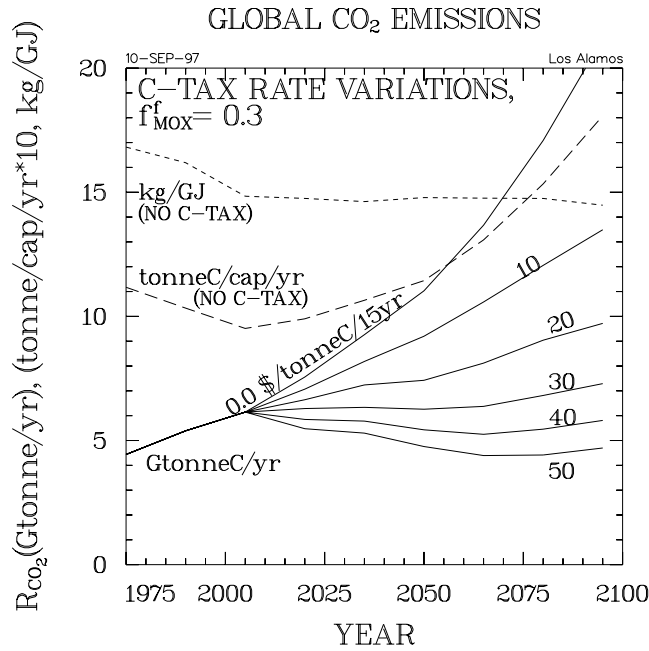


Figure 68A. Atmospheric carbon emission rates as a function of time, carbon tax rate, and region: Global atmospheric carbon emission rate as a function of time and rate at which carbon-tax is imposed; shown also for the zero carbon-tax case are global emission rates *per capita* and *per primary energy usage*.

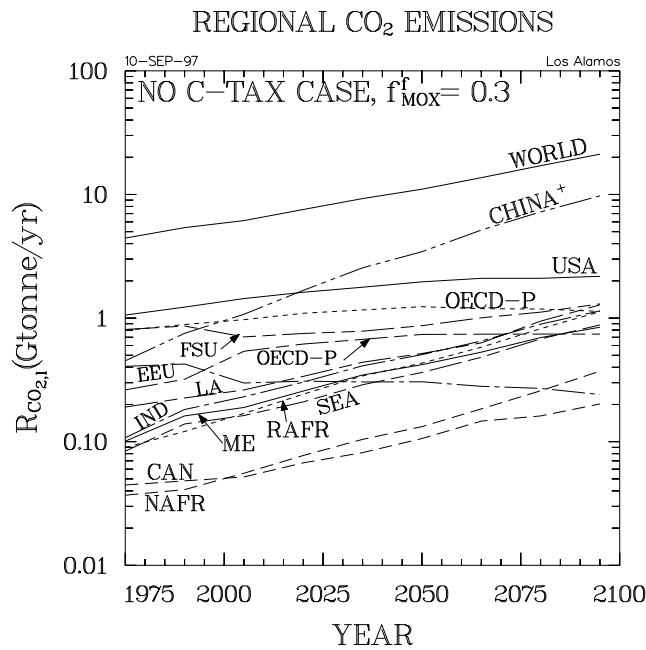


Figure 68B. Atmospheric carbon emission rates as a function of time, carbon tax rate, and region: Global atmospheric carbon emission rate as a function of time and region for the zero carbon-tax case (refer to Fig. 2 for regional notation).

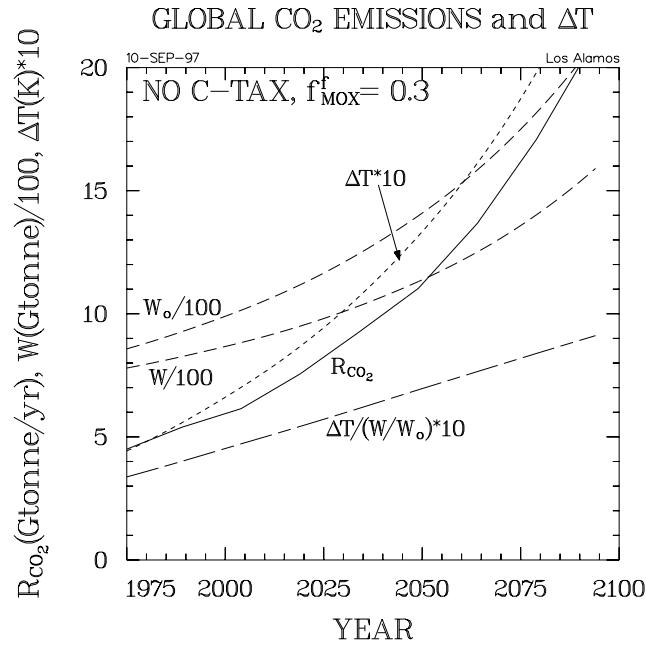


Figure 69. Time dependence of total CO₂ (carbon) emission, integrated emissions, atmospheric accumulation of emissions, and corresponding global average temperature rise, as determined from the linear integral- response model^{42,49}; results applied to the zero carbon-tax basis case⁹.

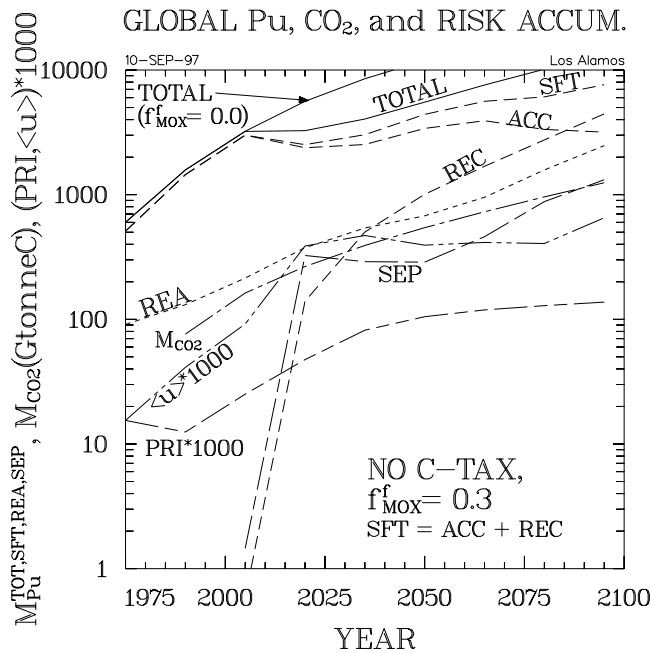


Figure 70. Time dependence of global plutonium inventories as a function of form (TOT, SFT = ACC + REC, SEP = FF + RP, and REA), as well as the evolution of the integrated CO₂ (carbon) emissions, the grand utility function for proliferation¹⁹, $\langle u \rangle$, and the proliferation- risk index, PRI, evaluated from a USA perspective and discounted at a rate $DR = 0.04$ 1/yr.

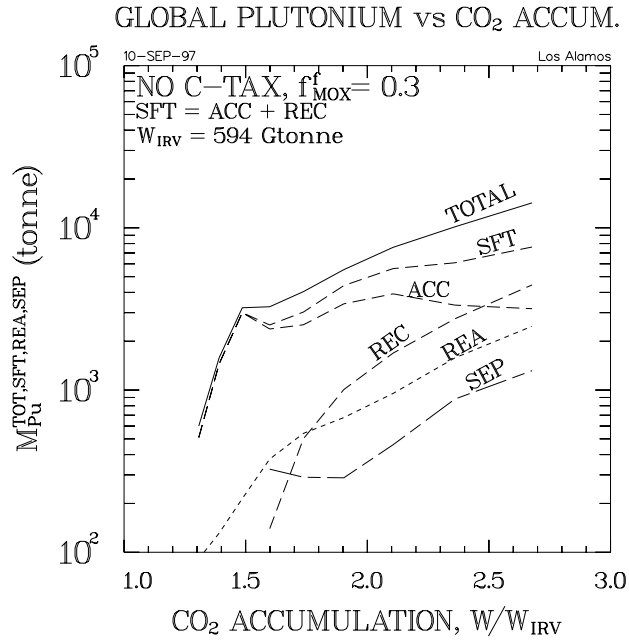


Figure 71A. Correlation of global plutonium inventories, by form, for no carbon taxes with atmospheric CO₂ (carbon) accumulation relative to pre-industrial levels ($W_{IRV} = 594$ Gtonne).

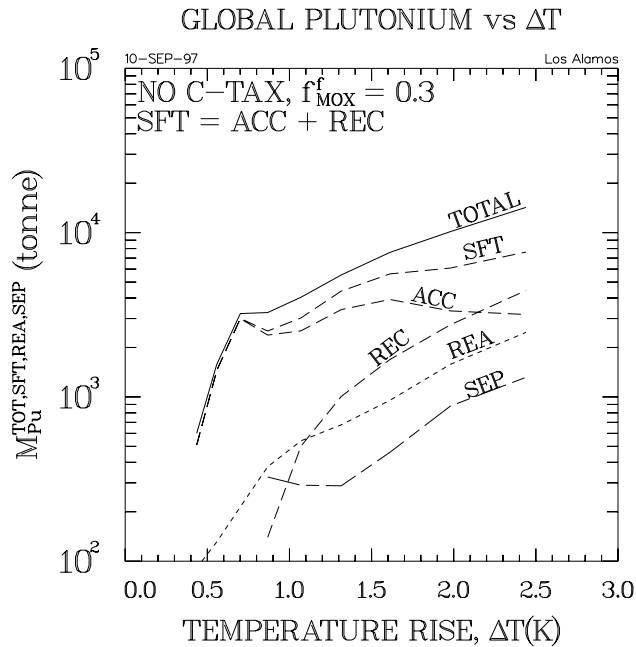


Figure 71B. Correlation of global plutonium inventories, by form, for no carbon taxes with average global temperature rise (ΔT measured from $t_{IRV} = 1800$).

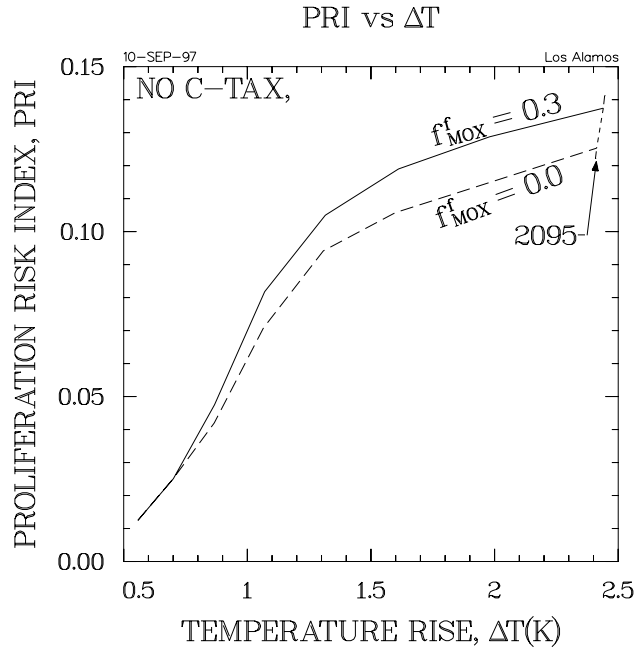


Figure 72. Correlation of proliferation-risk index with average global temperature rise for case without carbon tax imposed; comparison of PRI impacts of plutonium recycle (e.g., $f_{\text{MOX}}^f = 0.0$ versus 0.30) is shown (ΔT measured from $t_{\text{IRV}} = 1800$).

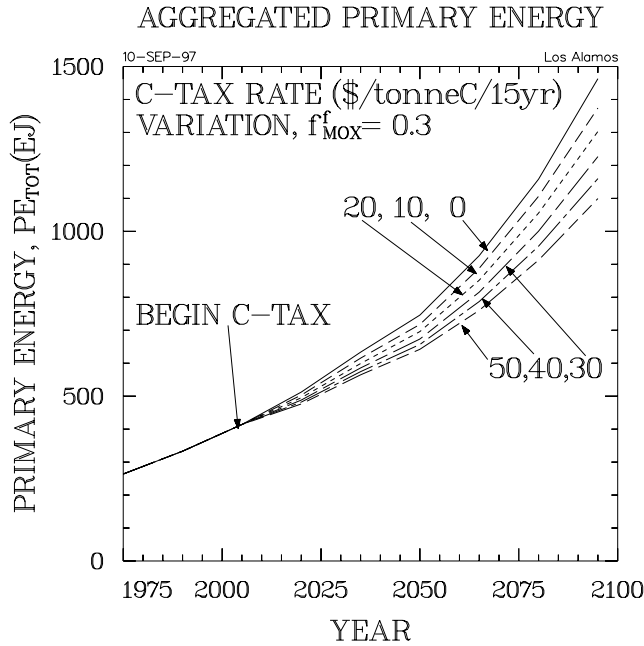


Figure 73. Impact of global carbon tax rates on primary energy demand.

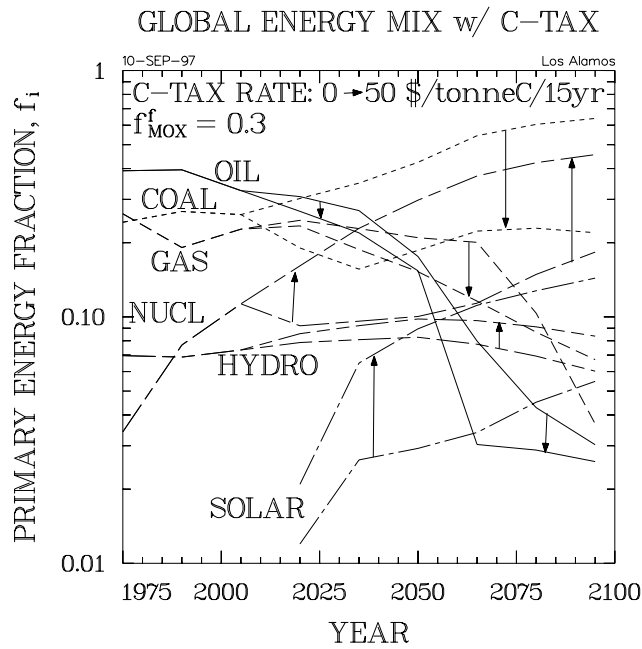


Figure 74. Shift in primary energy share fractions induced by strong carbon-tax rate (50 \$/tonneC/15yr).

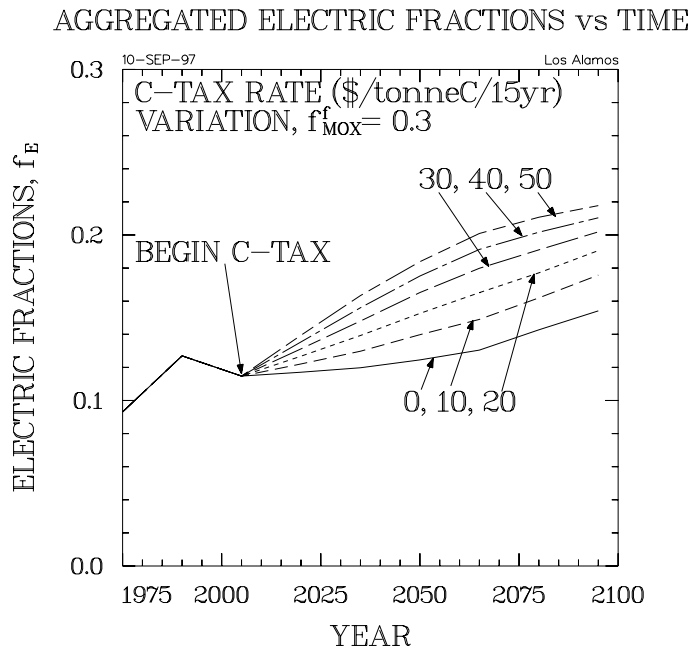


Figure 75. Impact of global carbon tax rates on fraction of primary energy used as electricity (not same energy basis).

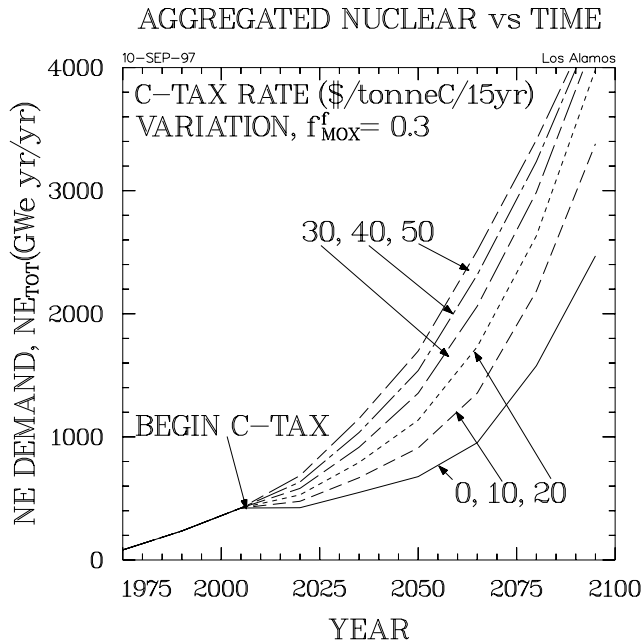


Figure 76. Impact of global carbon tax rates on nuclear energy demand.

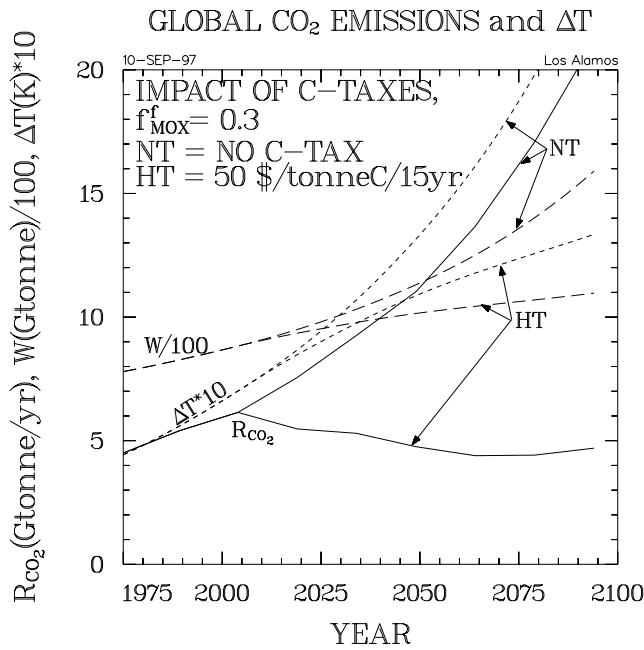


Figure 77. Impact of strong carbon-tax rate (50 \$/tonneC/15yr) of atmospheric carbon emissions, accumulations, and associated average global temperature rise.

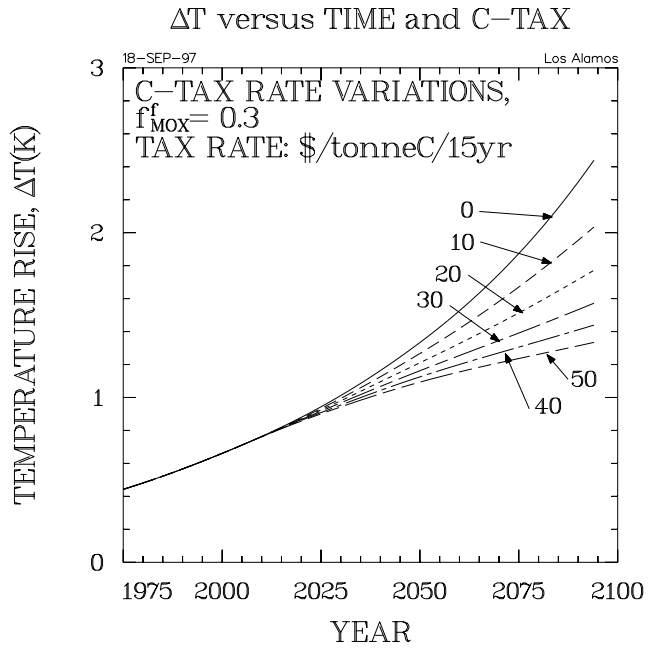


Figure 78. Global temperature rise *versus* time for a range of carbon tax rates.

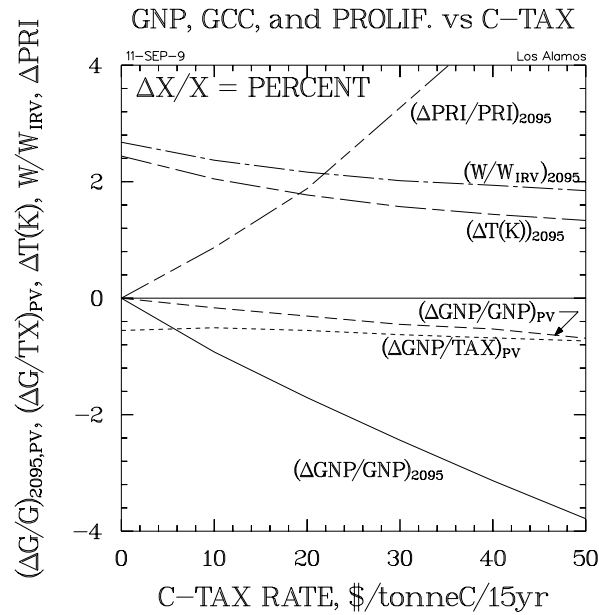


Figure 79A. Impact of carbon tax rates on either present value (PV) or last-year (2095) gross productivity ($G = \text{GWP}$), comparing GCC parameters (W/W_{IRV} and ΔT) with proliferation parameters (PRI); all relative changes $\Delta X/X$ are expressed as percentages:
 direct dependence on carbon tax rate;

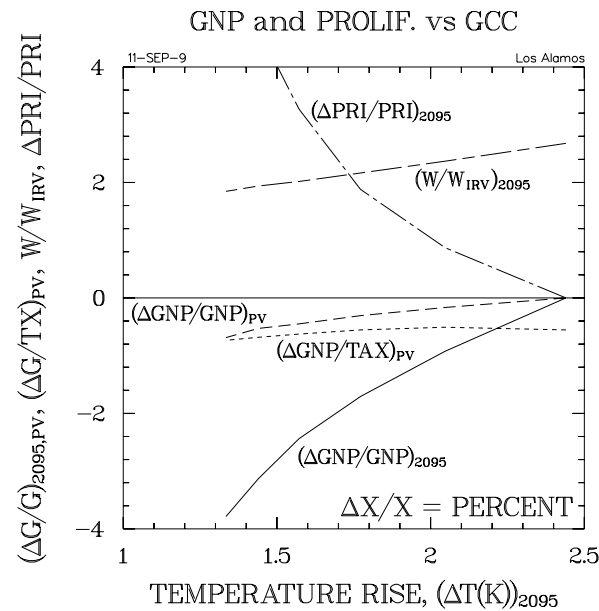


Figure 79B. Impact of carbon tax rates on either present value (PV) or last-year (2095) gross productivity ($G = \text{GWP}$), comparing GCC parameters (W/W_{IRV} and ΔT) with proliferation parameters (PRI); all relative changes $\Delta X/X$ are expressed as percentages:
 correlation with last-year (2095) temperature rise, as determined by carbon tax rate.

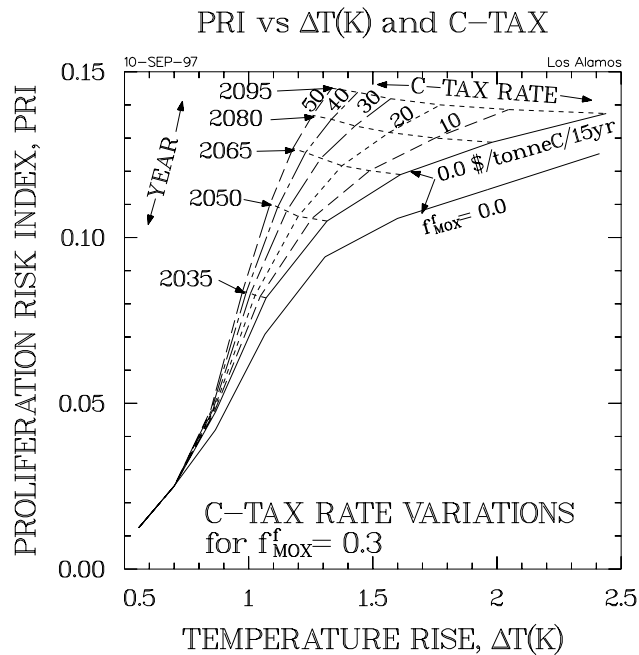


Figure 80A. Direct comparison of proliferation-risk-index *versus* atmospheric temperature-rise “operating curves” as the rate of carbon taxation is varied: direct comparison/evolution of PRI *versus* ΔT , showing isochrones;

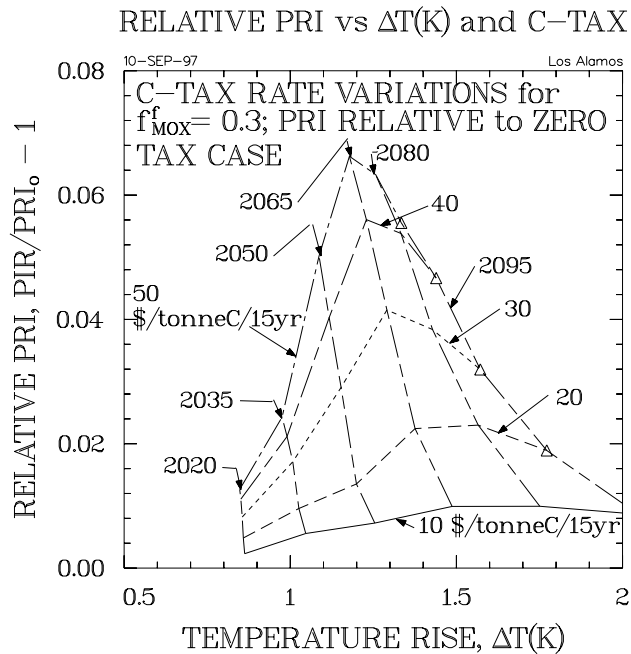


Figure 80B. Direct comparison of proliferation-risk-index *versus* atmospheric temperature-rise “operating curves” as the rate of carbon taxation is varied: change in PRI relative to the no-carbon-tax case, showing isochrones.

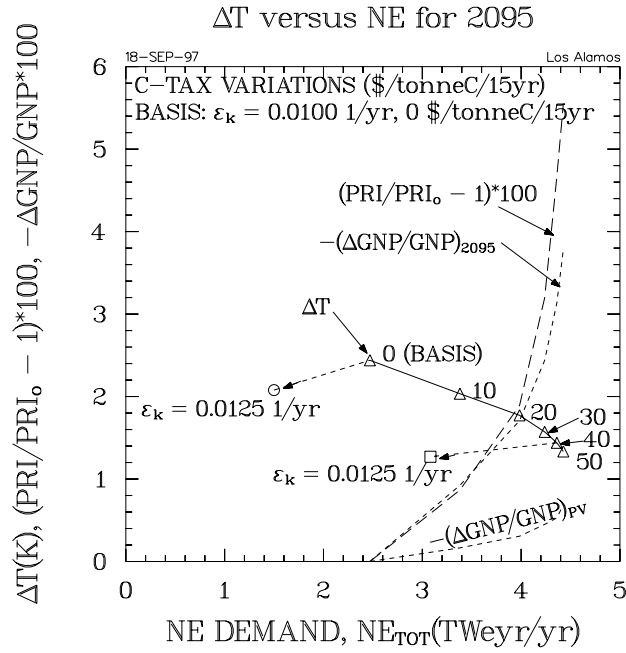


Figure 81. Global temperature rise in 2095 as a function of increased (carbon-tax-induced) nuclear energy demand; the relative increase in proliferation risk is also shown, as is the decrease in GNP (both in 2095 and on a present-value basis).

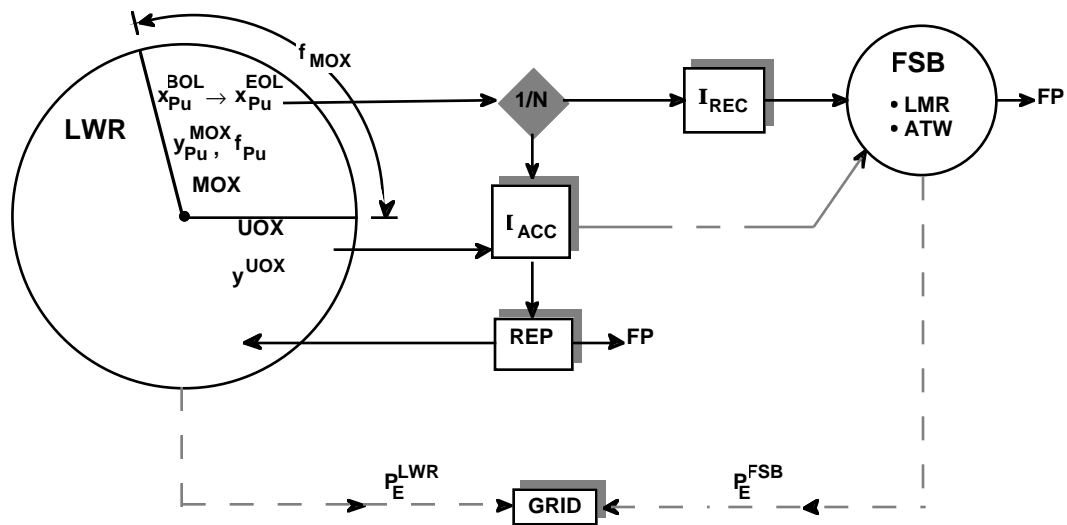


Figure A-1. Plutonium mass-flow model, where LWR-recyclable plutonium is accumulated as inventory I_{ACC} (kgPu), and plutonium that on the average has been recycled greater than N times to the LWR is stored as unrecyclable material under inventory I_{REC} (kgPu). Fast-spectrum burners (FSBs) of plutonium include LMRs or ATWs, which can consume both REC and ACC plutonium inventories.

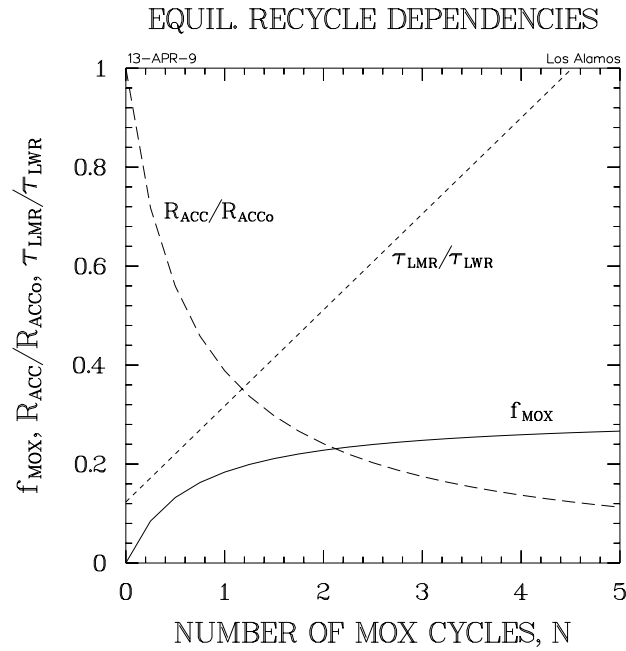


Figure A-2. Dependencies of MOX fraction, rates of (fully recycled) plutonium accumulation, and time to accumulated on LMR inventory as a function of number of LWR recycles under sustainable steady-state conditions described by Eq. (A-5); Eqs. (A-6) and (A-7) are also plotted.

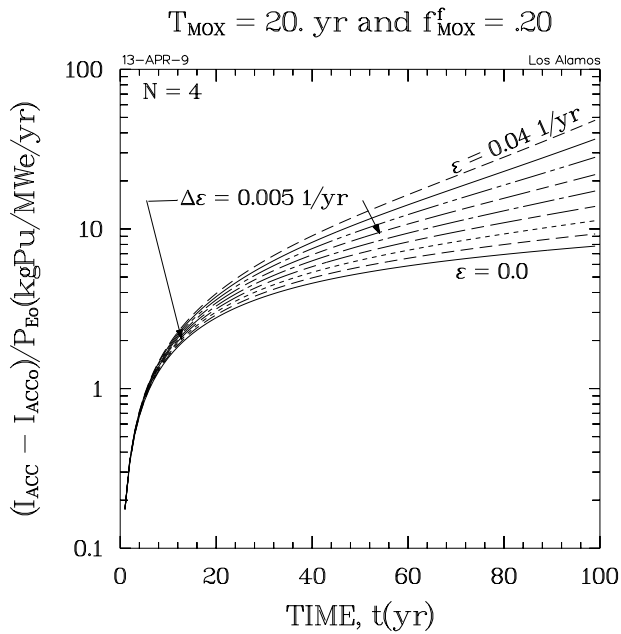


Figure A-3A. Time dependence of recyclable (to LWRs, ACC) plutonium inventories for a range of nuclear energy growth rates, ϵ , and asymptotic MOX core fractions, f_{MOX}^f , for the parameters listed in Table A-I:
 $f_{MOX}^f = 0.20$

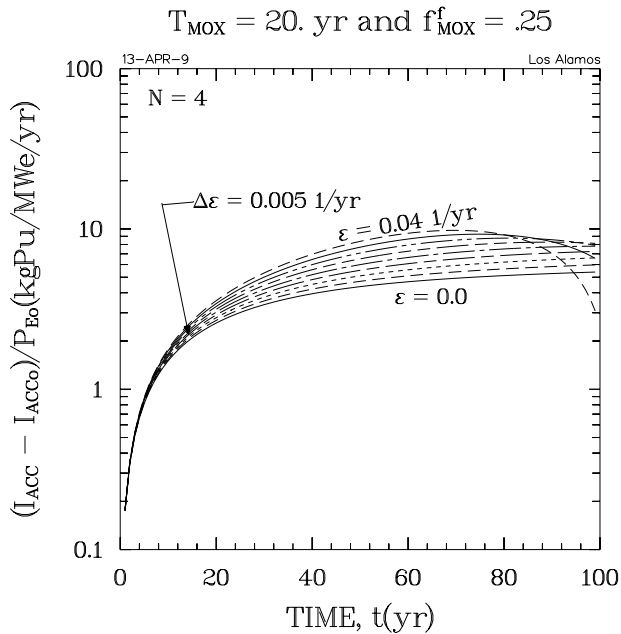


Figure A-3B. Time dependence of recyclable (to LWRs, ACC) plutonium inventories for a range of nuclear energy growth rates, ϵ , and asymptotic MOX core fractions, f_{MOX}^f , for the parameters listed in Table A-I:
 $f_{MOX}^f = 0.25$

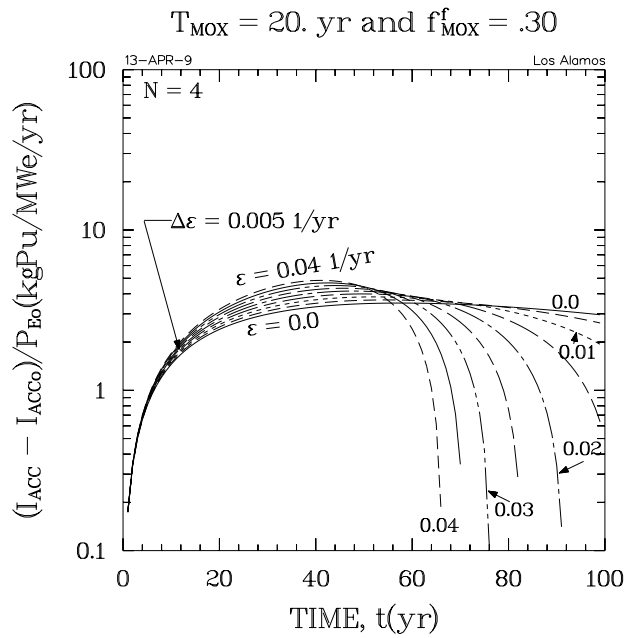


Figure A-3C. Time dependence of recyclable (to LWRs, ACC) plutonium inventories for a range of nuclear energy growth rates, ϵ , and asymptotic MOX core fractions, f_{MOX}^f , for the parameters listed in Table A-I:

$$f_{\text{MOX}}^f = 0.30$$